www.oftalmoloji.org

ISSN 2149-8695

TURKISH JOURNAL OF OPHTHALMOLOGY

TJO

July
August
2018
48 Volume
Issue 4

galenos

TURKISH JOURNAL OF OPHTHALMOLOGY

TJO

www.oftalmoloji.org

Publishing House
Molla Gürani Mah. Kaçamak Sokak No: 21,
34093 Fındıkzade-İstanbul-Turkey
Phone: +90 212 621 99 25 **Fax:** +90 212 621 99 27
E-mail: info@galenos.com.tr
Printed at: Özgün Ofset Ticaret Ltd. Şti.
Yeşilce Mah. Aytekin Sk. No: 21 34418 4. Levent, İstanbul, Türkiye
Phone: +90 212 280 00 09
Date of printing: September 2018
International scientific journal published bimonthly.
ISSN: 2149-8695 **E-ISSN:** 2149-8709

The Turkish Journal of Ophthalmology is an official journal of the Turkish Ophthalmological Association.
On Behalf of Turkish Ophthalmological Association Owner
T. Reha Ersöz,
Çukurova University Faculty of Medicine, Department of Ophthalmology, Adana, Turkey

TURKISH JOURNAL OF OPHTHALMOLOGY

TJO

www.oftalmoloji.org

ABOUT US

The Turkish Journal of Ophthalmology (TJO) is the only scientific periodical publication of the Turkish Ophthalmological Association and has been published since January 1929. In its early years, the journal was published in Turkish and French. Although there were temporary interruptions in the publication of the journal due to various challenges, the Turkish Journal of Ophthalmology has been published continually from 1971 to the present.

The Turkish Journal of Ophthalmology is currently published in Turkish and English languages. TJO is an independent international periodical journal based on single-blind peer-review principle. TJO is regularly published six times a year and special issues are occasionally released. The aim of TJO is to publish original research papers of the highest scientific and clinical value at an international level. Furthermore, review articles, case reports, editorial comments, letters to the editor, educational contributions and congress/meeting announcements are released.

The target audience includes specialists and physicians in training in ophthalmology in all relevant disciplines.

The editorial policies are based on the "Recommendations for the Conduct, Reporting, Editing, and Publication of Scholarly Work in Medical Journals (ICMJE Recommendations)" by the International Committee of Medical Journal Editors (2013, archived at http://www.icmje.org/) rules.

The Turkish Journal of Ophthalmology is indexed in the **PubMed Central (PMC), Web of Science-Emerging Sources Citation Index (ESCI), Scopus, TUBITAK/ULAKBIM, Directory of Open Access Journals (DOAJ), EBSCO Database, CINAHL, Proquest, Gale/Cengage Learning, Index Copernicus, J-Gate, Turk Medline** and **Turkish Citation Index.**

Open Access Policy

This journal provides immediate open access to its content on the principle that making research freely available to the public supports a greater global exchange of knowledge.

Open Access Policy is based on the rules of the Budapest Open Access Initiative (BOAI) http://www.budapestopenaccessinitiative.org/. By "open access" to peer-reviewed research literature, we mean its free availability on the public internet, permitting any users to read, download, copy, distribute, print, search, or link to the full texts of these articles, crawl them for indexing, pass them as data to software, or use them for any other lawful purpose, without financial, legal, or technical barriers other than those inseparable from gaining access to the internet itself. The only constraint on reproduction and distribution, and the only role for copyright in this domain, should be to give authors control over the integrity of their work and the right to be properly acknowledged and cited.

Subscription Information

TJO is sent free of charge to subscribers. Address changes should be immediately reported to the affiliates and to the managing editor. Subscribers who do not receive the journal in the relevant time period should contact the managing editor. All published volumes in full text can be reached free of charge through the website www.oftalmoloji.org. Requests for subscription should be addressed to the Turkish Ophthalmological Association.

Manuscripts can only be submitted electronically through the Journal Agent website (http://journalagent.com/tjo/) after creating an account. This system allows online submission and review.

Membership Procedures

Turkish Ophthalmological Association
Bank Account: Yapı Kredi Bankası, Şehremini Şubesi 65774842
IBAN: TR10 0006 7010 0000 0065 7748 42
Annual Subscription: Domestic: 100.-TL (Tax Incl)
Abroad: 100 USD (Tax Incl.)

Correspondence Address

Editor-in-Chief, Murat Irkeç, MD, Professor in Ophthalmology
Hacettepe University Faculty of Medicine, Department of Ophthalmology
06100 Sıhhiye-Ankara-Turkey
Phone: +90 212 801 44 36/37 Fax: +90 212 801 44 39
E-mail: mirkec@hacettepe.edu.tr

Secretary, Arzu Sevdasız

E-mail: dergi@oftalmoloji.org - sekreter@oftalmoloji.org
Address: Avrupa Konutları Kale, Maltepe Mah. Yedikule Çırpıcı Yolu Sk. 9. Blok No: 2 Kat:1 Ofis:1 Zeytinburnu-İstanbul-Turkey
Phone: +90 212 801 44 36/37 Fax: +90 212 801 44 39
Web Page: www.oftalmoloji.org

Permissions

Requests for permission to reproduce published material should be sent to the editorial office.
Editor-in-Chief: Murat İrkeç, MD, Professor in Ophthalmology
Address: Avrupa Konutları Kale, Maltepe Mah. Yedikule Çırpıcı Yolu Sk. 9. Blok No: 2 Kat:1 Ofis:1 Zeytinburnu-İstanbul-Turkey
Phone: +90 212 801 44 36/37 Fax: +90 212 801 44 39
Web Page: www.oftalmoloji.org
E-mail: dergi@oftalmoloji.org - sekreter@oftalmoloji.org

Advertisement

Applications for advertisement should be addressed to the editorial office.
Address: Avrupa Konutları Kale, Maltepe Mah. Yedikule Çırpıcı Yolu Sk. 9. Blok No: 2 Kat:1 Ofis:1 Zeytinburnu-İstanbul-Turkey
Phone: +90 212 801 44 36/37 Fax: +90 212 801 44 39
Web Page: www.oftalmoloji.org
E-mail: dergi@oftalmoloji.org - sekreter@oftalmoloji.org

Publisher Corresponding Address

Publisher: Erkan Mor
Galenos Yayınevi Tic. Ltd. Şti.
Address: Molla Gürani Mah. Kaçamak Sk. No: 21, 34093 Fındıkzade-İstanbul-Turkey
Phone: +90 212 621 99 25 Fax: +90 212 621 99 27
E-mail: info@galenos.com.tr

Instructions for Authors

Instructions for authors are published in the journal and on the website www.oftalmoloji.org

Material Disclaimer

The author(s) is (are) responsible for the articles published in the Turkish Journal of Ophthalmology.
The editor, editorial board and publisher do not accept any responsibility for the articles.

The journal is printed on acid-free paper.

TURKISH JOURNAL OF OPHTHALMOLOGY

TJO

www.oftalmoloji.org

INSTRUCTIONS TO AUTHORS

The Turkish Journal of Ophthalmology is an official peer-reviewed publication of the Turkish Ophthalmological Association. Accepted manuscripts are published in both Turkish and English languages.

Manuscripts written in Turkish should be in accordance with the Turkish Dictionary and Writing Guide ("Türkçe Sözlüğü ve Yazım Kılavuzu") of the Turkish Language Association. Turkish forms of ophthalmology-related terms should be checked in the TODNET Dictionary (http://www.todnet.org/sozluk/) and used accordingly.

The Turkish Journal of Ophthalmology does not charge any article submission or processing charges.

A manuscript will be considered only with the understanding that it is an original contribution that has not been published elsewhere.

Reviewed and accepted manuscripts are translated either from Turkish to English or from English to Turkish by the Journal through a professional translation service. Prior to printing, the translations are submitted to the authors for approval or correction requests, to be returned within 7 days. If no response is received from the corresponding author within this period, the translation is checked and approved by the editorial board.

The abbreviation of the Turkish Journal of Ophthalmology is TJO, however, it should be denoted as Turk J Ophthalmol when referenced. In the international index and database, the name of the journal has been registered as Turkish Journal of Ophthalmology and abbreviated as Turk J Ophthalmol.

The scientific and ethical liability of the manuscripts belongs to the authors and the copyright of the manuscripts belongs to the Turkish Journal of Ophthalmology. Authors are responsible for the contents of the manuscript and accuracy of the references.

All manuscripts submitted for publication must be accompanied by the Copyright Transfer Form. Once this form, signed by all the authors, has been submitted, it is understood that neither the manuscript nor the data it contains have been submitted elsewhere or previously published and authors declare the statement of scientific contributions and responsibilities of all authors.

All manuscripts submitted to the Turkish Journal of Ophthalmology are screened for plagiarism using the 'iThenticate' software. Results indicating plagiarism may result in manuscripts being returned or rejected.

Experimental, clinical and drug studies requiring approval by an ethics committee must be submitted to the Turkish Journal of Ophthalmology with an ethics committee approval report confirming that the study was conducted in accordance with international agreements and the Declaration of Helsinki (revised 2013) (https://www.wma.net/policies-post/wma-declaration-of-helsinki-ethical-principles-for-medical-research-involving-human-subjects/). The approval of the ethics committee and the fact that informed consent was given by the patients should be indicated in the Materials and Methods section. In experimental animal studies, the authors should indicate that the procedures followed were in accordance with animal rights as per the Guide for the Care and Use of Laboratory Animals (http://oacu.od.nih.gov/regs/guide/guide.pdf) and they should obtain animal ethics committee approval.

Authors must provide disclosure/acknowledgment of financial or material support, if any was received, for the current study.

If the article includes any direct or indirect commercial links or if any institution provided material support to the study, authors must state in the cover letter that they have no relationship with the commercial product, drug, pharmaceutical company, etc. concerned; or specify the type of relationship (consultant, other agreements), if any.

Authors must provide a statement on the absence of conflicts of interest among the authors and provide authorship contributions.

The Turkish Journal of Ophthalmology is an independent international journal based on single-blind peer-review principles. The manuscript is assigned to the Editor-in-Chief, who reviews the manuscript and makes an initial decision based on manuscript quality and editorial priorities. Manuscripts that pass initial evaluation are sent for external peer review, and the Editor-in-Chief assigns an Associate Editor. The Associate Editor sends the manuscript to three reviewers (internal and/or external reviewers). The reviewers must review the manuscript within 21 days. The Associate Editor recommends a decision based on the reviewers' recommendations and returns the manuscript to the Editor-in-Chief. The Editor-in-Chief makes a final decision based on editorial priorities, manuscript quality, and reviewer recommendations. If there are any conflicting recommendations from reviewers, the Editor-in-Chief can assign a new reviewer.

The scientific board guiding the selection of the papers to be published in the Journal consists of elected experts of the Journal and if necessary, selected from national and international authorities. The Editor-in-Chief, Associate Editors, biostatistics expert and English language consultant may make minor corrections to accepted manuscripts that do not change the main text of the paper.

In case of any suspicion or claim regarding scientific shortcomings or ethical infringement, the Journal reserves the right to submit the manuscript to the supporting institutions or other authorities for investigation. The Journal accepts the responsibility of initiating action but does not undertake any responsibility for an actual investigation or any power of decision.

The Editorial Policies and General Guidelines for manuscript preparation specified below are based on "Recommendations for the Conduct, Reporting, Editing, and Publication of Scholarly Work in Medical Journals (ICMJE Recommendations)" by the International Committee of Medical Journal Editors (2016, archived at http://www.icmje.org/).

Preparation of research articles, systematic reviews and meta-analyses must comply with study design guidelines:

CONSORT statement for randomized controlled trials (Moher D, Schultz KF, Altman D, for the CONSORT Group. The CONSORT statement revised recommendations for improving the quality of reports of parallel group randomized trials. JAMA 2001; 285: 1987-91) (http://www.consort-statement.org/);

PRISMA statement of preferred reporting items for systematic reviews and meta-analyses (Moher D, Liberati A, Tetzlaff J, Altman DG, The PRISMA Group. Preferred Reporting Items for Systematic Reviews and Meta-Analyses: The PRISMA Statement. PLoS Med 2009; 6(7): e1000097.) (http://www.prisma-statement.org/);

STARD checklist for the reporting of studies of diagnostic accuracy (Bossuyt PM, Reitsma JB, Bruns DE, Gatsonis CA, Glasziou PP, Irwig LM, et al., for the STARD Group. Towards complete and accurate reporting of studies of diagnostic accuracy: the STARD initiative. Ann Intern Med 2003;138:40-4.) (http://www.stard-statement.org/);

STROBE statement, a checklist of items that should be included in reports of observational studies (http://www.strobe-statement.org/);

MOOSE guidelines for meta-analysis and systemic reviews of observational studies (Stroup DF, Berlin JA, Morton SC, et al. Meta-analysis of observational studies in epidemiology: a proposal for reporting Meta-analysis of observational Studies in Epidemiology (MOOSE) group. JAMA 2000; 283: 2008-12).

GENERAL GUIDELINES

Manuscripts can only be submitted electronically through the Journal Agent website (http://journalagent.com/tjo/) after creating an account. This system allows online submission and review.

The manuscripts are archived according to ICMJE, Index Medicus (Medline/PubMed) and Ulakbim-Turkish Medicine Index Rules.

Format: Manuscripts should be prepared using Microsoft Word, size A4 with 2.5 cm margins on all sides, 12 pt Arial font and 1.5 line spacing.

Abbreviations: Abbreviations should be defined at first mention and used consistently thereafter. Internationally accepted abbreviations should be used; refer to scientific writing guides as necessary.

Cover letter: The cover letter should include statements about manuscript type, single-journal submission affirmation, conflict of interest statement, sources of outside funding, equipment (if applicable), approval of language for articles in English and approval of statistical analysis for original research articles.

REFERENCES

Authors are solely responsible for the accuracy of all references.

In-text citations: References should be indicated as a superscript immediately after the period/full stop of the relevant sentence. If the author(s) of a reference is/are indicated at the beginning of the sentence, this reference should be written as a superscript immediately after the author's name. If relevant research has been conducted in Turkey or by Turkish investigators, these studies should be given priority while citing the literature.

Presentations presented in congresses, unpublished manuscripts, theses, Internet addresses, and personal interviews or experiences should not be indicated as references. If such references are used, they should be indicated in parentheses at the end of the relevant sentence in the text, without reference number and written in full, in order to clarify their nature.

References section: References should be numbered consecutively in the order in which they are first mentioned in the text. All authors should be listed regardless of number. The titles of journals should be abbreviated according to the style used in the Index Medicus.

Reference Format

Journal: Last name(s) of the author(s) and initials, article title, publication title and its original abbreviation, publication date, volume, the inclusive page numbers. Example: Collin JR, Rathbun JE. Involutional entropion: a review with evaluation of

a procedure. Arch Ophthalmol. 1978;96:1058-1064.
Book: Last name(s) of the author(s) and initials, chapter title, book editors, book title, edition, place of publication, date of publication and inclusive page numbers of the extract cited.
Example: Herbert L. The Infectious Diseases (1st ed). Philadelphia; Mosby Harcourt; 1999:11;1-8.
Book Chapter: Last name(s) of the author(s) and initials, chapter title, book editors, book title, edition, place of publication, date of publication and inclusive page numbers of the cited piece.
Example: O'Brien TP, Green WR. Periocular Infections. In: Feigin RD, Cherry JD, eds. Textbook of Pediatric Infectious Diseases (4th ed). Philadelphia; W.B. Saunders Company;1998:1273-1278.
Books in which the editor and author are the same person: Last name(s) of the author(s) and initials, chapter title, book editors, book title, edition, place of publication, date of publication and inclusive page numbers of the cited piece.
Example: Solcia E, Capella C, Kloppel G. Tumors of the exocrine pancreas. In: Solcia E, Capella C, Kloppel G, eds. Tumors of the Pancreas. 2nd ed. Washington: Armed Forces Institute of Pathology; 1997:145-210.

TABLES, GRAPHICS, FIGURES, AND IMAGES

All visual materials together with their legends should be located on separate pages that follow the main text.
Images: Images (pictures) should be numbered and include a brief title. Permission to reproduce pictures that were published elsewhere must be included. All pictures should be of the highest quality possible, in
JPEG format, and at a minimum resolution of 300 dpi.
Tables, Graphics, Figures: All tables, graphics or figures should be enumerated according to their sequence within the text and a brief descriptive caption should be written. Any abbreviations used should be defined in the accompanying legend. Tables in particular should be explanatory and facilitate readers' understanding of the manuscript, and should not repeat data presented in the main text.

BIOSTATISTICS

To ensure controllability of the research findings, the study design, study sample, and the methodological approaches and applications should be explained and their sources should be presented.
The "P" value defined as the limit of significance along with appropriate indicators of measurement error and uncertainty (confidence interval, etc.) should be specified. Statistical terms, abbreviations and symbols used in the article should be described and the software used should be defined. Statistical terminology (random, significant, correlation, etc.) should not be used in non-statistical contexts.
All results of data and analysis should be presented in the Results section as tables, figures and graphics; biostatistical methods used and application details should be presented in the Materials and Methods section or under a separate title.

MANUSCRIPT TYPES

Original Articles

Clinical research should comprise clinical observation, new techniques or laboratories studies. Original research articles should include title, structured abstract, keywords relevant to the content of the article, introduction, materials and methods, results, discussion, study limitations, conclusion, references, tables/figures/images and acknowledgement sections. Title, abstract and key words should be written in both Turkish and English. The manuscript should be formatted in accordance with the above-mentioned guidelines and should not exceed sixteen A4 pages.
Title Page: This page should include the title of the manuscript, short title, name(s) of the authors and author information. The following descriptions should be stated in the given order:
1. Title of the manuscript (Turkish and English), as concise and explanatory as possible, including no abbreviations, up to 135 characters
2. Short title (Turkish and English), up to 60 characters
3. Name(s) and surname(s) of the author(s) (without abbreviations and academic titles) and affiliations
4. Name, address, e-mail, phone and fax number of the corresponding author
5. The place and date of scientific meeting in which the manuscript was presented and its abstract published in the abstract book, if applicable
Abstract: A summary of the manuscript should be written in both Turkish and English. References should not be cited in the abstract. Use of abbreviations should be avoided as much as possible; if any abbreviations are used, they must be taken into consideration independently of the abbreviations used in the text. For original articles, the structured abstract should include the following sub-headings:
Objectives: The aim of the study should be clearly stated.
Materials and Methods: The study and standard criteria used should be defined; it should also be indicated whether the study is randomized or not, whether it is retrospective or prospective, and the statistical methods applied should be indicated, if applicable.
Results: The detailed results of the study should be given and the statistical significance level should be indicated.
Conclusion: Should summarize the results of the study, the clinical applicability of the results should be defined, and the favorable and unfavorable aspects should be declared.
Keywords: A list of minimum 3, but no more than 5 key words must follow the abstract. Key words in English should be consistent with "Medical Subject Headings (MESH)" (www.nlm.nih.gov/mesh/MBrowser.html). Turkish key words should be direct translations of the terms in MESH.
Original research articles should have the following sections:
Introduction: Should consist of a brief explanation of the topic and indicate the objective of the study, supported by information from the literature.
Materials and Methods: The study plan should be clearly described, indicating whether the study is randomized or not, whether it is retrospective or prospective, the number of trials, the characteristics, and the statistical methods used.
Results: The results of the study should be stated, with tables/figures given in numerical order; the results should be evaluated according to the statistical analysis methods applied. See General Guidelines for details about the preparation of visual material.
Discussion: The study results should be discussed in terms of their favorable and unfavorable aspects and they should be compared with the literature. The conclusion of the study should be highlighted.
Study Limitations: Limitations of the study should be discussed. In addition, an evaluation of the implications of the obtained findings/results for future research should be outlined.
Conclusion: The conclusion of the study should be highlighted.
Acknowledgements: Any technical or financial support or editorial contributions (statistical analysis, English/Turkish evaluation) towards the study should appear at the end of the article.
References: Authors are responsible for the accuracy of the references. See General Guidelines for details about the usage and formatting required.

Case Reports

Case reports should present cases which are rarely seen, feature novelty in diagnosis and treatment, and contribute to our current knowledge. The first page should include the title in Turkish and English, an unstructured summary not exceeding 150 words, and key words. The main text should consist of introduction, case report, discussion and references. The entire text should not exceed 5 pages (A4, formatted as specified above).

Review Articles

Review articles can address any aspect of clinical or laboratory ophthalmology. Review articles must provide critical analyses of contemporary evidence and provide directions of current or future research. Most review articles are commissioned, but other review submissions are also welcome. Before sending a review, discussion with the editor is recommended.
Reviews articles analyze topics in depth, independently and objectively. The first chapter should include the title in Turkish and English, an unstructured summary and key words. Source of all citations should be indicated. The entire text should not exceed 25 pages (A4, formatted as specified above).

Letters to the Editor

Letters to the Editor should be short commentaries related to current developments in ophthalmology and their scientific and social aspects, or may be submitted to ask questions or offer further contributions in response to work that has been published in the Journal. Letters do not include a title or an abstract; they should not exceed 1,000 words and can have up to 5 references.

CORRESPONDENCE

All correspondence should be directed to the TJO editorial board:

Post: Turkish Ophthalmological Association
Adress: Avrupa Konutları Kale, Maltepe Mah. Yedikule Çırpıcı Yolu Sk. 9. Blok No: 2 Kat:1 Ofis:1 Zeytinburnu-İstanbul-Turkey
Phone: +90 212 801 44 36/37 Fax: +90 212 801 44 39
Web Page: www.oftalmoloji.org
E-mail: dergi@oftalmoloji.org / sekreter@oftalmoloji.org

TURKISH JOURNAL OF OPHTHALMOLOGY

TJO

www.oftalmoloji.org

CONTENTS

Original Articles

Review

Case Reports

TURKISH JOURNAL OF OPHTHALMOLOGY

TJO

www.oftalmoloji.org

EDITORIAL

2018 Issue 4 at a Glance:

This issue of our journal includes six original articles, a review, and four case reports we believe you will read with interest, selected from various areas of ophthalmology on topics concerning the cornea, contact lenses, glaucoma, the retina, and neuro-ophthalmology.

Keratoconus is a progressive, non-inflammatory degenerative disease in which the cornea gradually thins and becomes cone-shaped. Collagen cross-linking (CXL) is widely used to arrest progressive keratoconus. Küçümen et al. used the Ocular Response Analyzer (ORA) to assess corneal biomechanical changes after CXL in 35 eyes of 30 patients with progressive keratoconus and reported statistically insignificant increases in corneal hysteresis and corneal resistance factor and a decrease in central corneal thickness (see pages 160-165).

Çavdarlı and Topçu-Yılmaz determined that daily use of high oxygen permeable and low modulus silicone hydrogel spherical and toric soft contact lenses for 12 months caused no significant changes in corneal and anterior chamber parameters (see pages 166-170).

Gobeka et al. also utilized the ORA to compare corneal biomechanical parameters in both eyes of keratoconus patients who underwent unilateral penetrating keratoplasty (PKP). They reported that corneal hysteresis, corneal resistance factor, corneal-compensated intraocular pressure (IOP), Goldmann-correlated IOP, IOP measured by applanation, and central corneal thickness were significantly higher in the PKP eye than the fellow eye, with corneal biomechanical properties approaching normal values after PKP (see pages 171-177).

Optical coherence tomography (OCT) provides objective and reproducible measurements of the peripapillary retinal nerve fiber layer (RNFL) and the optic nerve head (ONH), and is among the main imaging modalities used to show glaucomatous structural damage for early diagnosis and progression monitoring. With the fovea-disc (FoDi) alignment software in the spectral domain OCT Spectralis (Heidelberg Engineering GmbH, Heidelberg, Germany), RNFL thickness is measured by automatically detecting the fovea and optical disc margins and delineating quadrants based on the anatomical axis connecting the ONH center and the fovea, thus eliminating rotational errors. Tuncer and Altuğ used this new FoDi software to investigate interindividual differences in the angle between the axis connecting the fovea center and optic disc center and the horizontal meridian through the OHN center in 260 eyes of 133 patients with suspected or diagnosed glaucoma. The angle of deviation of the fovea-disc axis from the horizontal axis (FoDi angle) ranged from -24.40° to +11.60°, with an average of -6.43±4.9°. The authors suggest that discrepancies between the anatomic axis and horizontal axis in glaucoma patients may affect RNFL thickness measurements and lead to errors in early glaucoma diagnosis (see pages 178-184).

Kıylıoğlu et al. describe a new pupillometry system they developed for evaluation of pupillary light reflexes. They demonstrated that pupil area can be accurately measured in video images obtained with infrared and white light reflected outside the pupil, and reported 87% and 86.8% reproducibility of the measurements for short (1 second) and long (2 second) stimuli, respectively. However, the authors emphasized that further development of the apparatus is necessary for it to be a cost-effective alternative (see pages 185-189).

Vascular endothelial growth factor A (VEGF-A) is the main mediator of angiogenesis and is associated with increased vascular permeability in vascular retinal diseases. Anti-VEGF agents block various types of VEGF when administered intravitreally, reduce the permeability of nascent vessel walls, and to lead to a reduction in edema of the retinal layers. Şahiner et al. applied aflibercept (0.5 mg/mL), bevacizumab (0.3125 mg/mL) and ranibizumab (0.125 mg/mL) to retinal pigment epithelium cell cultures isolated from the enucleated eyes of New Zealand white rabbits. After 72 hours of drug exposure, the treated cells and controls were compared in terms of viability, apoptosis, proliferation, and senescence. Cultures treated with aflibercept exhibited a decrease in apoptosis and increase in viability ($p<0.05$), while cultures treated with bevacizumab and ranibizumab showed significantly increased apoptosis and reduced viability compared to the control group ($p<0.05$). There were no differences between the groups in terms of proliferation or senescence ($p>0.05$) (see pages 190-195).

For this issue, Gábor Holló, who has numerous previous studies in the literature, prepared an extensive review encompassing current and potential future applications

TURKISH JOURNAL OF OPHTHALMOLOGY

TJO

www.oftalmoloji.org

EDITORIAL

of optical coherence tomography angiography (OCTA) in glaucoma. The principle of measurement in OCTA is based on split spectrum amplitude decomposition algorithm, which detects red blood cell motion independent of direction. Vascular dysfunction is common in glaucoma patients, and RNFL peripapillary vessel density (angioflow vessel density) and macular superficial perifoveal vessel density are measured using OCTA, with high reproducibility demonstrated in previous studies. Vessel density is the perfusion area expressed as the percentage of the area examined or of predetermined sectors in the retinal layer being investigated. Studies have shown a relationship between vessel density and glaucoma damage. In the future, OCTA will continue to be an exciting clinical research area used in the diagnosis and follow-up of glaucoma patients (see pages 196-201).

Sarcoidosis can affect multiple organs and is histologically characterized by non-caseified granulomas. In the first case report of this issue, Tanyıldız et al. diagnosed neurosarcoidosis in a young female patient with bilateral granulomatous anterior uveitis, vitritis, optic neuropathy, and unilateral macular ischemia based on the results of mediastinal lymph node biopsy, cranial magnetic resonance imaging, and lumbar puncture. She was successfully treated with high-dose intravenous followed by oral methylprednisolone, and methotrexate (see pages 202-205).

Papillophlebitis is a rare ocular disease of unknown etiology that is characterized by retinal hemorrhage, optic disc edema, and tortuosity of the retinal vessels. Unlike classic central retinal vein occlusion, it is seen in healthy patients younger than 50 years of age. Guillain-Barre syndrome (GBS), an immunologically mediated acute polyneuropathy that involves motor neurons and causes paralysis, is the most common cause of acute muscle weakness associated with peripheral neuropathy in adults. In the second case report, Çoban Karataş and Soylu discuss the clinical findings, diagnostic tests, and effectiveness of intravenous immunoglobulin therapy in a patient with papillophlebitis possibly associated with GBS (see pages 206-208).

Sympathetic ophthalmia (SO) is bilateral granulomatous inflammation of the uvea following trauma or surgery. Choroidal neovascular membrane (CNV) is a rare complication and can have a negative impact on vision. Saatçi et al. observed type 2 CNV on fundus fluorescein angiography (FFA) and OCT in a 38-year-old patient taking systemic steroid therapy for SO, and report favorable anatomic and functional outcomes after treatment with 5 injections of 2 mg intravitreal aflibercept (see pages 209-211).

In the final case report, Kahraman et al. present the clinical findings, FFA, and family screening results of a 49-year-old male patient with familial exudative vitreoretinopathy (AEVR) and discuss the case in the context of the literature. AEVR is a rare hereditary disease that affects retinal vascular development, and can manifest clinically with avascular peripheral retina, neovascularization, fibrosis, posterior pole traction, retinal folds, and retinal detachment. The authors emphasized the key importance of screening family members when diagnosing AEVR (see pages 212-214).

Respectfully on behalf of the Editorial Board,
Banu Bozkurt, MD

DOI: 10.4274/tjo.56750
Turk J Ophthalmol 2018;48:160-165

Original Article

Evaluation of Corneal Biomechanical Changes After Collagen Crosslinking in Patients with Progressive Keratoconus by Ocular Response Analyzer

Raciha Beril Küçümen*, Berna Şahan*, Canan Aslı Yıldırım**, Ferda Çiftçi*

*Yeditepe University Faculty of Medicine, Department of Ophthalmology, İstanbul, Turkey
**Dokuz Eylül University Faculty of Medicine, Department of Ophthalmology, İzmir, Turkey

Abstract

Objectives: To evaluate corneal biomechanics before and after collagen crosslinking (CXL) in patients with progressive keratoconus.

Materials and Methods: In this prospective study, CXL was performed under topical anesthesia after removal of the epithelium (epi-off technique) by applying ultraviolet A (UVA) light at a wavelength of 365 nm and power of 3 mW/cm^2 or 5.4 joule/cm^2. Isoosmolar 0.1% riboflavin solution was administered before and during UVA irradiation. In addition to ophthalmologic examination, ocular response analyzer measurements were performed pre- and postoperatively. Corneal hysteresis (CH), corneal resistance factor (CRF), corneal compensated intraocular pressure (IOPcc), Goldmann-correlated intraocular pressure (IOPg), and central corneal thickness (CCT) were recorded.

Results: The study included 35 eyes of 30 patients with progressive keratoconus. The mean age was 28.2±6.5 years and postoperative follow-up time was 20.2±14.7 months (range: 6-74 months). The mean CH was 8.60±1.23 mmHg preoperatively, 8.96±2.05 mmHg in the early postoperative period (1-6 months), (p=0.28) and 8.96±1.28 mmHg in the late postoperative period (10-29 months) (p=0.48). Mean CRF was 7.13±1.50 mmHg preoperatively, 8.48±2.16 mmHg in the early postoperative period (p=0.009), and 7.71±1.29 mmHg in the late postoperative period (p=0.40). Mean IOPcc was 12.78±2.34 mmHg preoperatively, 15.38±4.21 mmHg in the early postoperative period (p=0.12) and 13.68±3.61 mmHg in the late postoperative period (p=0.48). Mean IOPg was 9.56±2.73 mmHg preoperatively, 13.01±4.45 mmHg in the early postoperative period (p=0.046), and 10.86±3.47 mmHg in the late postoperative period (p=0.44). Mean CCT was 484.43±41.26 µm preoperatively, 474.16±64.74 µm in the early postoperative period (p=0.70), and 470.38±33.64 µm in the late postoperative period (p=0.71).

Conclusion: CXL is a treatment modality believed to affect corneal biomechanics in keratoconus, but the results of larger patient series with longer follow-up periods may enable a better evaluation.

Keywords: Keratoconus, collagen crosslinking, corneal biomechanics

Introduction

Keratoconus is a progressive, non-inflammatory degenerative disease in which the cornea gradually thins and becomes cone-shaped.[1,2] Decreased corneal stability leads to stromal thinning and protrusion. It causes irregular corneal astigmatism and myopia, thus reducing visual acuity. Visual impairment often appears in adolescence. Even in cases of bilateral involvement, the eyes are affected asymmetrically.[3] Although the prevalence of keratoconus varies depending on ethnic and geographical factors, it is reported as 50-600 per 100,000 in the general population.[4]

The course of keratoconus is highly variable and disease stage affects the treatment strategy. In the early stages, irregular astigmatism can be treated with hard or custom-made contact lenses.[5,6] Intracorneal ring segment implantation is another treatment option for patients who are averse to or cannot tolerate

Address for Correspondence: Raciha Beril Küçümen MD, Yeditepe University Faculty of Medicine, Department of Ophthalmology, İstanbul, Turkey
Phone: +90 216 369 14 01 E-mail: berilkucumen@hotmail.com **ORCID-ID:** orcid.org/0000-0002-6053-3947
Received: 16.02.2016 **Accepted:** 31.10.2016

wearing contact lenses, and it enables visual rehabilitation by correcting refraction.[6,7] Intracorneal rings are also thought to contribute to corneal stability by affecting the biomechanics of the cornea.[8,9] When these options are inadequate in patients with severe irregular astigmatism and stromal scarring, deep anterior lamellar keratoplasty or penetrating keratoplasty may be preferred.[4,10]

Collagen crosslinking (CXL) has gained attention in recent years as a treatment approach to keratoconus. It is universally accepted for the treatment of advanced keratoconus. CXL halts or delays the progression of the disease, thus reducing the need for lamellar or penetrating keratoplasty. In the corneal stroma, riboflavin (vitamin B2) and ultraviolet-A (UVA) undergo a photochemical reaction with environmental oxygen and generate free oxygen radicals. This photochemical reaction forms additional covalent bonds between the collagen fibrils in the stroma, thus reinforcing the structure of the corneal stroma. Therefore, CXL induces a process that influences and reshapes the biomechanics of the cornea.[11]

In this study, we aimed to use an ocular response analyzer (ORA, Ocular Response Analyzer, Reichert Ophthalmic Instruments, Corp., NY, USA) to examine eyes that underwent CXL treatment at our clinic due to progressive keratoconus, and evaluate the biomechanical changes that may occur in the cornea.

Materials and Methods

Thirty-five eyes of 30 patients who were diagnosed with progressive keratoconus at the Yeditepe University Eye Center between September 2011 and August 2015 were included in this prospective study. CXL treatment was planned for all patients; the research protocol was explained to all patients before the intervention and informed consent forms were obtained. The study was conducted in compliance with the Declaration of Helsinki principles and was approved by the hospital ethics committee. The patients underwent preoperative and postoperative examination including ophthalmologic examination, corneal topography using two different technologies, the GALILEI™ Dual Scheimpflug Analyzer (Ziemer Group AG, Switzerland) and the Wavelight Allegro Topolyzer (Alcon Laboratories, Inc., Fort Worth, TX, USA), and ORA measurement. The patients were clinically and topographically diagnosed with keratoconus based on clinical and biomicroscopic findings such as a scissoring reflex on retinoscopy, Munson's sign, thinning of the cornea, Vogt striae, and Fleischer rings, and keratoconus patterns and corneal index changes on corneal topography. An increase of more than 1.00 diopter (D) in the vertical keratometry value within the last 12 months and/or a 0.50 D increase in spherical refraction, and a 1.00 D increase in the cylindrical refraction value were accepted as criteria for progression.[11,12]

Study inclusion criteria were being 18-40 years of age, having no ocular pathology other than keratoconus, and having a minimum corneal thickness of 400 microns and progression of keratoconus in the last 12 months. Patients with herpetic keratitis, severe dry eye, blepharitis, corneal infection, corneal scarring, and/or a history of autoimmune disease and patients who had undergone ocular surgery were excluded from the study. None of the patients had a history of smoking or diabetes. Pregnant women and breastfeeding mothers were also not included in the study.

The ORA delivers a rapid air pulse to the cornea during measurement, similar to air-puff tonometers; it then makes calculations by eliminating the potential interference between the pressure and the force. The first recording is acquired as the air jet creates the first applanation in the cornea. As the air jet continues to exert pressure, the cornea becomes concave. The air pulse is discontinued within milliseconds (ms). The cornea flattens again with the decrease in force, and the second recording is made during the second applanation. The cornea then returns to its normal convex state. Measurements are taken from the 3.0 mm-diameter area of the central cornea. An electrooptic detector monitors the area for 20 ms. A graph is made from the recorded values (Graphic 1). The two peaks clearly visible at the top of the graph indicate the first and second applanations (P1 and P2). The viscoelastic nature of the cornea results in different pressure values at the applanations. The intersection points of the applied pressure and applanation pressure curves are identified, and the difference in height between them is defined as corneal hysteresis (CH) (Graphic 1). In other words, CH refers to the energy the cornea loses in order to return to its former state after being deformed by the airjet during ORA measurements. Another parameter provided by the ORA is corneal resistance factor (CRF). This parameter shows the total viscoelastic resistance of the cornea. The value is determined by calculating the linear function between the two applanation pressures (P1 and P2). The formula is defined as CRF=k1 x (P1-0.7xP2) + k2, where k1 and k2 are constants. Other ORA parameters are corneal compensated intraocular pressure (IOPcc), Goldmann-correlated intraocular pressure (IOPg), and central corneal thickness (CCT). The CCT measurement is taken after the ORA measurement with an ultrasonic pachymeter adapted to the device.

Surgical Technique

CXL was performed under sterile conditions and surgical microscopy. After applying topical anesthesia (2-3 drops of 0.5% proparacaine hydrochloride) to the target eye, the periorbital area and lids were cleaned with 10% povidone iodine, as in preparation

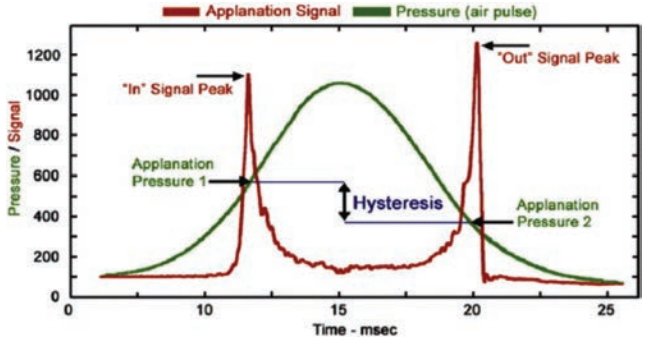

Graphic 1. The two peaks on the red line represent the first and second applanations (P1 and P2). The green curve shows the air pressure applied by the device. The difference in height between the two intersection points corresponds to the histeresis value in mmHg (translated from the manufacturer's user guide)

for refractive surgery. With a sterile drape, the eyelashes were drawn back, the eye was covered, and a blepharostat was placed. The ocular surface was irrigated with a balanced salt solution (BSS). Several measurements were taken from the cornea using an ultrasonic pachymeter (PacScan 300AP, Sonomed Inc., NY, USA) and the minimum corneal thickness of at least 400 µm was reconfirmed. The cornea was prepared by placing 20% alcohol in a 9 mm diameter ring centered on the cornea for 45 seconds. After rinsing the surface with ample BSS, the corneal epithelium was removed as a flap. A solution containing riboflavin (0.1% riboflavin, 20% dextran) was instilled every 3 minutes for the first half hour in accordance with the Dresden protocol.[16] During the second half hour, 365-nm UVA at a dose of 3 mW/cm^2 or 5.4 J/cm^2 was applied to the corneal apex from a distance of 5 cm using a CXL device (PESCHKE Trade CCL-VARIO Cross-linking). During irradiation, the riboflavin solution was instilled every 2.5 minutes and artificial tears (3 mg/mL hydroxypropylmethylcellulose, Tears Naturale® II, Alcon, Belgium) were instilled between drops of riboflavin in order to prevent dehydration of the cornea. Topical antibiotic (0.5% moxifloxacin, 4 times daily), topical corticosteroid (1% prednisolone acetate, 4 times daily), and artificial tear drops were prescribed postoperatively.

Statistical Analysis

In addition to ophthalmologic examination, the patients were evaluated with ORA before surgery, in the early postoperative period (1-6 months), and in the late postoperative period (10-29 months). ORA measurements were made between 10:00 and 12:00 in the morning. At least 3 measurements were taken from the patients and the most qualitative measurement with the highest waveform score was used for evaluation. In the statistical analysis, the pre-CXL and post-CXL CH, CRF, IOPg, IOPcc, and CCT values were evaluated using a dependent paired-samples t-test in SPSS (Statistical Package for the Social Sciences Inc., Chicago, IL, USA) software. Change in a parameter with a p value of <0.05 was considered a significant difference.

Results

Thirty-five eyes of 30 patients were included in the study. Twenty-two patients (73%) were male and 8 (27%) were female. The mean age was 28.2±6.5 years (18-38 years). The mean postoperative follow-up period was 20.2±4.7 months (10-29 months) (Table 1). The results of 3 male patients (4 eyes) and 1 female patient (1 eye) who were lost to follow-up after the first month were excluded from the statistical analysis.

Table 2 shows the uncorrected and best corrected visual acuity, refraction, and topographic results of the patients before and after surgery. Significant improvement was found in all parameters (p<0.05).

Preoperative and early and late postoperative ORA parameters are shown in Table 3.

The mean CH was found to be higher in the early and late postoperative periods compared to the preoperative value, but the difference was not statistically significant (p_1=0.25, p_2=0.48). The mean CFR was significantly higher in the early postoperative period compared to the preoperative value (p_1=0.009), but there was no statistically significant increase in the late postoperative period compared to the preoperative value (p_2=0.40). There was a significant increase in mean IOPg in the early postoperative period compared to the preoperative value (p_1=0.46). The late postoperative mean IOPg was higher than the preoperative value but the difference was not statistically significant (p_2=0.44). Mean IOPcc was higher in the early and late postoperative period than the preoperative value, but this difference was also not statistically significant (p_1=0.12; p_2=0.48). Early and late postoperative mean CCT was thinner in the early and late postoperative period compared to the preoperatively, but the difference was not statistically significant (p_1=0.70; p_2=0.71). There was no significant difference between the early and late postoperative period means of ORA parameters (CH, CRF, IOPg, IOPcc, CCT) (Table 3, p_3 values).

Discussion

In recent years, it has been reported that CXL therapy slows, stops, and even reverses keratoconus.[17,18,19] In vitro studies

Table 1. Demographic characteristics of the patients

	Patients (n=30)
Sex	8 female (27%) 22 male (73%)
Age distribution (years) 18-28 years 29-38 years	 23 patients (76.6%) 7 patients (23.3%)
Mean age, years (mean ± SD)	28.2±6.5
Mean follow-up time, months (mean ± SD)	20.2±4.7

SD: Standard deviation

Table 2. Patients' preoperative and late postoperative visual acuity, refraction, and topographic findings

Parameter	Preoperative (n=30)	Late postoperative period (n=30)	p
Corrected VA (decimal)	0.27±0.26	0.34±0.26	p<0.05
BCVA (decimal)	0.49±0.29	0.66±0.26	p<0.05
Refraction (spheric equivalent) (diopters)	-2.67±2.31	-1.781±1.68	p<0.05
Astigmatism (diopters)	-3.04±1.48	-2.31±1.24	p<0.05
$SimK_{avg}$ (diopters)	48.16±3.83	45.96±2.86	p<0.05
$SimK_s$ (diopters)	49.74±4.56	48.03±2.96	p<0.05

VA: Visual acuity, BCVA: Best corrected visual acuity, $SimK_{avg}$: Simulated keratometric average measured via topography, $SimK_s$: Simulated vertical keratometric value measured via topography

Table 3. Preoperative, early postoperative, and late postoperative ocular response analyzer results of patients who underwent collagen crosslinking therapy

Parameter	Preoperative (n=30)	Early postoperative period (n=30)	Late postoperative period (n=30)	p_1	p_2	p_3
CH (mmHg)	8.60±1.23	8.96±2.05	8.96±1.28	0.28	0.48	0.85
CRF (mmHg)	7.13±1.50	8.48±2.16	7.71±1.29	0.009	0.40	0.67
IOPg (mmHg)	9.56±2.73	13.01±4.45	10.86±3.47	0.046	0.44	0.60
IOPcc (mmHg)	12.78±2.34	15.38±4.21	13.68±3.61	0.12	0.48	0.63
CCT (micron)	484.43±41.26	474.16±64.74	470.38±33.64	0.70	0.71	0.51

CH: Corneal hysteresis, CRF: Corneal resistance factor, IOPg: Goldmann intraocular pressure, IOPcc: Corneal compensated intraocular pressure, CCT: Central corneal thickness, p_1: Statistical comparison of preoperative and early postoperative means ($p<0.05$ was accepted as significant), p_2: Statistical comparison of preoperative and late postoperative means ($p<0.05$ was accepted as significant), p_3: Statistical comparison of early and late postoperative means ($p<0.05$ was accepted as significant)

have demonstrated that the treatment increases the number of crosslinks in the stroma and thus enhances the biomechanical resistance of the cornea.[20,21] In a 2003 in vitro study conducted with a strip extensometer, Wollensak et al.[22] experimentally demonstrated that Young's modulus, which indicates the biomechanical rigidity of the cornea, increased 4.5 times in the human cornea and 1.8 times in the porcine cornea after CXL. However, this method is not suitable for clinical use because it is done with stripped corneal tissue.

Devices that assess corneal biomechanics in vivo are the ORA, the Corvis tonometer (Corvis® ST OCULUS Optikgeräte GmbH, Wetzlar, Germany), and applanation resonance technology.[23,24] The ORA is most commonly used in the clinic for evaluating corneal biomechanics, and there are many studies based on ORA results after various ocular pathologies and eye surgeries.[9,13,14,15,25,26,27,28] ORA studies performed in keratoconus have reported lower CH and CRF parameters compared with normal eyes.[16] Following corneal transplantation in eyes with advanced keratoconus, CH and CRF were increased but were found to be lower compared to normal eyes.[10]

In our study, mean CH was increased in the early and late post-CXL periods compared to the preoperative level, but the difference was not statistically significant. On the other hand, mean CRF, which is considered an important parameter in keratoconus, has been found to be significantly increased in the early post-CXL period.[29] Mean CRF also increased in the late post-CXL period compared to the preoperative period, but the change was not statistically significant.

The low IOP measurements in eyes with keratoconus are attributed to low corneal rigidity and corneal thinning.[30] In our study, we observed increases in both mean IOPg and IOPcc in the early and late postoperative periods after CXL. However, only the increase in IOPg seen in the early postoperative period was statistically significant. Mean CCT showed statistically insignificant thinning in the early and late post-CXL periods. This thinning may be explained by the collagen fibers becoming more compact due to the increased crosslinkage in the stroma and scar formation.[12,30]

ORA studies performed in eyes with keratoconus following CXL report different results regarding biomechanical changes. Statistically insignificant increases in CH and CRF values were reported at 6 months after treatment in 2 studies and at 1 year after treatment in another.[31,32,33] Çağıl et al.[12] also found a nonsignificant increase in CH or CRF values at postoperative 1 and 6 months, but observed a significant decrease in CCT. Vinciguerra et al.[19] reported significant increases in CH and CRF values at postoperative 1 month. However, they found no significant differences at postoperative 6 and 12 months compared to the preoperative values, and reported statistically insignificant reduction in CCT at postoperative 12 months. Greenstein et al.[34] also found a significant increase in CRF in 1 and 3 months, but found no significant difference at 1 year. While our results are consistent with the literature, the small differences among these studies are also noteworthy.

CXL therapy aims to increase the rigidity and resistance of the cornea. An increase in the values of parameters that measure corneal biomechanics is expected after CXL. Therefore, theoretically, a statistically significant increase would be expected after CXL in the biomechanical indicators assessed by the ORA device, especially the CH and CRF values. In our study, we observed that two of the ORA parameters (CH and IOPg) increased significantly in the early post-CXL period, while four of them (CH, CRF, IOPg, IOPcc) increased in the late period, albeit statistically insignificantly. The fact that our results are largely statistically insignificant may be due to various reasons. The first reason is the low number of patients, which is the main limitation of our study. The second may be the collagen lamellae becoming compact after CXL. As the cornea becomes thinner, the measurements decrease. In the present study, mean CCT measurements showed reductions of 10 µm in the early postoperative period and 14 µm in the late postoperative period, which may have caused the parametric values to be lower than expected. Another reason may be that each eye with keratoconus has different configuration, pachymetric, topographic, and therefore biomechanical properties. It is argued that because the cornea is not homogeneous, the ORA device may not be technologically sufficient for measurements. Other studies have similarly addressed the possibility of optical irregularities in ectatic corneas obscuring actual biomechanical changes by altering ORA signals.[35,36] With time, the development of more precise versions and/or new devices may yield more meaningful results.

Conclusion

In summary, CXL is a promising new treatment modality for keratoconus patients and may affect corneal biomechanics. Larger patient series and more advanced technologies are needed to fully understand corneal biomechanics and to quantitatively and precisely assess them. Devices that can accurately measure these changes and are suitable for clinical use have not yet been developed, including the ORA. To understand the mechanism of action of this therapy on the cornea, there is a need for multicenter, randomized, prospective studies including large patient populations with long postoperative follow-up periods, which will provide more statistically valuable results.

Ethics

Ethics Committee Approval: Yeditepe University Clinical Reserach Ethics Committee, approval number: 826.

Informed Consent: Have been taken.

Peer-review: Externally and internally peer-reviewed.

Authorship Contributions

Surgical and Medical Practices: Raciha Beril Küçümen, Canan Aslı Yıldırım, Concept: Raciha Beril Küçümen, Design: Raciha Beril Küçümen, Ferda Çiftçi, Data Collection or Processing: Raciha Beril Küçümen, Berna Şahan Analysis or Interpretation: Raciha Beril Küçümen, Berna Şahan, Literature Search: Berna Şahan, Writing: Raciha Beril Küçümen, Berna Şahan.

Conflict of Interest: No conflict of interest was declared by the authors.

Financial Disclosure: The authors declared that this study received no financial support.

References

1. Rabinowitz YS. Keratoconus. Surv Ophthalmol. 1998;42:297-319.
2. Zadnik K, Barr JT, Edrington TB, Everett DF, Jameson M, McMahon TT, Shin JA, Sterling JL, Wagner H, Gordon MO. Baseline findings in the Collaborative Longitudinal Evaluation of Keratoconus (CLEK) Study. Invest Ophthalmol Vis Sci. 1998;39:2537-2546.
3. Kymes SM, Walline JJ, Zadnik K, Sterling J, Gordon MO; Collaborative Longitudinal Evaluation of Keratoconus Study Group. Changes in the quality-of-life of people with keratoconus. Am J Ophthalmol. 2008;145:611-617.
4. Maeno A, Naor J, Lee HM, Hunter WS, Rootman DS. Three decades of corneal transplantation: indications and patient characteristics. Cornea. 2000;19:7-11.
5. Tan DT, Por YM. Current treatment options for corneal ectasia. Curr Opin Ophthalmol. 2007;18:284-289.
6. Küçümen RB, Başar D, Alimgil ML. Keratokonusta femtosaniye laser yardımıyla kornea içi halka (Keraring) takılması. Turk J Ophthalmol. 2009;39:96-102.
7. Colin J, Cochener B, Savary G, Malet F. Correcting keratoconus with intracorneal rings. J Cataract Refract Surg. 2000;26:1117-1122.
8. Miralles MG, Martínez CP, Pascual FP. Biomechanical corneal response measurement after manula insertion of intrastromal rings in patients with keratoconus. J Emmetropia. 2010;1:206-212.
9. Gorgun E, Kucumen RB, Yenerel NM. Influence of intrastromal corneal ring segment implantation on corneal biomechanical parameters in keratoconic eyes. Jpn J Ophthalmol. 2011;55:467-471.
10. Yenerel NM, Kucumen RB, Gorgun E. Changes in corneal biomechanics in patients with keratoconus after penetrating keratoplasty. Cornea. 2010;29:1247-1251.
11. Sorkin N, Varssano D. Corneal collagen crosslinking: a systematic review. Ophthalmologica. 2014;232:10-27.
12. Çağıl N, Saraç Ö, Akçay E, Aksoy B, Uğurlu N, Ayan M. Keratokonus hastalarında korneal kollajen çapraz bağlama tedavisinin kısa dönemde kornea biyomekaniği üzerine etkileri. MN Oftalmoloji. 2014;21:152-156.
13. Luce DA. Determining in vivo biomechanical properties of the cornea with an ocular response analyzer. J Cataract Refract Surg. 2005;31:156-162.
14. Medeiros FA, Weinreb RN. Evaluation of the influence of corneal biomechanical properties on intraocular pressure measurements using the ocular response analyzer. J Glaucoma. 2006;15:364-370.
15. Küçümen RB, Yenerel NM, Görgün E, Kohen MC, Başar D, Alimgil ME. Evaluation of changes in corneal biomechanical properties by Ocular Response Analyzer after femtosecond laser assisted LASIK. Turk J Ophtalmol. 2009;39:250-255.
16. Terai N, Raiskup F, Haustein M, Pillunat LE, Spoerl E. Identification of biomechanical properties of the cornea: the ocular response analyzer. Curr Eye Res. 2012;37:553-562.
17. Wollensak G, Spoerl E, Seiler T. Riboflavin/ultraviolet-a-induced collagen crosslinking for the treatment of keratoconus. Am J Ophthalmol. 2003;135: 620-627.
18. Goldich Y, Marcovich AL, Barkana Y, Mandel Y, Hirsh A, Morad Y, Avni I, Zadok D. Clinical and corneal biomechanical changes after collagen cross-linking with riboflavin and UV irradiation in patients with progressive keratoconus: results after 2 years of follow-up. Cornea. 2012;31:609-614.
19. Vinciguerra P, Albè E, Mahmoud AM, Trazza S, Hafezi F, Roberts CJ. Intra- and postoperative variation in ocular response analyzer parameters in keratoconic eyes after corneal cross-linking. J Refract Surg. 2010;26:669-676.
20. Spoerl E, Huhle M, Seiler T. Induction of cross-links in corneal tissue. Exp Eye Res. 1998;66:97-103.
21. Beshtawi IM, O'Donnell C, Radhakrishnan H. Biomechanical properties of corneal tissue after ultraviolet-A-riboflavin crosslinking. J Cataract Refract Surg. 2013;39:451-462.
22. Wollensak G, Spoerl E, Seiler T. Stress-strain measurements of human and porcine corneas after riboflavin-ultraviolet-A-induced cross-linking. J Cataract Refract Surg. 2003;29:1780-1785.
23. Ji C, Yu J, Li T, Tian L, Huang Y, Wang Y, Zheng Y. Dynamic curvature topography for evaluating the anterior corneal surface change with Corvis ST. Biomed Eng Online. 2015;14:53.
24. Beckman Rehnman J, Behndig A, Hallberg P, Lindén C. Increased corneal hysteresis after corneal collagen crosslinking: a study based on applanation resonance technology. JAMA Ophthalmol. 2014;132:1426-1432.
25. Kucumen RB, Yenerel NM, Gorgun E, Kulacoglu DN, Oncel B, Kohen MC, Alimgil ML. Corneal biomechanical properties and intraocular pressure changes after phacoemulsification and intraocular lens implantation. J Cataract RefractSurg. 2008;34:2096-2098.
26. Yenerel NM, Gorgun E, Kucumen RB, Oral D, Dinc UA, Ciftci F. Corneal biomechanical properties of patients with pseudoexfoliation syndrome. Cornea. 2011;30:983-986.
27. Abitbol O, Bouden J, Doan S, Hoang-Xuan T, Gatinel D. Corneal hysteresis measured with the Ocular Response Analyzer in normal and glaucomatous eyes. Acta Ophthalmol. 2010;88:116-119.
28. Mansouri K, Leite MT, Weinreb RN, Tafreshi A, Zangwill LM, Medeiros FA. Association between corneal biomechanical properties and glaucoma severity. Am J Ophthalmol. 2012;153:419-427.
29. Galletti JG, Pförtner T, Bonthoux FF. Improved keratoconus detection by ocular response analyzer testing after consideration of corneal thickness as a confounding factor. J Refract Surg. 2012;28:202-208.
30. Kasumovic SS, Mavija M, Kasumovic A, Lepara O, Duric-Colic B, Cabric E, Muhamedagic L, Sakovic-Racic A, Jankov M. Intraocular Pressure Measurements Referring to the Corneal Thickness in Keratoconic Eyes

After Corneal Crosslinking with Riboflavin and Ultraviolet A. Med Arch. 2015;69:334-338.
31. Sedaghat M, Naderi M, Zarei-Ghanavati M. Biomechanical parameters of the cornea after collagen crosslinking measured by waveform analysis. J Cataract Refract Surg. 2010;36:1728-1731.
32. De Bernardo M, Capasso L, Tortori A, Lanza M, Caliendo L, Rosa N. Trans epithelial corneal collagen crosslinking for progressive keratoconus: 6 months follow up. Cont Lens Anterior Eye. 2014;37:438-441.
33. Spoerl E, Terai N, Scholz F, Raiskup F, Pillunat LE. Detection of biomechanical changes after corneal cross-linking using Ocular Response Analyzer software. J Refract Surg. 2011;27:452-457.
34. Greenstein SA, Fry KL, Hersh PS. In vivo biomechanical changes after corneal collagen cross-linking for keratoconus and corneal ectasia: 1-year analysis of a randomized, controlled, clinical trial. Cornea. 2012;31:21-25.
35. Shah S, Laiquzzaman M, Cunliffe I, Mantry S. The use of the Reichert ocular response analyser to establish the relationship between ocular hysteresis, corneal resistance factor and central corneal thickness in normal eyes. Cont Lens Anterior Eye. 2006;29:257-262.
36. Vinciguerra P, Albè E, Trazza S, Rosetta P, Vinciguerra R, Seiler T, Epstein D. Refractive, topographic, tomographic, and aberrometric analysis of keratoconic eyes undergoing corneal cross-linking. Ophthalmology. 2009;116:369-378.

DOI: 10.4274/tjo.53486
Turk J Ophthalmol 2018;48:166-170

Original Article

Does Long-term Soft Contact Lens Wear Affect Corneal and Anterior Chamber Parameters?

Cemal Çavdarlı, Pınar Topçu-Yılmaz
University of Health Sciences, Ankara Numune Training and Research Hospital, Ophthalmology Clinic, Ankara, Turkey

Abstract

Objectives: To assess the long-term effects of soft contact lenses (SCL) on the cornea and anterior chamber by topography.

Materials and Methods: Thirty-nine eyes of 22 healthy patients were included in this prospective study. Changes in corneal and anterior chamber parameters before and after 12 months of daily SCL use (Air Optix Aqua, Air Optix Aqua for Astigmatism, Acuvue Oasys and Acuvue Oasys for Astigmatism) were evaluated with Pentacam (Oculus, Germany).

Results: Best corrected visual acuity with toric SCL was significantly better compared to spectacles in the toric SCL group (0.98±0.34 vs 0.94±0.72, p=0.004). None of the corneal (horizontal and vertical keratometry, corneal volume, anterior and posterior corneal astigmatism, corneal pachymetry of apex and thinnest location) and anterior chamber (anterior chamber depth, volume and angle) parameters showed a statistically significant change after long-term daily wear of SCLs.

Conclusion: The results of this study revealed that long-term wear of current high oxygen permeable and relatively low modulus silicone hydrogel SCLs does not impact cornea and anterior chamber morphology or volumetric parameters. Furthermore, toric silicone hydrogel SCLs can provide better visual performance than spectacles.

Keywords: Soft, contact lens, cornea, anterior chamber, topography

Introduction

Soft contact lenses (SCL) are currently one of the most popular modes of refractive error correction. With the advances in contact lens technology, they have become more comfortable and safer; however, they still carry the risks associated with modification of corneal morphology. The primary goal in SCL design is to create a contact lens which provides biocompatibility with both the cornea and the surrounding ocular environment (e.g. tear film, conjunctiva, eyelids). The mechanical properties of the SCL (edge design, diameter, modulus) should not increase corneal and conjunctival epithelial irritation and should allow maximum tear circulation.[1]

Despite the developments in contact lens technology, the alterations in corneal metabolism and the mechanical forces associated with contact lens wear can affect the anterior shape of the cornea and result in central corneal steepening or flattening, loss of radial symmetry, and changes in astigmatism or optical higher order aberrations.[2,3,4,5,6] Significant improvements in silicone hydrogel lenses have made them the first choice for new contact lens wearers.[7] Silicone hydrogel lenses have eliminated corneal hypoxia.[8] However, despite their high oxygen transmission levels, SCL-related central and peripheral corneal swelling which results in increased central corneal thickness and significant thinning of the central corneal epithelium has been reported.[9,10]

Both the anterior corneal surface and corneal thickness are critical variables to consider before any clinical intervention, particularly refractive surgery. Furthermore, changes in the posterior corneal surface are useful in monitoring corneal pathologies and in the early detection of corneal ectatic disorders.[11] Thus, monitoring changes in the anterior and posterior cornea is important in contact lens wearers who are candidates for keratorefractive surgery.

The purpose of this study was to assess changes in corneal and anterior chamber parameters after 12 months of SCL wear.

Address for Correspondence: Cemal Çavdarlı MD, University of Health Sciences, Ankara Numune Training and Research Hospital, Ophthalmology Clinic, Ankara, Turkey Phone: +90 312 430 57 46 E-mail: ccavdarli@gmail.com **ORCID-ID:** orcid.org/0000-0001-8379-4384

Received: 05.09.2017 **Accepted:** 04.01.2018

Materials and Methods

Thirty-nine eyes of 22 individuals who attended the contact lens clinic of Ankara Numune Training and Research Hospital between January 2014 and January 2016 were included in this prospective study. Patients with known history of ocular and/or systemic diseases, previous ocular surgery, prior contact lens use, ocular or systemic medication use, and more than 3.5 diopters of cylindrical and/or 6 diopters of spherical refractive error were not included. All subjects underwent complete ophthalmologic evaluation to ensure the presence of Snellen best corrected visual acuity of 20/25 or better, normal anterior and posterior segment biomicroscopy, normal tear film functions (Schirmer test >15 mm/5 minute and tear break-up time ≥10 second) and normal intraocular pressure. Informed consent was obtained from all subjects and the study was carried out with approval from the ethics committee of Ankara Numune Training and Research Hospital.

Refractive and topometric maps obtained with Pentacam (Oculus, Germany) were used to evaluate anterior and posterior corneal axial curvature, corneal volume, central corneal thickness, corneal thickness at the thinnest point, anterior chamber depth, anterior chamber angle, and anterior chamber volume before contact lens fitting. All measurements were performed by a single author (C.C.) between 10:00 and 12:00 a.m. to avoid diurnal variations. Only reliable scans that marked "quality specification" of Pentacam were included in analysis.

After the completion of Pentacam measurements, each patient was fitted with a suitable Lotrafilcon B (Air Optix Aqua, Air Optix Aqua for Astigmatism, CIBA Vision, Duluth, USA) or Senofilcon A (Acuvue Oasys, Acuvue Oasys for Astigmatism, Johnson&Johnson, Jacksonville, USA) SCL according to their manifest refraction. Subjects were instructed to wear these contact lenses in daily wear mode before returning for the final visit at 12 months. The cornea and anterior chamber were re-evaluated with Pentacam (Oculus, Germany) at the final visit, at least 1 hour after contact lens removal to avoid lens-related mechanical changes. Subjects who wore their contact lenses regularly (>4 days/week) in daily wear mode were included in the final analysis.

Statistical Analysis

Statistical analyses were performed using SPSS version 13.0 (Chicago, IL, USA) software. Student's paired t-test was used to compare changes in visual acuity, keratometry, corneal volume, central corneal thickness, corneal thickness at thinnest point, anterior chamber depth, anterior chamber angle, and anterior chamber volume over time. P value less than 0.05 was considered to be statistically significant.

Results

Thirty-nine eyes of 22 patients were initially included in the study, but 2 of the subjects were excluded due to irregular SCL wear. Thus, the study was completed with a total of 37 eyes of 20 patients (12 female, 8 male). Mean age was 20.52±3.18 years (range 15-28 years). Nineteen eyes were fitted with spherical soft lenses and 18 eyes were fitted with toric soft lenses.

Best corrected distance visual acuity (BCVA) for patients fitted with spherical lenses was 20/20 at baseline and final examination. There was a statistically significant increase in the distance BCVA of toric lens wearers (0.94±0.72 vs 0.98±0.34, p=0.004) (Table 1), and the significance in the total group seems to originate from the toric group.

The corneal (keratometry, corneal volume, anterior and posterior astigmatism, corneal apex, and thinnest-point corneal pachymetry) and anterior chamber parameters (anterior chamber depth, anterior chamber volume, and chamber angle) as evaluated by Pentacam are summarized in Tables 2 and 3, respectively. None of these parameters showed a statistically significant change after long-term contact lens wear.

Discussion

Contact lenses are a popular mode of refractive error correction due to advantages such as a larger field of vision, better optical quality, and cosmetic appeal. However, they still have the disadvantage of interfering with normal corneal physiology and curvature.[11] The purpose of our study was to investigate the long-term effects of SCL wear on corneal and anterior chamber parameters measured by Pentacam. To our knowledge, this is the first prospective study to investigate long-term SCL-associated changes in the cornea (keratometry, corneal volume, central corneal thickness, corneal thickness at thinnest point) and the anterior chamber (anterior chamber depth, angle, and volume) with Pentacam. This device has been found to be highly reliable and showed excellent repeatability in previous studies.[12,13]

Snellen best corrected visual acuity of 20/20 was our targeted value for SCL wearers when prescribing contact lenses. Thus, some of the patients might have better visual acuity after SCL fitting. While we were unable to find a significant difference in the visual acuity of spherical lens wearers, a more detailed visual acuity study could also reveal significance in the spherical group. Visual performance in toric lens wearers was better with SCLs compared to spectacles. This result is in line with previous studies that have found improved visual quality and acuity with toric SCLs in low and moderate astigmatic eyes.[14,15] We believe that with a good SCL-cornea adaptation process, the mechanical properties of contact lenses and the toric designs result in fewer aberrations with toric lenses compared to glasses.

Several studies have investigated the changes in corneal shape and thickness associated with contact lens wear. However,

Table 1. Snellen best corrected visual acuity at baseline and after 12 months of contact lenses wear

Parameter	Lens type	Baseline	12 month	n	p[a]
Visual acuity	Total	0.97±0.06	0.99±0.02	37	**0.006**
	Spheric	1.0	1.0	19	-
	Toric	0.94±0.72	0.98±0.34	18	**0.004**

[a]Statistical significance with paired t-test (p<0.05)

the follow-up for most of these studies was very short. Liu and Pflugfelder[16] evaluated corneal thickness and topography in long-term contact lens wearers and healthy controls. They found that corneal thickness was significantly reduced by 30-50 µm in contact lens wearers. Furthermore, corneal curvature and surface irregularity were increased in eyes wearing contact lenses. Yeniad et al.[17] evaluated changes in corneal curvature and thickness after 1, 6, and 18 months of rigid gas-permeable and soft lens

Table 2. Evaluation of corneal parameters at baseline and 12-month follow-up

Corneal parameters	Lens type	Baseline	12 months	n	p[a]
Rh (mm)	Total	7.94±0.22	7.94±0.24	37	0.98
	Spheric	7.86±0.17	7.85±0.17	19	0.131
	Toric	8.02±0.23	8.05±0.25	18	0.288
Rv (mm)	Total	7.67±0.24	7.67±0.24	37	0.454
	Spheric	7.72±0.22	7.71±0.21	19	0.154
	Toric	7.62±0.26	7.63±0.25	18	0.968
Corneal volume (mm3)	Total	62.29±3.47	60.85±9.39	37	0.406
	Spheric	61.78±2.64	58.66±12.24	19	0.360
	Toric	62.82±4.19	63.17±4.12	18	0.116
Anterior astigmatism (diopters)	Total	1.58±1.07	1.57±1.07	37	0.802
	Spheric	0.84±0.38	0.85±0.34	19	0.778
	Toric	2.36±1.00	2.33±1.05	18	0.616
Posterior astigmatism (diopters)	Total	0.41±0.23	0.43±0.21	37	0.073
	Spheric	0.29±0.13	0.30±0.12	19	0.431
	Toric	0.53±0.26	0.57±0.19	18	0.111
Corneal thickness at the apex (µm)	Total	553.64±23.22	555.76±23.39	37	0.163
	Spheric	547.35±17.91	550.24±17.91	19	0.214
	Toric	560.31±26.25	561.63±27.45	18	0.214
Corneal thickness at thinnest point (µm)	Total	549.03±22.75	550.82±23.57	37	0.247
	Spheric	543.65±16.84	545±17.44	19	0.559
	Toric	554.75±27.09	557±27.96	18	0.293

Rh: Horizontal radius of cornea, Rv: Vertical radius of cornea, [a]Statistical significance with paired t-test ($p<0.05$)

Table 3. Evaluation of anterior chamber parameters at baseline and 12-month follow-up

	Lens type	Baseline	12 months	n	p[a]
Anterior chamber depth (mm)	Total	3.24±0.17	3.23±0.15	37	0.285
	Spheric	3.29±0.15	3.26±0.15	19	0.055
	Toric	3.19±0.17	3.20±0.15	18	0.532
Anterior chamber volume (mm^3)	Total	203.61±23.31	203.88±18.46	37	0.872
	Spheric	208.30±20.50	208.00±16.78	19	0.884
	Toric	198.62±25.67	199.50±19.67	18	0.759
Anterior chamber angle (°)	Total	40.012±5.553	41.157±5.502	37	0.175
	Spheric	40.35±6.20	43.42±5.02	19	0.221
	Toric	39.64±4.93	38.74±5.06	18	0.328

[a]Statistical significance with paired t-test ($p<0.05$)

wear. SCL wearers in their study showed corneal thickening at 1 month, followed by corneal thinning at 6 and 18 months. An increase in radius of corneal curvature and central corneal thinning associated with continuous wear of first-generation high-Dk SCLs were previously reported in a small sample of patients.[18]

Contrary to these studies, Alba-Bueno et al.[2] compared corneal topographical changes with 3 months daily wear of silicone hydrogel (SiH) lenses and found that corneal topographic indices were stable with daily wear of SiH lenses. The magnitude of corneal morphological changes associated with 8 hours wear of daily disposable lenses was also small.[19] Radaie-Moghadam et al.[20] investigated corneal hysteresis, corneal resistance factor, central corneal thickness, and keratometry on toric SCL wearers with negative history of SCL wear and concluded that corneal hysteresis and corneal resistance factor decreased at 1 month and returned to baseline after 3 months, while central corneal thickness and corneal curvature values did not change significantly.

In the present study; Acuvue Oasys, Acuvue Oasys for Astigmatism, Air Optix Aqua, and Air Optix Aqua for Astigmatism were selected to evaluate the presumptive corneal alterations. These SCLs constitute the majority of SCL prescriptions in our clinic. The mean CCT was 553.64±23.22 at baseline and none of the corneal parameters showed significant difference after 12 months of SiH contact lens wear. Conflicting results in different studies are most likely due to differences in contact lens material, oxygen transmissibility, water content, and modulus. The results of our study show that low modulus, high oxygen transmissible lenses can prevent the corneal alterations associated with SCL use. Early corneal biomechanical and curvature changes which develop in the first few months of SCL wear regress in long-term follow-up after the cornea-contact lens adaptation process.

This study also investigated changes in anterior chamber volume, depth, and angle with SCL wear. As expected, no significant changes were observed in anterior chamber parameters.

Study Limitations

This study has several limitations. First, our sample size was relatively small and did not allow for segregation of patients into subgroups depending on the modulus of lens materials.

Another limitation is the lack of aberrometry measurements, which would be helpful to explain the improvement in visual acuity in the toric SCL group.

Conclusion

In conclusion, the results of this study revealed that previously reported short-term SCL-associated corneal changes probably diminish in long-term follow-up. Long-term wear of current highly oxygen permeable and relatively low modulus SiH SCLs do not change corneal or anterior chamber morphology and volumetric parameters. Furthermore, toric SiH SCLs may provide better visual performance compared to spectacles. Further studies with a larger sample size and longitudinal follow-up are necessary to confirm these findings.

Ethics

Ethics Committee Approval: The study was carried out with approval from the Ethics Committee of University of Health Sciences, Ankara Numune Training and Research Hospital, approval number: 15-520.

Informed Consent: All participants were informed about the objective and content of study. Informed consent was obtained from all patients.

Peer-review: Externally peer-reviewed.

Authorship Contributions

Surgical and Medical Practices: Cemal Çavdarlı, Concept: Cemal Çavdarlı, Design: Cemal Çavdarlı, Data Collection or Processing: Cemal Çavdarlı, Pınar Topçu-Yılmaz, Analysis or Interpretation: Cemal Çavdarlı, Pınar Topçu-Yılmaz, Literature Search: Cemal Çavdarlı, Pınar Topçu-Yılmaz, Writing: Cemal Çavdarlı, Pınar Topçu-Yılmaz.

Conflict of Interest: No conflict of interest was declared by the authors.

Financial Disclosure: The authors declared that this study received no financial support.

References

1. Stapleton F, Stretton S, Papas E, Skotnitsky C, Sweeney DF. Silicone hydrogel contact lenses and the ocular surface. Ocul Surf. 2006;4:24-43.
2. Alba-Bueno F, Beltran-Masgoret A, Sanjuan C, Biarnes M, Marin J. Corneal shape changes induced by first and second generation silicone hydrogel contact lenses in daily wear. Cont Lens Anterior Eye. 2009;32:88-92.
3. Arranz I, Gonzalez-Garcia MJ, Galarreta DJ, Cisneros AB, Calonge M, Herreras JM. Low water content hydrogel contact lenses (HCL) induce corneal irregularity. Invest Ophthalmol Vis Sci. 2003;44:3701.
4. Alipour F, Letafatnejad M, Beheshtnejad AH, Mohammadi SF, Ghaffary SR, Hassanpoor N, Yaseri M. Corneal Biomechanical Findings in Contact Lens Induced Corneal Warpage. J Ophthalmol. 2016;2016:5603763.
5. Ruiz-Montenegro J, Mafra CH, Wilson SE, Jumper JM, Klyce SD, Mendelson EN. Corneal topographic alterations in normal contact lens wearers. Ophthalmology. 1993;100:128-134.
6. Lu F, Mao X, Qu J, Xu D, He JC. Monochromatic Wavefront Aberrations in the Human Eye with Contact Lenses. Optom Vis Sci. 2003;80:135-141.
7. Sankaridurg P, Lazon de la Jara P, Holden B. The future of silicone hydrogels. Eye Contact Lens. 2013;39:125-129.
8. Sweeney DF. Have silicone hydrogel lenses eliminated hypoxia? Eye Contact Lens. 2013;39:53-60.
9. Tyagi G, Collins M, Read S, Davis B. Regional changes in corneal thickness and shape with soft contact lenses. Optom Vis Sci. 2010;87:567-575.
10. Ren DH, Yamamoto K, Ladage PM, Molai BSM, Li L, Petroll WM, Jester JV, Cavanagh HD. Adaptive effects of 30-night wear of hyper-O2 transmissible contact lenses on bacterial binding and corneal epithelium: a 1-year clinical trial. Ophthalmology. 2002;109:27-39.
11. Ichijima H, Imayasu M, Tanaka H, Ren DH, Cavanagh HD. Effects of RGP lens extended wear on glucose-lactate metabolism and stromal swelling in the rabbit cornea. CLAO J 2000;26:30-36.
12. Chen D, Lam AK. Reliability and repeatability of the pentacam on corneal curvatures. Clin Exp Optom. 2009;92:110-118.
13. O'Donnell C, Maldonado-Codina C. Agreement and repeatability of central thickness measurement in normal corneas using Ultrasound pachymetry and the Oculus Pentacam. Cornea. 2005;24:920-924.

14. Demir M, Kurna SA, Sengor T, Atakan TG, Sahin T. Assessment of aberrations and visual quality differences between myopic and astigmatic eyes before and after contact lens application. North Clin Istanb. 2015;2:1-6.
15. Richdale K, Berntsen DA, Mack CJ, Merchea MM, Barr JT. Visual acuity with spherical and toric soft contact lenses in low- to moderate-astigmatic eyes. Optom Vis Sci. 2007;84:969-975.
16. Liu Z, Pflugfelder SC. The effects of long-term contact lens wear on corneal thickness, curvature, and surface regularity. Ophthalmology. 2000;107:105-111.
17. Yeniad B, Yiğit B, Işsever H, Közer Bilgin L. Effects of contact lenses on corneal thickness and corneal curvature during usage. Eye Contact Lens. 2003;29:223-229.
18. González-Méijome JM, González-Pérez J, Cerviño A, Yebra-Pimentel E, Parafita MA. Changes in corneal structure with continuous wear of high-Dk soft contact lenses: a pilot study. Optom Vis Sci. 2003;80:440-446.
19. Del Águila-Carrasco AJ, Domínguez-Vicent A, Pérez-Vives C, Ferrer-Blasco T, Montés-Micó R. Assessment of corneal morphological changes induced by the use of daily disposable contact lenses. Cont Lens Anterior Eye. 2015;38:28-33.
20. Radaie-Moghadam S, Hashemi H, Jafarzadehpur E, Yekta AA, Khabazkhoob M. Corneal Biomechanical Changes Following Toric Soft Contact Lens Wear. J Ophthalmic Vis Res. 2016;11:131-135.

DOI: 10.4274/tjo.79664
Turk J Ophthalmol 2018;48:171-177

Original Article

Corneal Biomechanical Properties of Keratoconic Eyes Following Penetrating Keratoplasty

Hamidu Gobeka, Özlem Barut Selver, Melis Palamar Onay, Sait Eğrilmez, Ayşe Yağcı
Ege University Faculty of Medicine, Department of Ophthalmology, İzmir, Turkey

Abstract

Objectives: To investigate the corneal biomechanical properties of keratoconic eyes following penetrating keratoplasty (PKP).

Materials and Methods: Thirty-five patients (70 eyes) were enrolled to this prospective study. Operated and contralateral keratoconic eyes were defined as Group 1 and 2, respectively. All patients underwent ophthalmological examination and measurements of corneal biomechanical properties by Ocular Response Analyzer (ORA), intraocular pressure (IOP) by Goldmann applanation tonometry, and central corneal thickness (CCT) by Pentacam. Shapiro-Wilk W test was performed to test normality of the data. The statistical significance was evaluated with the paired t-test and Wilcoxon signed ranks test. Pearson correlation and Spearman rho tests were used for correlation analysis.

Results: The average age and male/female ratio were 31.34±11.65 (15-60) years and 21/14, respectively. The mean values of the data obtained from Group 1 and 2 respectively were: corneal hysteresis (CH): 9.35±1.66, 8.18±1.84 mmHg (p=0.013), corneal resistance factor (CRF): 9.48±1.96, 7.14±2.05 mmHg (p<0.001), IOPcc: 16.90±4.32, 14.26±3.69 mmHg (p=0.004), IOPg: 15.45±4.61, 10.91±3.97 mmHg (p<0.001), IOPapl: 14.26±3.11, 13.09±2.54 mmHg (p=0.046), and central corneal thickness (CCT): 545.64±60.82, 442.60±68.14 µM (p<0.001). The positive correlation between CH and CRF was moderate (r=0.444) in Group 1 and strong (r=0.770) in Group 2. There was a moderate negative correlation between CH and IOPcc in both groups (r=-0.426, r=-0.423), but CH was not correlated with IOPg or IOPapl in either group. There were weak to strong positive correlations between CRF and all IOP values in both groups. There was no correlation between CRF and CCT in Group 1 (r=0.075) and a very weak correlation in Group 2 (r=0.237). Only IOPcc and IOPg were strongly correlated in both groups.

Conclusion: Better understanding of corneal biomechanical properties is essential for elucidating the pathophysiology and diagnosis of several corneal pathologies such as keratoconus. The biomechanical properties of keratoconic eyes seem to be closer to normal values after PKP.

Keywords: Corneal biomechanical properties, Ocular Response Analyzer, keratoconus, penetrating keratoplasty

Introduction

The cornea has unique viscoelastic properties that enable it to deform under stress and then return to its original state. Collectively, these are called the biomechanical properties of the cornea. In recent years, the in vivo evaluation of corneal biomechanical properties has gained importance. Although new devices are under development for such analyses, the Ocular Response Analyzer (ORA) device is currently in widespread use.[1]

Since the introduction of this device into clinical practice, several studies have been conducted on the biomechanical properties of the cornea.[2] These studies examine a wide range of findings, from demographic data to the effects of corneal surgeries and various corneal pathologies on corneal biomechanical properties.[1,2,3,4,5,6,7,8,9,10,11,12]

Address for Correspondence: Ayşe Yağcı MD, Ege University Faculty of Medicine, Department of Ophthalmology, İzmir, Turkey
Phone: +90 542 481 17 00 E-mail: drayseyagci@gmail.com **ORCID-ID:** orcid.org/0000-0002-4713-2831
Received: 10.07.2017 **Accepted:** 03.01.2018

Keratoconus is a progressive degenerative disorder of the cornea which inevitably affects its biomechanical parameters. Moreover, corneal transplant by keratoplasty, the surgical treatment option for advanced keratoconus, results in another change in biomechanical parameters.[2]

In this study, we aimed to evaluate and compare corneal biomechanical parameters in both eyes of patients with bilateral keratoconus who underwent unilateral penetrating keratoplasty (PKP). We also examined the relationship between the results and patients' demographic characteristics.

Materials and Methods

In this study, we prospectively examined the corneal biomechanical properties of the operated and unoperated eyes of patients diagnosed with keratoconus who underwent unilateral PKP between 2013 and 2015 in the Cornea, Contact Lens, and Oculoplasty Unit in the Ege University Faculty of Medicine, Department of Ophthalmology. Eyes that underwent PKP were designated as Group 1 (study group) and the unoperated keratoconus eyes were designated as Group 2 (control group). The study was approved by the Ege University Faculty of Medicine, Clinical Research Ethics Committee. Voluntary informed consent forms were obtained from all patients.

Thirty-five patients aged 15-61 years were included in the study. All patients were diagnosed with keratoconus and underwent unilateral PKP surgery. Inclusion criteria included the absence of postoperative complications, absence of accompanying systemic (e.g. diabetes) or ocular diseases (e.g. glaucoma), no contact lens use, and no prior ocular surgery other than PKP (e.g. cataract surgery, LASIK).

The patients were examined no earlier than 15 days after the corneal sutures were removed. All patients underwent detailed ophthalmologic examination, best corrected visual acuity measurement, slit-lamp anterior segment examination, and posterior segment examination with a 90 diopter (D) lens following pupil dilation with 1% tropicamide. Intraocular pressure (IOP) was measured with a Goldmann applanation tonometer (Haag-Streit AG, Koning, Switzerland) (IOPapl) and an ORA was used to measure the following corneal biomechanical properties: corneal hysteresis (CH), corneal resistance factor (CRF), corneal compensated IOP (IOPcc), and Goldmann-correlated IOP (IOPg). The average of 4 measurements was recorded. In addition, central corneal thickness (CCT) was measured with a Pentacam (Oculus Pentacam version 1.20/10 Germany) device.

Statistical Analysis

Data obtained in the study were statistically analyzed using SPSS (SPSS Inc., Chicago, IL, USA) version 16 for Windows software package. The conformity of the data to normal distribution was assessed with a Shapiro-Wilk W test. Parametric data conforming to normal distribution were evaluated in terms of statistical significance with a dependent t-test; data not conforming to normal distribution and other non-parametric data were evaluated using a Wilcoxon signed rank test. For correlation analysis, normally distributed parametric data were analyzed with Pearson correlation test while data not conforming to normal distribution and non-parametric data were analyzed with a Spearman rho test. Absolute correlation values of 0 to 0.25 were interpreted as very weak or no correlation, 0.25-0.50 as weak correlation, 0.50-0.75 as moderate correlation, and >0.75 as strong correlation. The intragroup consistency (reliability) of IOP measurements was assessed using an F-test. P values of <0.05 were considered statistically significant.

Results

The mean age of the patients was 31.34±11.65 (15-60) years. The female to male ratio was 14:21 (2:3). Simple interrupted sutures were used in all procedures. Graft diameter was 7.75 mm in 23 patients (65.7%), 7.50 mm in 9 patients (25.7%), 8 mm in 2 patients (5.7%), and 9 mm in 1 patient (2.9%).

As expected, there was a significant increase in vision in all Group 1 eyes. Median pre- and postoperative visual acuity values were 1.3 (0.7-3.1) logMAR and 0.3 (0-1.5) logMAR, respectively (p<0.001).

The median interval between suture removal and ORA measurement was 10 months (0.5-492 months). All measured data (except for waveform score [WS]) conformed to normal distribution according to the Shapiro-Wilk W test.

The mean CH, CRF, IOPcc, IOPg, IOPapl, and CCT values of the groups are shown in Table 1. There were statistically significant differences between Groups 1 and 2 in all variables.

The median WS was 4.10 (2.20-7.50) in Group 1 and 5.10 (1.20-8.50) in Group 2 (p=0.376).

Analysis of correlations between age and corneal biomechanical parameters (CH, CRF, IOPcc, IOPg, and IOPapl) (Table 2) revealed no significant results other than very weak negative correlations between age and CH and CRF in Group 2 (r=-0.216, -0.242).

In the evaluation of gender differences in the corneal biomechanical properties of the eyes in Group 2, it was observed that females had higher CH (8.69 vs. 7.84 mmHg) and CRF (7.61 vs. 6.82 mmHg) values, but the differences were not statistically significant (p=0.186 and p=0.275, respectively).

As shown in Table 3, intragroup comparisons revealed a moderate positive correlation between CH and CRF values in Group 1 (r=0.444) and strong positive correlation in Group 2 (r=0.770). Moderate negative correlations were observed between CH and IOPcc in both Group 1 and Group 2 (r=-0.426, r=-0.423). There was no correlation between CH and IOPg, IOPapl, or CCT in either group. CRF and IOPcc were weakly or very weakly correlated in Group 1 (r=0.334) and Group 2 (r=0.178). CRF and IOPg showed a strong positive correlation in Group 1 (r=0.663) and a moderate positive correlation in Group 2 (r=0.575). There was a weak correlation between CRF and IOPapl in both Group 1 and Group 2 (r=0.277, r=0.298). CRF and CCT were not correlated in Group 1 (r=0.075), but showed a very weak correlation in Group 2 (r=0.237). There was a very strong positive correlation between IOPcc and IOPg in Group 1 (r=0.911) and a moderate positive correlation between them in

Group 2 (r=0.771). Weak correlations were observed between IOPcc and IOPapl in both groups (r=0.357, r=0.371). There were also weak correlations between the IOPg and IOPapl values in both groups (r=0.362, r=0.384). CCT was not correlated with any corneal biomechanical parameter in Group 1, but was very weakly correlated with CRF (r=0.237) and IOPcc (r=0.487) and moderately correlated with IOPg (r=0.529) in Group 2.

Table 1. Comparison of mean ocular response analyzer corneal parameters in Groups 1 and 2

	Group 1	Group 2	p value
CH	9.35±1.66	8.18±1.84	p=0.013
CRF	9.48±1.96	7.14±2.05	p<0.001
IOPcc	16.90±4.32	14.26±3.69	p=0.004
IOPg	15.45±4.61	10.91±3.97	p<0.001
IOPapl	14.26±3.11	13.09±2.54	p=0.046
CCT	545.64±60.82	442.60±68.14	p<0.001

CH: Corneal hysteresis, CRF: Corneal resistance factor, CCT: Central corneal thickness, IOPapl: Intraocular pressure measured by applanation, IOPcc: Corneal-compensated intraocular pressure, IOPg: Goldmann-correlated intraocular pressure

Table 2. Analyses of statistical significance and correlation between age and Ocular Response Analyzer corneal parameters

	Age			
	p value		Correlation (r)	
	Group 1	Group 2	Group 1	Group 2
CH	0.662	0.212	-0.077	-0.216
CRF	0.298	0.162	-0.181	-0.242
IOPcc	0.347	0.693	-0.164	-0.069
IOPg	0.396	0.925	-0.148	-0.016
IOPapl	0.959	0.314	-0.009	0.175

CH: Corneal hysteresis, CRF: Corneal resistance factor, IOPapl: Intraocular pressure measured by applanation, IOPcc: Corneal-compensated intraocular pressure, IOPg: Goldmann-correlated intraocular pressure

In our evaluation of the consistency between IOP values, intragroup correlation coefficients (ICC) for IOPapl and IOPcc in Groups 1 and 2 were 0.276 (95% confidence interval [CI]=-0.027-0.543; p=0.022, F-test) and 0.330 (CI=0.019-0.588; p=0.019, F-test), respectively (Table 4). ICC values for IOPapl value and IOPg were 0.327 (95% CI=0.010-0.588, p=0.023, F-test) in Group 1 and 0.291 (CI=-0.013-0.556, p=0.019, F-test) in Group 2. For IOPcc and IOPg values, ICC values in Groups 1 and 2 were 0.866 (95% CI=0.563-0.947, p<0.0001, F-test) and 0.559 (CI=-0.073-0.828, p<0.0001, F-test), respectively.

Discussion

Keratoconus is a degenerative process that causes changes in corneal biomechanical parameters. In eyes with keratoconus that undergo keratoplasty, another change in biomechanical parameters is expected.[2]

The reliability of the ORA device is the main factor in the ability to accurately evaluate corneal biomechanical parameters. Version 2.04 of the ORA includes WS as a scale of 0-10, with higher values corresponding to greater measurement reliability. In previous studies on the reliability of using ORA, Lam et al.[13] recommended taking 3 measurements with WS ≥3.5, while Ehrlich et al.[14] recommended a WS cut-off of 6.5. In another study, Mandalos et al.[15] used a cut-off value of 6.0. Ayala and Chen[16] recommended using measurements with WS of 7 or above whenever possible in order to increase reliability. In our study, the mean WS was 4.10 in eyes that underwent PKP and 5.10 in unoperated keratoconus eyes. These values are consistent with the reliability values reported by Lam et al.[13] The low WS values in our study, particularly in the corneas that underwent keratoplasty, may be attributable to scar tissue at the recipient bed-graft junction in eyes that underwent keratoplasty and the presence of abnormal topographic changes in both groups. Detailed WS data were not provided in other studies with patient populations similar to ours, thus precluding comparison with other studies on this point.

Regarding the effect of sex on corneal biomechanical parameters, there are studies in the literature indicating no

Table 3. Intragroup correlations between corneal biomechanical parameters

	CH		CRF		IOPcc		IOPg		IOPapl		CCT	
	Group 1	Group 2	Group 1	Group 2	Group 1	Group 2	Group 1	Group 2	Group 1	Group 2	Group 1	Group 2
CH	1.000		0.444	0.770	-0.426	-0.423	-0.160	0.039	-0.131	0.092	0.126	-0.047
CRF	0.444	0.770	1.000		0.334	0.178	0.663	0.575	0.277	0.298	0.075	0.237
IOPcc	-0.426	-0.423	0.334	0.178	1.000		0.911	0.771	0.357	0.371	0.034	0.487
IOPg	-0.160	0.039	0.663	0.575	0.911	0.771	1.000		0.362	0384	0.016	0.529
IOPapl	-0.131	0.092	0.277	0.298	0.357	0.371	0.362	0.384	1.000		0.051	0.086
CCT	0.126	-0.047	0.075	0.237	-0.034	0.487	0.016	0.529	0.051	0.086	1.000	

CH: Corneal hysteresis, CRF: Corneal resistance factor, CCT: Central corneal thickness, IOPapl: Intraocular pressure measured by applanation, IOPcc: Corneal-compensated intraocular pressure, IOPg: Goldmann-correlated intraocular pressure

Table 4. Consistency between intraocular pressure measurements within Groups 1 and 2

	Group	Correlation coefficient	Confidence interval and F test
IOPapl vs IOPcc	Group 1	0.276	-0.027-0.543, p=0.022
	Group 2	0.330	0.019-0.588, p=0.019
IOPapl vs IOPg	Group 1	0.327	0.010-0588, p=0.023
	Group 2	0.291	-0.013-0.556, p=0.019
IOPcc vs IOPg	Group 1	**0.866**	0.563-0.947, p<0.0001
	Group 2	**0.559**	-0.073-0.828, p<0.0001

IOPapl: Intraocular pressure measured by applanation, IOPcc: Corneal-compensated intraocular pressure, IOPg: Goldmann-correlated intraocular pressure

significant effect[17,18,19] as well as studies reporting statistically significant differences.[20,21] It is conceivable that sex differences in corneal biomechanical properties may vary between different ethnicities, explaining these conflicting results. Our evaluation of sex-based differences in the corneal biomechanical properties of unoperated keratoconus eyes in this study showed that CH and CRF values were higher in women, but that the difference was not statistically significant.

Investigation of the effect of age on corneal biomechanical parameters has revealed no clinically significant differences in many previous studies. In a study by Kamiya et al.[17] involving 204 eyes of healthy individuals with a mean age of 46.7±19.4 years, a minimal but statistically significant negative correlation was observed between CH and CRF values, while Ortiz et al.[22] reported significant differences in CH and CRF values only in individuals younger than 14 and older than 60 years of age. However, a linear correlation was not observed between age and these two biomechanical parameters. Kotecha et al.[23] reported that CH decreased by 0.28 every decade, while Foster et al.[24] observed that CH decreased by 0.34 and CRF value decreased by 0.31 with each decade of age. In our study, there was a negative correlation, albeit very weak, between age and CRF in unoperated eyes with keratoconus (r=-0.242). Due to the progressive nature of keratoconus, these findings may be related to age-related progression and the presence of more advanced disease in older patients. However, because normal corneas were not included in our evaluation of the effects of age and sex on CH and CRF values, we believe the sex differences observed in this study may not reflect those in the healthy population.

In keratoconus, corneal biomechanical properties are affected by various factors including collagen fibrils and the organization of the main corneal components and cells within the tissue.[25,26,27,28] In previous studies concerning the biomechanical parameters of keratoconic eyes, it is reported that CH and CRF values are lower compared to normal corneas, and that this decrease is correlated with disease stage.[1,22,29,30,31,32,33] Kirwan et al.[34] examined corneal biomechanical properties in 3 groups (normal eyes, advanced keratoconus, and forme fruste [early] keratoconus [FFK]) and reported that CH and CRF values were significantly lower in eyes with keratoconus compared to FFK and normal eyes. Consistent with previous studies, we also found that the corneal biomechanical values of eyes with keratoconus (CH: 8.18±1.84 mmHg, CRF: 7.14±2.05 mmHg) were lower compared to literature data on normal healthy eyes (normal range, CH: 9.3±1.4-11.4±1.5 mmHg, CRF: 9.2±1.4-11.9±1.5 mmHg).[35]

The impact of keratoplasty on corneal biomechanical properties seems unavoidable.[3,5,6,7] There are studies reporting that this effect differs in lamellar and PKP.[7,8,9] The main factors that can contribute to changes in CH and CRF values after PKP are the biomechanical properties of the transplanted graft, the graft diameter, fibrotic wound healing at the graft-host junction, and the biomechanical properties of the recipient corneoscleral rim. While the first three factors have a positive effect on CH and CRF values, the presence of weak tissue from the keratoconic cornea in the corneoscleral rim of the recipient bed negatively affects CH and CRF values. In the relevant literature, Yenerel et al.[3] reported that CH and CRF values were higher in eyes that underwent PKP compared to eyes with FFK or advanced keratoconus. It has also been shown that both CH and CRF approach values seen in normal eyes after PKP. Goldhagen et al.[36] detected CH and CRF values close to those of normal corneas in keratoconus eyes that underwent PKP. Consistent with the literature, we observed in the present study that CH and CRF values were significantly higher after PKP when compared with unoperated keratoconus eyes (CH: p=0.013, CRF: p<0.001).

Strong correlation has been reported between CH value and CRF value, which are corneal viscoelastic parameters.[37] Similarly, in the present study there was a moderate positive correlation between CH and CRF values in PKP eyes (r=0.444) and strong positive correlation in unoperated keratoconus eyes (r=0.770). The weaker correlation in eyes that underwent keratoplasty may be due to the effect of the fibrotic scar on cumulative values.

It is known that CH and CRF values are strongly correlated with CCT.[38,39,40,41] Most studies in the literature have reported a strong positive correlation between CH and CRF values and CCT in normal eyes.[38,42,43,44,45,46,47] Unlike these studies, Broman et al.[48] observed different CH values in eyes with the same CCT value, which they attributed to the possible influence of other unidentified factors on corneal biomechanical properties.[34,49] In our comparison of unoperated keratoconus corneas and keratoconus corneas that underwent PKP, we did not observe the correlation between CH and CRF values and CCT that exists in normal corneas, which supports the theory of multiple unidentified factors.

Studies investigating the relationship between CH and CRF values and IOP values have shown that CH is negatively correlated with IOPcc.[42,49,50,51,52] This is likely due to the interaction between CH and CCT.[39] As CCT increases, CH and the measured IOPg value also increase, while IOPg and IOPcc diverge.[38,42] However, a study by Liu and Roberts[28] demonstrated that the correlation between CCT and IOP values is not a simple linear relationship, but a complex and non-linear association. Furthermore, some believe that IOPcc value is a more accurate because it is obtained by eliminating the effect of CCT.[5] Similar

to the literature, correlation analysis between CH and CRF values and IOP values in our study revealed a moderate negative correlation between the CH value and the IOPcc value in both groups, but CH value was not correlated with IOPg or IOPapl values.

In the literature, CRF value is reported to be positively correlated with IOP values in healthy eyes.[53] In parallel to existing data, we also observed positive correlations between CRF and all IOP values, ranging in strength from weak to strong, in both groups of eyes in our study. However, the correlations were weaker than those seen in healthy corneas.

The accepted strong positive correlations between CCT value and IOPapl and IOPg values are a result of the CCT increasing corneal resistance to applanation. Because IOPcc is obtained by correcting for the effect of corneal thickness on IOP, this value is least dependent on CCT.[54,55] In our study, we detected no correlation between CCT and IOP values in either group. We believe that because our study involved eyes that underwent PKP and eyes with keratoconus, the relationship between biomechanical factors and IOP and CCT may have been affected by different variables than those reported in the literature.

Regarding consistency between IOP values, Ouyang et al.[56] showed that in a normal population, repeated ORA IOP measurements are equivalent to IOPapl values and that ORA IOP values are valid and reliable. In our analysis of the intragroup consistency of measured IOP values, we did not observe significant agreement between IOPcc and IOPg values and IOPapl values in the eyes that underwent PKP or the keratoconus eyes. However, there was significant consistency between IOPcc and IOPg values in both groups. This is because IOPcc and IOPg values are both ORA IOP values and were obtained from the same device.

Aside from all these data, another factor that is likely to affect ORA parameters in eyes that undergo PKP is graft diameter. Corneal biomechanical results after keratoplasty using a large graft are reported to be closer to normal values. Large grafts have several advantages: there is less postoperative astigmatism due to a more peripheral graft-recipient interface, and the maximum amount of abnormal cornea is removed and replaced with normal donor tissue. In terms of graft biomechanical properties in keratoconus, a large graft may be expected to provide the best results and yield more stable postoperative refractive outcomes; however, grafts with large diameters (>8.5 mm) have certain limitations such as high graft rejection and failure rates.[9,57] Therefore, we believe that when performing keratoplasty, these factors should be evaluated and graft diameter should be selected so as to bring the biomechanical properties of the cornea closer to normal while assessing the risks and benefits. The majority of the grafts used in the keratoplasty procedures in our study were 7.5 mm or 7.75 mm in diameter, which was not considered adequate data for a comparison of graft diameter. Therefore, we did not evaluate the effect of graft diameter on corneal biomechanical properties.

Conclusion

In conclusion, while the biomechanical properties of eyes with keratoconus approach normal values after PKP, there are still important limitations to the comparison of these eyes using an ORA. Because measurements are taken 3-4 mm from the central cornea, keratoconic corneas with decentralized irregularity may be overlooked with this device and it may not be possible to evaluate response of the entire cornea in cases where the central 7-8 mm has been replaced, as in keratoplasty. In addition, central corneal surface irregularity and the presence of a corneal scar can interfere with the infrared specular reflection beam of the ORA, leading to a waveform change. Therefore, all of these potential limitations should be taken into consideration and the importance of reliability should not be overlooked in the ORA examination of all non-normal corneas.

Ethics

Ethics Committee Approval: Ege University Faculty of Medicine, Clinical Research Ethics Committee (decision number: 13-6.1/3).

Informed Consent: Retrospective study.

Peer-review: Externally and internally peer-reviewed.

Authorship Contributions

Surgical and Medical Practices: Hamidu Gobeka, Ayşe Yağcı, Concept: Hamidu Gobeka, Melis Palamar Onay, Sait Eğrilmez, Ayşe Yağcı, Design: Ayşe Yağcı, Data Collection or Processing: Hamidu Gobeka, Özlem Barut Selver, Melis Palamar Onay, Sait Eğrilmez, Ayşe Yağcı, Analysis or Interpretation: Hamidu Gobeka, Özlem Barut Selver, Melis Palamar Onay, Sait Eğrilmez, Ayşe Yağcı, Literature Search: Hamidu Gobeka, Özlem Barut Selver, Melis Palamar Onay, Sait Eğrilmez, Ayşe Yağcı, Writing: Hamidu Gobeka, Özlem Barut Selver, Melis Palamar Onay, Sait Eğrilmez, Ayşe Yağcı.

Conflict of Interest: No conflict of interest was declared by the authors.

Financial Disclosure: The authors declared that this study received no financial support.

References

1. Luce DA. Determining in vivo biomechanical properties of the cornea with an ocular response analyzer. J Cataract Refract Surg. 2005;31:156-162.
2. Edmund C. Corneal elasticity and ocular rigidity in normal and keratoconic eyes. Acta Ophthalmol (Copenh). 1988;66:134-140.
3. Yenerel NM, Kucumen RB, Gorgun E. Changes in corneal biomechanics in patients with keratoconus after penetrating keratoplasty. Cornea. 2010;29:1247-1251.
4. Gatinel D, Chaabouni S, Adam PA, Munck J, Puech M, Hoang-Xuan T. Corneal hysteresis, resistance factor, topography, and pachymetry after corneal lamellar flap. J Refract Surg. 2007;23:76-84.
5. Shin JY, Choi JS, Oh JY, Kim MK, Lee JH, Wee WR. Evaluation of corneal biomechanical properties following penetrating keratoplasty using the ocular response analyzer. Korean J Ophthalmol. 2010;24:139-142.
6. Laiquzzaman M, Tambe K, Shah S. Comparison of biomechanical parameters in penetrating keratoplasty and normal eyes using the Ocular Response Analyser. Clin Exp Ophthalmol. 2010;38:758-763.

7. Hosny M, Hassaballa MA, Shalaby A. Changes in corneal biomechanics following different keratoplasty techniques. Clin Ophthalmol. 2011;5:767-770.
8. Jafarinasab MR, Feizi S, Javadi MA, Hashemloo A. Graft biomechanical properties after penetrating keratoplasty versus deep anterior lamellar keratoplasty. Curr Eye Res. 2011;36:417-421.
9. Feizi S, Einollahi B, Yazdani S, Hashemloo A. Graft biomechanical properties after penetrating keratoplasty in keratoconus. Cornea. 2012;31:855-858.
10. Feizi S, Hashemloo A, Rastegarpour A. Comparison of the ocular response analyzer and the Goldmann applanation tonometer for measuring intraocular pressure after deep anterior lamellar keratoplasty. Invest Ophthalmol Vis Sci. 2011;52:5887-5891.
11. Murugesan V, Bypareddy R, Kumar M, Tanuj D, Anita P. Evaluation of corneal biomechanical properties following penetrating keratoplasty using ocular response analyzer. Indian J Ophthalmol. 2014;62:454-460.
12. Fabian ID, Barequet IS, Skaat A, Rechtman E, Goldenfeld M, Roberts CJ, Melamed S. Intraocular pressure measurements and biomechanical properties of the cornea in eyes after penetrating keratoplasty. Am J Ophthalmol. 2011;151:774-781.
13. Lam AK, Chen D, Tse J. The usefulness of waveform score from the ocular response analyzer. Optom Vis Sci. 2010;87:195-199.
14. Ehrlich JR, Haseltine S, Shimmyo M, Radcliffe NM. Evaluation of agreement between intraocular pressure measurements using Goldmann applanation tonometry and Goldmann correlated intraocular pressure by Reichert's ocular response analyser. Eye (Lond). 2010;24:1555-1560.
15. Mandalos A, Anastasopoulos E, Makris L, Dervenis N, Kilintzis V, Topouzis F. Inter-examiner reproducibility of Ocular Response Analyzer using the waveform score quality index in healthy subjects. J Glaucoma. 2013;22:152-155.
16. Ayala M, Chen E. Measuring corneal hysteresis: threshold estimation of the waveform score from the Ocular Response Analyzer. Graefes Arch Clin Exp Ophthalmol. 2012;250:1803-1806.
17. Kamiya K, Shimizu K, Ohmoto F. Effect of aging on corneal biomechanical parameters using the ocular response analyzer. J Refract Surg. 2009;25:888-893.
18. Jiang Z, Shen M, Mao G, Chen D, Wang J, Qu J, Lu F. Association between corneal biomechanical properties and myopia in Chinese subjects. Eye (Lond). 2011;25:1083-1089.
19. Wang J, Cayer MM, Descovich D, Kamdeu-Fansi A, Harasymowycz PJ, Li G, Lesk MR. Assessment of factors affecting the difference in intraocular pressure measurements between dynamic contour tonometry and goldmann applanation tonometry. J Glaucoma. 2011;20:482-487.
20. Strobbe E, Cellini M, Barbaresi U, Campos EC. Influence of age and gender on corneal biomechanical properties in a healthy Italian population. Cornea. 2014;33:968-972.
21. Fontes BM, Ambrósio R Jr, Alonso RS, Jardim D, Velarde GC, Nosé W. Corneal biomechanical metrics in eyes with refraction of -19.00 to +9.00 D in healthy Brazilian patients. J Refract Surg. 2008;24:941-945.
22. Ortiz D, Piñero D, Shabayek MH, Arnalich-Montiel F, Alió JL. Corneal biomechanical properties in normal, post-laser in situ keratomileusis, and keratoconic eyes. J Cataract Refract Surg. 2007;33:1371-1375.
23. Kotecha A, Elsheikh A, Roberts CR, Zhu H, Garway-Heath DF. Corneal thickness- and age-related biomechanical properties of the cornea measured with the ocular response analyzer. Invest Ophthalmol Vis Sci. 2006;47:5337-5347.
24. Foster PJ, Broadway DC, Garway-Heath DF, Yip JL, Luben R, Hayat S, Dalzell N, Wareham NJ, Khaw KT. Intraocular pressure and corneal biomechanics in an adult British population: the EPIC-Norfolk eye study. Invest Ophthalmol Vis Sci. 2011;52:8179-8185.
25. Ogbuehi KC, Osuagwu UL. Corneal biomechanical properties: precision and influence on tonometry. Cont Lens Anterior Eye. 2014;37:124-131.
26. Daxer A, Fratzl P. Collagen fibril orientation in the human corneal stroma and its implication in keratoconus. Invest Ophthalmol Vis Sci. 1997;38:121-129.
27. Fratzl P, Daxer A. Structural transformation of collagen fibrils in corneal stroma during drying. An x-ray scattering study. Biophys J. 1993;64:1210-1214.
28. Liu J, Roberts CJ. Influence of corneal biomechanical properties on intraocular pressure measurement: quantitative analysis. J Cataract Refract Surg. 2005;31:146-155.
29. Touboul D, Roberts C, Kérautret J, Garra C, Maurice-Tison S, Saubusse E, Colin J. Correlations between corneal hysteresis, intraocular pressure, and corneal central pachymetry. J Cataract Refract Surg. 2008;34:616-622.
30. Schweitzer C, Roberts CJ, Mahmoud AM, Colin J, Maurice-Tison S, Kerautret J. Screening of forme fruste keratoconus with the ocular response analyzer. Invest Ophthalmol Vis Sci. 2010;51:2403-2410.
31. Fontes BM, Ambrósio R, Jardim D, Velarde GC, Nosé W. Corneal biomechanical metrics and anterior segment parameters in mild keratoconus. Ophthalmology. 2010;117:673-679.
32. Mollan SP, Wolffsohn JS, Nessim M, Laiquzzaman M, Sivakumar S, Hartley S, Shah S. Accuracy of Goldmann, ocular response analyser, Pascal and TonoPen XL tonometry in keratoconic and normal eyes. Br J Ophthalmol. 2008;92:1661-1665.
33. Çankaya AB, Anayol A, İleri D, Yılmazbaş P, Öztürk F. Keratokonus Hastalarında Kontakt Lens Kullanımının Korneal Biyomekanik Parametreler Üzerine Etkisi. Turk J Ophthalmol. 2012;3:197-201.
34. Kirwan C, O'Malley D, O'Keefe M. Corneal hysteresis and corneal resistance factor in keratoectasia: findings using the Reichert ocular response analyzer. Ophthalmologica. 2008;222:334-337.
35. Piñero DP, Alcón N. In vivo characterization of corneal biomechanics. J Cataract Refract Surg. 2014;40:870-887.
36. Goldhagen BE, Hwang RY, Kuo AN, Afshari NA. Changes in Corneal Biomechanics after Penetrating Keratoplasty in Keratoconus. Invest Ophthalmol Vis Sci. 2012;53:1511.
37. Glass DH, Roberts CJ, Litsky AS, Weber PA. A viscoelastic biomechanical model of the cornea describing the effect of viscosity and elasticity on hysteresis. Invest Ophthalmol Vis Sci. 2008;49:3919-3926.
38. Lam A, Chen D, Chiu R, Chui WS. Comparison of IOP measurements between ORA and GAT in normal Chinese. Optom Vis Sci 2007;84:909-914.
39. Shah S, Laiquzzaman M, Cunliffe I, Mantry S. The use of the Reichert ocular response analyser to establish the relationship between ocular hysteresis, corneal resistance factor and central corneal thickness in normal eyes. Cont Lens Anterior Eye. 2006;29:257-262.
40. Fontes BM, Ambrósio R Jr, Alonso RS, Jardim D, Velarde GC, Nosé W. Corneal biomechanical metrics in eyes with refraction of -19.00 to +9.00 D in healthy Brazilian patients. J Refract Surg. 2008;24:941-945.
41. Montard R, Kopito R, Touzeau O, Allouch C, Letaief I, Borderie V, Laroche L. [Ocular response analyzer: feasibility study and correlation with normal eyes]. J Fr Ophtalmol. 2007;30:978-984.
42. Franco S, Lira M. Biomechanical properties of the cornea measured by the Ocular Response Analyzer and their association with intraocular pressure and the central corneal curvature. Clin Exp Optom. 2009;92:469-475.
43. del Buey MA, Cristóbal JA, Ascaso FJ, Lavilla L, Lanchares E. Biomechanical properties of the cornea in Fuchs' corneal dystrophy. Invest Ophthalmol Vis Sci. 2009;50:3199-3202.
44. Rosa N, Lanza M, De Bernardo M, Signoriello G, Chiodini P. Relationship Between Corneal Hysteresis and Corneal Resistance Factor with Other Ocular Parameters. Semin Ophthalmol. 2015;30:335-339.
45. Ostadimoghaddam H, Sedaghat MR, Yazdi SHH, Niyazmand H. The Correlation between Biomechanical Properties of Normal Cornea with Tomographic Parameters of Pentacam. Iranian Journal of Ophthalmology. 2012;24:11-18.
46. Plakitsi A, O'Donnell C, Miranda MA, Charman WN, Radhakrishnan H. Corneal biomechanical properties measured with the Ocular Response Analyser in a myopic population. Ophthalmic Physiol Opt. 2011;31:404-412.
47. Touboul D, Roberts C, Kérautret J, Garra C, Maurice-Tison S, Saubusse E, Colin J. Correlations between corneal hysteresis, intraocular pressure, and corneal central pachymetry. J Cataract Refract Surg. 2008;34:616-622.

48. Broman AT, Congdon NG, Bandeen-Roche K, Quigley HA. Influence of corneal structure, corneal responsiveness, and other ocular parameters on tonometric measurement of intraocular pressure. J Glaucoma. 2007;16:581-588.
49. Kamiya K, Hagishima M, Fujimura F, Shimizu K. Factors affecting corneal hysteresis in normal eyes. Graefes Arch Clin Exp Ophthalmol. 2008;246:1491-1494.
50. Oncel B, Dinc U, Orge F, Yalvac B. Comparison of IOP measurement by ocular response analyzer, dynamic contour, Goldmann applanation, and noncontact tonometry. Eur J Ophthalmol. 2009;19:936-941.
51. Alhamad TA, Meek KM. Comparison of factors that influence the measurement of corneal hysteresis in vivo and in vitro. Acta Ophthalmol. 2011;89:443-450.
52. Hirneiss C, Neubauer AS, Yu A, Kampik A, Kernt M. Corneal biomechanics measured with the ocular response analyser in patients with unilateral open-angle glaucoma. Acta Ophthalmol. 2011;89:189-192.
53. Terai N, Raiskup F, Haustein M, Pillunat LE, Spoerl E. Identification of biomechanical properties of the cornea: the ocular response analyzer. Curr Eye Res. 2012;37:553-562.
54. Luce DA. Methodology for corneal compensated IOP and corneal resistance factor for An Ocular Response Analyzer. Available at http://www.ocularresponseanalyzer.com/ downloads/luce-2006-1.pdf. Accessed May 26, 2010.
55. Luce DA, Taylor D. Reichert Ocular Response Analyzer measures corneal biomechanical properties and IOP. White Paper. Available at http://www.ocularresponseanalyzer.com/ocular%20response%20analyzer%20white%20paper.pdf. Accessed May 26, 2010.
56. Ouyang PB, Li CY, Zhu XH, Duan XC. Assessment of intraocular pressure measured by Reichert Ocular Response Analyzer, Goldmann Applanation Tonometry, and Dynamic Contour Tonometry in healthy individuals. Int J Ophthalmol. 2012;5:102-107.
57. Skeens HM, Holland EJ. Large-diameter penetrating keratoplasty: indications and outcomes. Cornea. 2010;29:296-301.

DOI: 10.4274/tjo.56254
Turk J Ophthalmol 2018;48:178-184

Original Article

Does Foveal Position Relative to the Optic Disc Affect Optical Coherence Tomography Measurements in Glaucoma?

Zerrin Tuncer, Mitat Altuğ

Göz Vakfı, Bayrampaşa Eye Hospital, Ophthalmology Clinic, İstanbul, Turkey

Abstract

Objectives: To determine interindividual variability in the angle between the anatomic axis connecting the fovea and optic disc center and the horizontal meridian using spectral domain optical coherence tomography (OCT).

Materials and Methods: A total of 260 eyes of 133 subjects (81 women, 52 men) with glaucoma or suspected glaucoma were included in the study retrospectively. Fovea-disc angle (FoDi angle) measurements, determined as the angle between the horizontal meridian passing through the Bruch's membrane opening (BMO) center and the line connecting the fovea and BMO center, were recorded from spectral domain-OCT scans performed by the same investigator. FoDi angle was defined as negative if the fovea was located below the horizontal meridian through the BMO center and positive if the fovea was located above it.

Results: The mean age of the participants was 56.5±14.6 years (27-83 years). The mean FoDi angle was -6.43±4.96° (range: -24.40° to +11.60°). Absolute deviation of the fovea BMO axis from the horizontal axis was 0-5° in 83 eyes (31.92%), 5-10° in 124 eyes (47.69%), 10-15° in 41 eyes (15.76%), 15-20° in 10 eyes (3.84%), and greater than 20° in 2 eyes (0.79%).

Conclusion: Most OCT devices currently used in the treatment and follow-up of glaucoma patients provide peripapillary retinal nerve fiber layer (RNFL) thickness measurements that are made based on a clinical axis in reference to the horizontal meridian passing through the optic disc center. The results of our study reveal interindividual variation in FoDi angle as well as intraindividual differences in FoDi angle between fellow eyes in the same individual. Disparity between clinical and anatomic quadrants could impact RNFL thickness measurements, which may lead to errors in the diagnosis of glaucoma.

Keywords: Optical coherence tomography, Bruch's membrane opening, minimum rim width, optic disc, glaucoma

Introduction

Glaucoma is among the leading causes of blindness worldwide.[1] Optical coherence tomography (OCT) parameters are reported to be more sensitive than visual field parameters for the early diagnosis of glaucoma.[2] OCT provides objective, measurable, and reproducible values pertaining to peripapillary retinal nerve fiber layer (RNFL) thickness and the optic nerve head (ONH), making it an important tool for early diagnosis and progression monitoring in glaucoma.[3]

Following the first publication on OCT over 25 years ago, various studies have shown that OCT is an important technological development for glaucoma diagnosis.[4,5,6,7,8] The use of spectral-domain OCT (SD-OCT) technology enables the acquisition of more detailed information with higher image resolution and scanning speed compared to time-domain

Address for Correspondence: Zerrin Tuncer MD, Göz Vakfı, Bayrampaşa Eye Hospital, Ophthalmology Clinic, İstanbul, Turkey
Phone: +90 212 674 75 00/517 E-mail: zrrnt@yahoo.com **ORCID-ID:** orcid.org/0000-0003-0082-6921
Received: 30.06.2017 **Accepted:** 17.01.2018

devices (TD-OCT).[9,10] Nevertheless, the value and reliability of OCT for early diagnosis and follow-up in clinical practice are still a subject of debate.[11,12,13] With the widely used SD-OCT devices, the optic disc margins are estimated clinically and RNFL thickness measurements are made by accepting the 0-180° horizontal line passing through the ONH center as the horizontal meridian (Figure 1). In addition, achieving the same head position and measuring through exactly the same points in repeated scans done to assess progression is entirely a matter of chance, which raises questions about reliability.

In the March 2015 update to the SD-OCT (Spectralis; Heidelberg Engineering GmbH, Heidelberg, Germany) device, fovea-disc (FoDi) alignment software was added with version 6.0. When measuring RNFL thickness with this new software, the fovea is first identified automatically (Figure 2), then the optic disc margins are automatically detected (Figure 3), and RNFL thickness is measured based on quadrants determined using the anatomic axis connecting the fovea and ONH center (Figure 4). As the same axis is used when preparing the database, the results obtained from data analysis are more accurate and rotational errors are eliminated. In addition, the FoDi system enables comparison of the same points in serial measurements of the same patient, allowing a more accurate assessment of progression.

The aim of this study was to utilize the FoDi software to investigate interindividual differences in the angle between the axis connecting the fovea center and optic disc center and the horizontal meridian through the OHN center among patients with suspected or diagnosed glaucoma. Considering that RNFL measurements with other devices are made using quadrants based on a standard 0-180° horizontal axis, we wanted to bring attention to the possible effect the discrepancy between these axes may have on diagnostic evaluation.

Materials and Methods

Two hundred sixty eyes of 133 patients (81 females, 52 males) who were diagnosed with glaucoma or were being followed for suspected glaucoma at our hospital were retrospectively included in the study. Patients having a best corrected visual acuity of 20/40 or better, refractive errors with a spherical equivalent of less than ±5.00 diopter, and no macular pathology were included in the study. Patients with a history of previous eye trauma or surgery, peripapillary atrophy, and tilted discs were not included. Data from previous routine ophthalmological examinations, including visual acuity measurements, refractive error assessment, slit-lamp and fundus examinations, and intraocular pressure measurements with Goldmann applanation tonometry, were recorded.

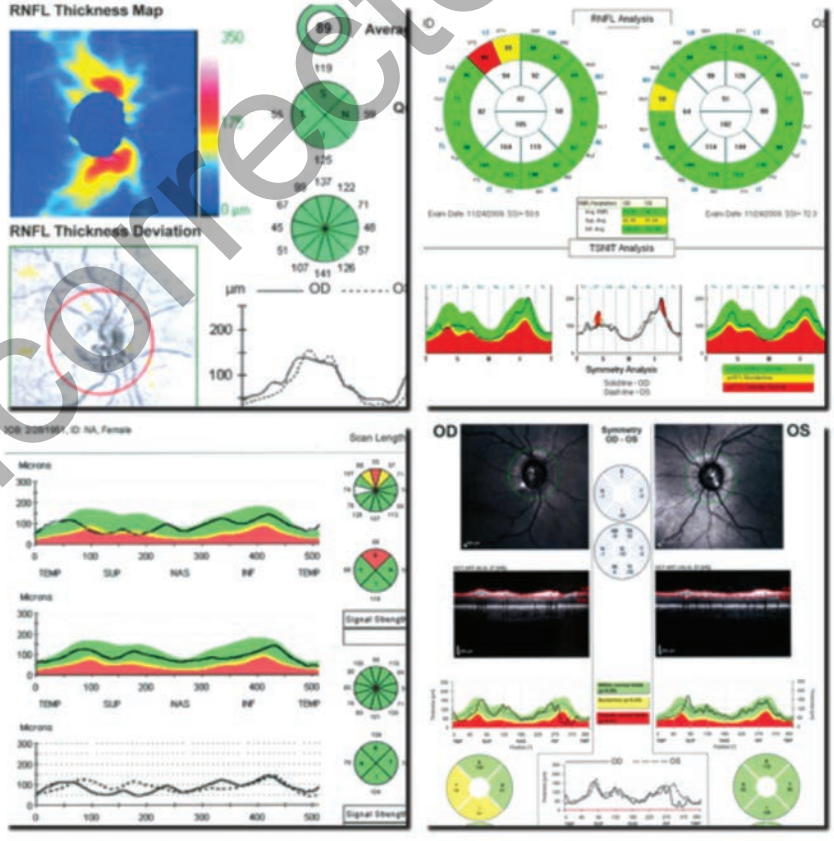

Figure 1. Measurements made in various optical coherence tomography devices based on a 0-180° horizontal meridian
RFNL: Retinal nerve fiber layer, OD: Right eye, OS: Left eye

Prior to OCT, all patients' pupils were dilated with 1% tropicamide. Patients were asked to look at the internal foveal fixation point during measurement. All RNFL thickness measurements were obtained by the same experienced physician (T.Z.) using the glaucoma module (software version 6.0f) of the SD-OCT device (Spectralis; Heidelberg Engineering GmbH, Heidelberg, Germany). Measurements were repeated for eyes with measurement quality less than 15. The angles between the axis connecting the fovea center and optic disc center and the horizontal axis passing through the disc center (FoDi angle, automatically provided in the OCT output) were recorded. In the OCT output, angles were recorded as negative values if the fovea center was below the horizontal axis through the ONH center and as positive values if the fovea center was above the horizontal axis. Absolute deviation values between the anatomic axis and horizontal axis (irrespective of positive/negative direction of FoDi angle) were also recorded.

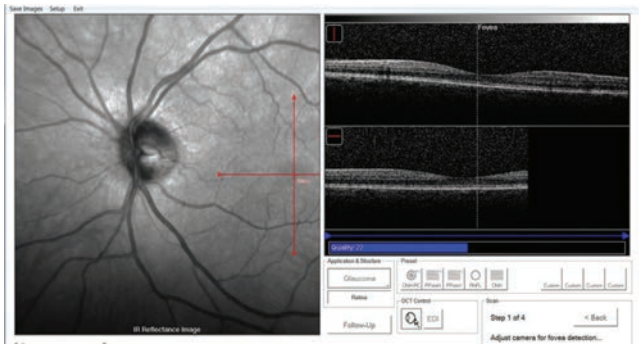

Figure 2. Automatic fovea detection in the fovea-disc software

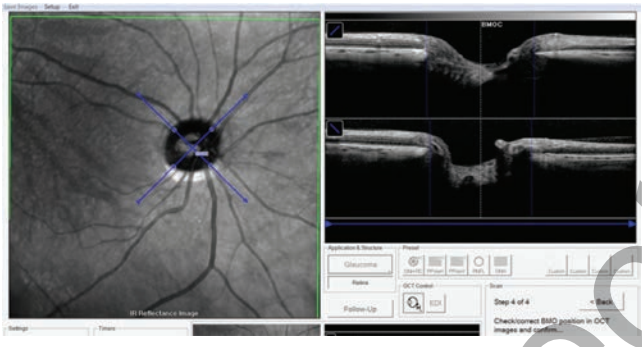

Figure 3. Determination of optic disc margins based on the Bruch's membrane opening in the fovea-disc software

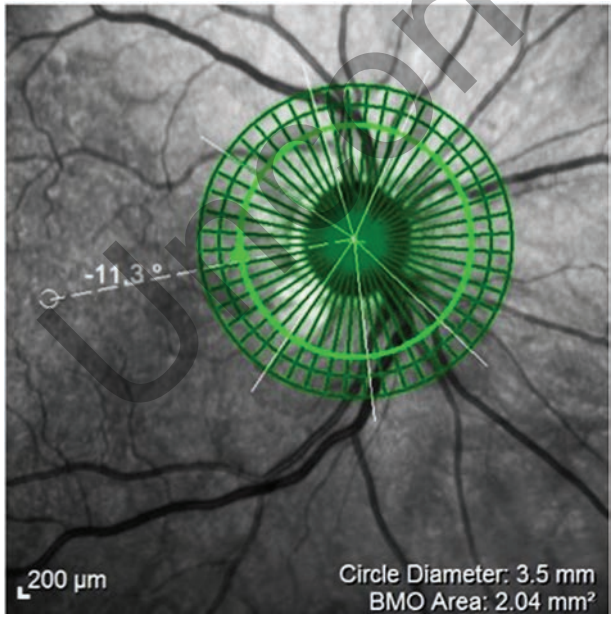

Figure 4. Retinal nerve fiber layer thickness measurement with the fovea-disc software
BMO: Bruch's membrane opening

Statistical Analysis

SPSS software (version 22.0, SPSS, Inc.) was used for statistical analyses. The one-sample Kolmogorov-Smirnov test was used to assess the normality of FoDi angle distribution and the distribution of absolute misalignment angle according to the horizontal axis.

Results

The patients ranged in age from 27 to 83 years, with a mean age of 56.5±14.6 years.

FoDi angles ranged between -24.40° and +11.60°, and the mean value taking into account positive and negative direction was -6.43±4.96°. Of the 260 eyes in the study, FoDi angle was negative in 243 eyes (93.46%) and positive in 16 eyes (6.15%). The anatomical axis and the horizontal axis were on the same plane in only 1 eye. According to the one-sample Kolmogorov-Smirnov test, FoDi angle distribution was normal (p=0.002) (Graphic 1). Analysis of deviations between 0° and 24.4° without regard to positive or negative sign yielded a mean absolute deviation of 7.14±3.95° between the anatomic axis and the horizontal axis. The distribution of absolute deviation values was also normal according to one-sample Kolmogorov-Smirnov test (p=0.2) (Graphic 2).

Deviation from the horizontal axis was 0-5° in 83 eyes (31.92%), 5-10° in 124 eyes (47.69%), 10-15° in 41 eyes (15.76%), 15-20° in 10 eyes (3.84%), and greater than 20° in 2 eyes (0.79%).

Discussion

Morphological changes in glaucoma are detected by assessing the optic nerve head and RNFL. Visual field testing, which is also used in glaucoma diagnosis and follow-up, is a subjective method. OCT emerged in the early 1990s but was more widely used after the introduction of the TD Stratus OCT (Carl Zeiss Meditec) in 2001. The production of the Optovue OCT (Optovue Inc., Fremont, California, USA) device in 2006 and the Cirrus OCT (Carl Zeiss Meditec) device in 2007 using SD-OCT technology enabled more detailed examination of the optic nerve

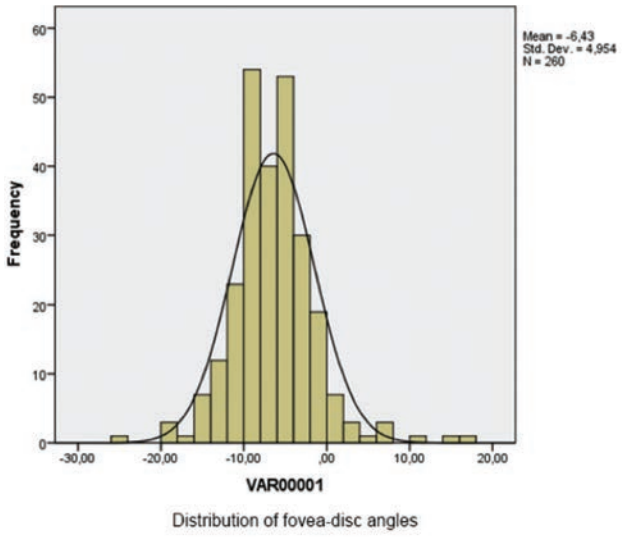

Graphic 1. Distribution of fovea-disc angles between -24.40° and +11.60° (x axis: fovea-disc angles in degrees; y axis: number of eyes)

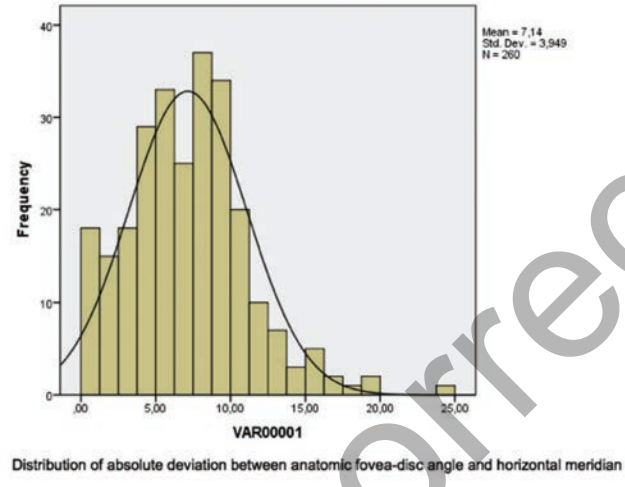

Graphic 2. Distribution of absolute deviation of anatomic fovea-disc angle from horizontal meridian, ranging from 0° to 24.4° (x axis: absolute deviation in degrees; y axis: number of eyes)

head in addition to the RNFL, and the use of OCT became increasingly widespread. Improvements in SD-OCT technology have enabled the visualization of various anatomic features in the assessment of the ONH which were not available until recently.

The glaucoma module of the Spectralis SD-OCT device (software version 6.0; Heidelberg Engineering GmbH, Heidelberg, Germany) evaluates the neuroretinal rim by automatically determining the shortest distance from the inner rim of the BMO to the internal limiting membrane as a reference and measuring RNFL thickness (Figure 5). The BMO minimum rim width (BMO-MRW) is now defined as a new parameter for the diagnosis of glaucoma. Determining MRW in this way is said to result in the most geometrically accurate measurement compared to scanning methods that have been in use since the introduction of OCT.[7,14] Kook et al.[5] reported that in the ONH, BMO-MRW represents the outer margin of the neuroretinal rim and is an anatomically definitive structure that allows neuroretinal rim measurements. When making measurements with standard OCT devices, the optic disc margins are determined by clinical estimation, which is very error-prone (Figure 6). In their study, Helvacioglu et al.[15] emphasized the importance of correctly positioning the 3.4 mm circle when measuring RNFL thickness. Reis et al.[20] stated in their study that due to clinically invisible extensions of the Bruch membrane and sectoral differences, the clinically observable disc margin is not the true disc margin. Numerous studies have emphasized the

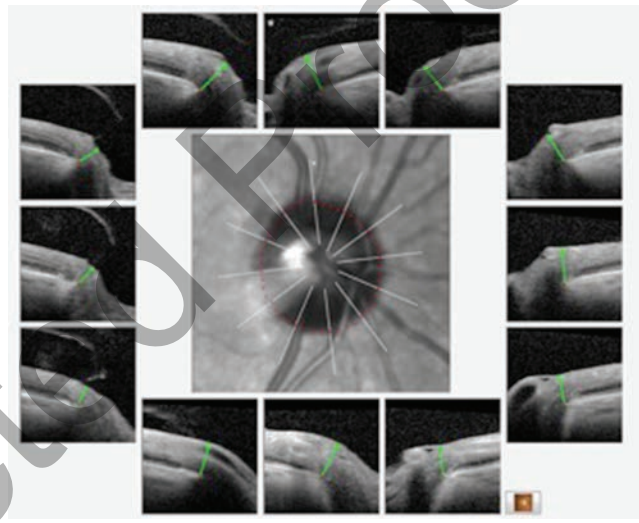

Figure 5. Determination of optic disc margins based on Bruch's membrane opening in the fovea-disc software

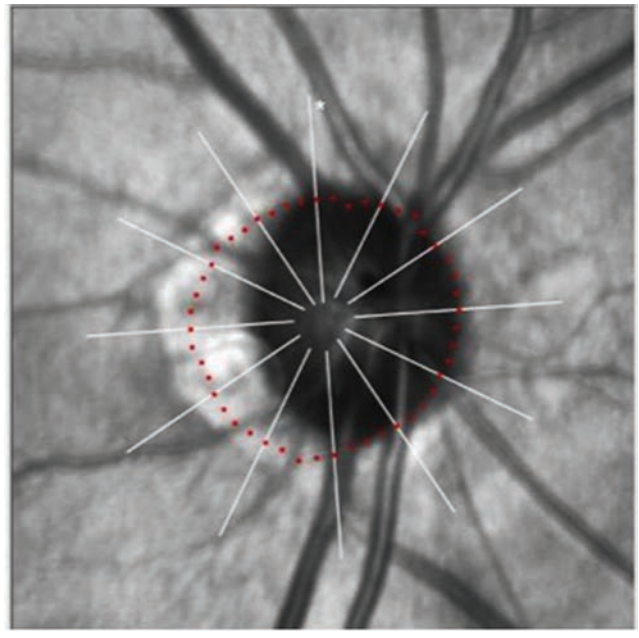

Figure 6. Anatomic disc margins according to Bruch's membrane opening-minimum rim width

importance in preperimetric glaucoma of OCT measurements of RNFL thickness taking into account BMO.[17,18,19,20]

The position of the fovea relative to the optic disc center has recently attracted the attention of some glaucoma researchers and new software has been developed. This is because measurements based on a horizontal meridian do not allow measurements at the same points when monitoring progression, and errors related to head position can lead to misleading results.

The FoDi software add-on found in the glaucoma module of the Heidelberg SD-OCT device automatically provides values for the ocular torsion angle. With the Anatomic Positioning System (APS) in the glaucoma module of Heidelberg SD-OCT, disc margins can be detected automatically based on BMO.[7,9] Using a device with this updated software, the line connecting the center of the optic disc margins automatically determined based on BMO (optic disc center) and the automatically determined fovea center was identified as the anatomical axis. The superior, inferior, nasal, and temporal quadrants are determined based on this axis (Figure 7). We believe this increased the accuracy of the RNFL thickness measurement values we obtained in this study.

There are various studies in the literature concerning the importance of FoDi alignment in the measurement of peripapillary RNFL thickness. In a study analyzing Stratus OCT data of 94 healthy individuals, Vizzeri et al.[9] reported positive linear relationships between signal strength and horizontal deviation and mean RNFL thickness. Similarly, Chauhan and Burgoyn[21] stated that the axis between the fovea and center of the BMO-based optic disc must be used in neuroretinal rim and peripapillary RNFL thickness measurements, otherwise the diagnostic sensitivity of SD-OCT measurements may be reduced.

Helvacioglu et al.[15] measured RNFL thickness in 42 eyes of 21 patients using Optovue SD-OCT and compared measurements made by perfectly centering to the ONH with measurements that were misaligned to the 4 quadrants (superior, inferior, nasal, temporal), and found that misalignment led to falsely low thickness measurements in that quadrant and higher thickness measurements in the opposite quadrant. Similarly, in their study including 222 eyes of 222 patients with ocular hypertension or glaucoma, He et al.[22] emphasized the importance of foveal position relative to the optic disc for normal RNFL thickness distribution. In another study including 164 eyes of 164 non-glaucomatous myopic patients, Choi et al.[23] reported that in eyes with a more negative FoDi angle, the peripapillary RNFL thickness profile was thinner in the superior quadrant and thicker in the inferior quadrant.

Contrary to these studies, Mwanza et al.[24] reported that FoDi alignment had no marked effect on RNFL thickness measurements in their Cirrus HD OCT study including 282 healthy (normative database), 46 non-glaucomatous myopic, and 86 glaucomatous individuals.

The aim of the present study was to emphasize the interindividual variation in FoDi angle, which affects peripapillary RNFL thickness, and to suggest that this variability may impact RNFL thickness measurements and ultimately lead to

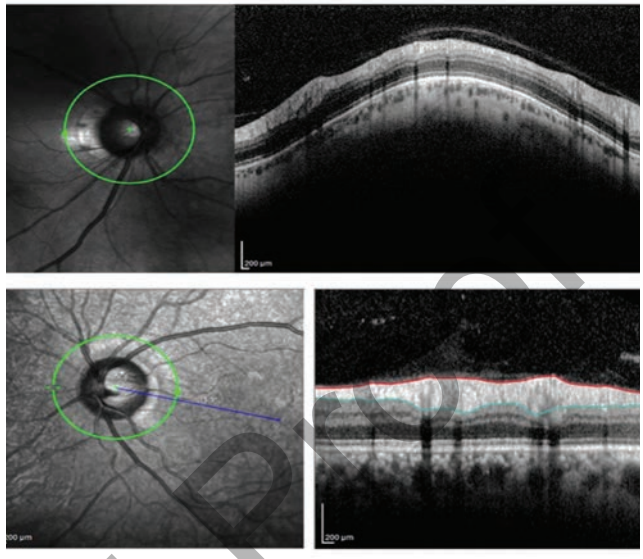

Figure 7. Retinal nerve fiber layer thickness measurement before and after fovea-disc software

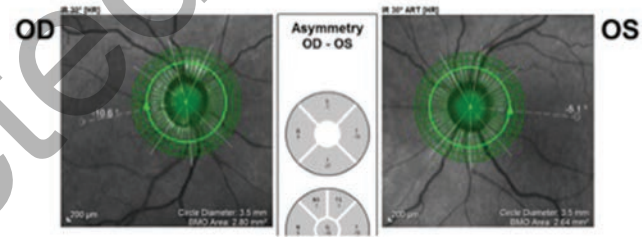

Figure 8. Fovea-disc angle differences between fellow eyes of the same patient
OD: Right eye, OS: Left eye

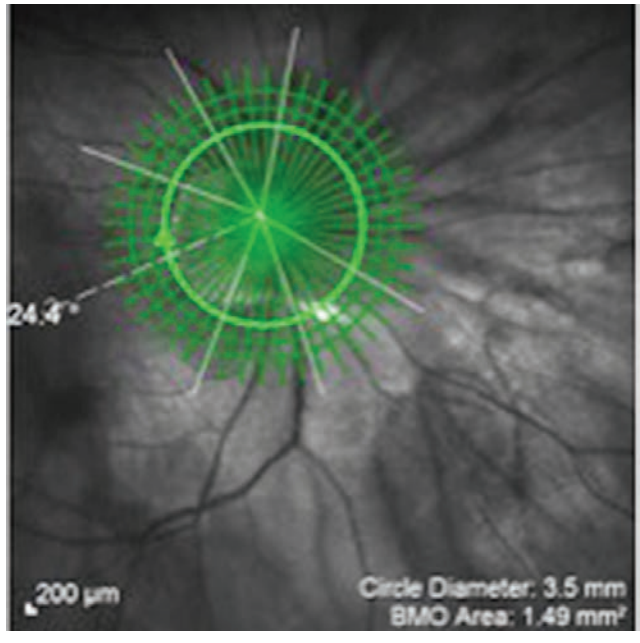

Figure 9. Fovea-disc angle of 24.4°

inaccuracy in glaucoma diagnosis. There are also various studies in the literature attempting to determine this difference. Reis et al.[25] found in their study that the optic disc margin tissue is variable and the angle between the horizontal axis and the axis connecting the fovea and the optic disc center varies between individuals and even between fellow eyes of the same individual. We also observed this intraindividual difference in FoDi angle in all of our patients (Figure 8).

In previous studies, mean FoDi angle values range between -5.6° and -7.7° and the FoDi distribution is between -17° (the fovea is 17° below the disc) and +7° (the fovea is 7° above the disc).[19,26,27,28] Consistent with the literature, the range of FoDi angles in our patients was -24.4° to +11.6° and the mean value was -6.43±4.96°. The range of absolute deviation angles between the anatomical axis and the horizontal axis was 0-24.4°, and the mean absolute deviation was 7.14±3.95°. In our study, the anatomical axis and the horizontal axis were on the same plane in only 1 of 260 eyes. We observed FoDi angles greater than 10° in 20.39% of the eyes (53 eyes) and greater than 20° in 0.79% of the eyes (2 eyes) (Figure 9).

Conclusion

In conclusion, we believe that the disparity between the anatomic axis and horizontal axis observed among patients with diagnosed or suspected glaucoma in our study may affect RNFL thickness measurements and lead to errors in early glaucoma diagnosis. Comparative studies on larger patient series are needed for more definitive results.

Ethics

Ethics Committee Approval: İstanbul University İstanbul Faculty of Medicine Ethics Committee for Clinical Investigations, (number: 1310, decision no: 18).

Informed Consent: Retrospective study.

Peer-review: Externally peer-reviewed.

Authorship Contributions

Concept: Zerrin Tuncer, Mitat Altuğ, Design: Zerrin Tuncer, Mitat Altuğ, Data Collection or Processing: Zerrin Tuncer, Mitat Altuğ, Analysis or Interpretation: Zerrin Tuncer, Literature Search: Zerrin Tuncer, Mitat Altuğ, Writing: Zerrin Tuncer, Mitat Altuğ.

Conflict of Interest: No conflict of interest was declared by the authors.

Financial Disclosure: The authors declared that this study received no financial support.

References

1. Quigley HA, Broman AT. The number of people with glaucoma worldwide in 2010 and 2020. Br J Ophthalmol. 2006;90:262-267.
2. Zaky AG, Yassin AT, El Sayid SH. Short wave-automated perimetry (SWAP) versus optical coherence tomography in early detection of glaucoma. Clin Ophthalmol. 2016;10:1819-1824.
3. Hood DC, De Cuir N, Blumberg DM, Liebmann JM, Jarukasetphon R, Ritch R, De Moraes CG. A SingleWide-Field OCT Protocol Can Provide Compelling Information for the Diagnosis of Early Glaucoma.Transl Vis Sci Technol. 2016;5:4.
4. Huang D, Swanson EA, Lin CP, Schuman JS, Stinson WG, Chang W, Hee MR, Flotte T, Gregory K, Puliafito CA, et al. Optical cohorens tomography. Science. 1991;254:1178-1181.
5. Kook MS, Sung K, Kim S, Park R, Kang W. Study of retinal nevre fibre layer thickness in eyes with high tension glaucoma and hemifield defect. Br J Ophthalmol. 2001;85:1167-1170.
6. Schuaman JS, Hee MR, Puliafitro CA, Wong C, Pedut-Kloizman T, Lin CP, Hertzmark E, Izatt JA, Swanson EA, Fujimoto JG. Quantification of nevre fiber layer thickness in normal and glaucomatous eyes using optical coherence tomography. Arch Ophthalmol. 1995;113:586-596.
7. Ferreras A, Pablo LE, Garway-Heath DF, Fogagnolo P, García-Feijoo J. Mapping Standard automated perimetry to the peripapillary retinal nevre fiber layer in glaucoma. Invest Ophthalmol Vis Sci. 2008;49:3018-3025.
8. Korkmaz B, Yiğit U, Ağaçhan A, Helvacıoğlu F, Bilen H, Tuğcu B. Glokomlu ve normal olgularda optik koherens tomografi ile retina sinir lifi tabakası ve ganglion hücre kompleksi ilişkisinin değerlendirilmesi.Turkish J Ophthalmol. 2010; 40:338-342.
9. Vizzeri G, Bowd C, Medeiros FA, Weinreb RN, Zangwill LM. Effect of signal strength and improper alignment on the variability of stratus optical coherence tomography retinal nerve fiber layer thickness measurements. Am J Ophthalmol. 2009;148:249-255.
10. Chen HY, Chang YC, Lane HY. Correlation in retinal nevre fiber layer thickness between two OCT units. OptopmVis Sci. 2011;88:1326-1332.
11. Ziya A, Arıkan G, Günenç Ü, Çılgıl G. Primer Açık Açılı Glokom, Normal Tansiyonlu Glokom ve Oküler Hipertansiyonda Humphrey Görme Alanı, Optik Koherens Tomografi ve Heidelberg Retina Tomografi Parametrelerinin Korelasyonu. Turk J Ophthalmol. 2011;41:143-150.
12. Çömez AT, Eser İ, Bakar C, Kömür B. Is single measurement enough to get a reliable result with optic coherence tomography? Turk J Ophthalmol. 2012:43:11-15.
13. Mumcuoğlu T, Erdurman C, Durukan AH. Optik Koherens Tomografi Prensipleri ve Uygulamadaki Yenilikler- Olgu Sunumu. Turk J Ophthalmol. 2008;38:168-175.
14. Almobarak FA, O'Leary N, Reis AS, Sharpe GP, Hutchison DM, Nicolela MT, Chauhan BC. Automated Segmentation of Optic Nerve Head Structures With Optical Coherence Tomography. Invest Ophthalmol Vis Sci. 2014;55:1161-1168.
15. Helvacioglu F, Uyar OM, Sencan S, Tunc Z, Kapran Z. Helvacioglu reproducibility index: a new algorithm to evaluate the effects of misalignments on the measurements of retinal nerve fiber layer by spectral-domain OCT. Int J Ophthalmol. 2015:18;8:1008-1012.
16. Gmeiner JM, Schrems WA, Mardin CY, Laemmer R, Kruse FE, Schrems-Hoesl LM. Comparison of Bruch's Membrane Opening Minimum Rim Width and Peripapillary Retinal Nerve Fiber Layer Thickness in Early Glaucoma Assessment. Invest Ophthalmol Vis Sci. 2016;57:575-584.
17. Lu AT, Wang M, Varma R, Schuman JS, Greenfield DS, Smith SD, Huang D; Advanced Imaging for Glaucoma Study Group. Combining nerve fiber layer parameters to optimize glaucoma diagnosis with optical coherence tomography. Ophthalmology. 2008;115:1352-1357.
18. Wu H, de Boer JF, Chen TC. Diagnostic capability of spectral-domain optical coherence tomography for glaucoma. Am J Ophthalmol. 2012;153:815-826.
19. Chen HY, Huang ML. Discrimination between normal and glaucomatous eyes using Stratus optica lcoherence tomography in Taiwan Chinese subjects. Graefes Arch Clin Exp Ophthalmol. 2005;243:894-902.
20. Reis AS, O'Leary N, Nicolela MT, Burgoyne CF, Chauhan BC. Influence of clinically invisible, but optical coherence tomography detected, optic disc magrin anatomy on neuroretinal rimevaluation. Invest Ophthalmol Vis Sci. 2012;53:1852-1860.
21. Chauhan BC, Burgoyne CF. From clinical examination of theoptic disc to clinical assesment of the optic nevre head: a paradigm change. Am J Ophthalmol. 2013;156:218-227.
22. He L, Ren R, Yang H, Hardin C, Reyes L, Reynaud J, Gardiner SK, Fortune B, Demirel S, Burgoyne CF. Anatomic vs. acquired image frame discordance in spectral domain optical cohorence tomography minimum rim measurements. Plos One. 2014;9:e92225.

23. Choi JA, Kim JS, Park CK. The foveal position relative to the optic disc and the retinal nerve fiber layer thickness profile in myopia. Invest Ophthalmol Vis Sci. 2014;55:1419-1426.
24. Mwanza JC, Lee G, Budenz DL. Effect of adjusting retinal nerve fiber layer profile to fovea-disc angle axis on the thickness and glaucoma diagnostic performance. Am J Ophthalmol. 2016;161:12-21.
25. Reis AS, Sharpe GP, Yang H, Nicolela MT, Burgoyne CF, Chauhan BC. Optic disc margin anatomy in patients with glaucoma and normal controls with spectral domain optical coherence tomography. Ophthalmology. 2012;119:738-747.
26. Megias AV, de-la-Casa JMM, Garcia MS, Larrosa JM, Feijoo JG. Clinical relevance of foveal location on retinal nevre fiber layer thickness using the new FoDi software in spectralis optical cohorence tomography. Invest Ophthalmol Vis Sci. 2013;54:5771-5776.
27. Rohrschneider K. Determination of the location of the fovea on the fundus. Invest Ophthalmol Vis Sci. 2004;45:3257-3258.
28. Piedrabita Alanso E, Valverde Megias A. Gomezd de Liano R. Rotation of retinal vascular arcades and comparison with disc fovea angle in the assesement of cycloposition. Br J Ophthalmol. 2014;98:115-119.

DOI: 10.4274/tjo.39049
Turk J Ophthalmol 2018;48:185-189

Original Article

A Custom-made Pupillometer System for Characterizing Pupillary Light Response

Nefati Kıylıoğlu*, Mahmut Alp Kılıç*, Tolga Kocatürk**, Seyhan Bahar Özkan**, Mehmet Bilgen***
*Adnan Menderes University Faculty of Medicine, Department of Neurology, Division of Clinical Neurophysiology, Aydın, Turkey
**Adnan Menderes University Faculty of Medicine, Department of Ophthalmology, Aydın, Turkey
***Adnan Menderes University Faculty of Medicine, Department of Biophysics, Aydın, Turkey

Abstract

Objectives: This paper presents the design and construction of a viable pupillometer system and demonstrates its merits with extensive validation tests.

Materials and Methods: A web camera was modified by removing its infrared filter and mounted on a chin rest. Light emitting diodes (LEDs) operating at infrared and visible spectra were integrated to provide background and light stimulus, respectively. The LEDs were controlled by a microprocessor board. Stimulation was presented using a periodic paradigm with variable period and duty cycle. Videos of both pupils were recorded at 30 frames/second and processed offline using software developed in-house. The overall system was validated with data gathered from individuals with healthy vision under different stimulation paradigms. Temporal variations in pupil size were determined and analyzed statistically.

Results: The analysis revealed that the pupil sizes were accurately measured from the video frames provided that reflections from both infrared and visible lights remain outside the pupil. The system achieved moderate to excellent repeatability scores (87.8 and 86.8% for short 1 second and long 2 second pulses, respectively), which demonstrated its effectiveness and confirmed that it can be used reliably as a pupillometer.

Conclusion: The proposed pupillometer system produces useful, quantitative data characterizing pupillary light response. However, further development and implementation are needed to potentially turn it into a low-cost alternative for other studies involving the autonomic nervous system, cognitive function, drug metabolism, pain response, psychology, fatigue, and sleep disorders.

Keywords: Pupillary light reflex, pupillary response, pupillometer

Introduction

The pupil is an important functional structure that balances the amount of illumination entering the eye to enable clear vision. The sphincter pupilla and dilator pupilla muscles act together under the control of the parasympathetic and sympathetic nervous systems. The muscles are respectively governed by the oculomotor nerve, sympathetic nervous system tracts and fibers that are located in the mesencephalon and the cervical spinal cord. The functional status of these structures (optic nerve, mesencephalon, spinal cord, oculomotor nerve, cervical sympathetic fibers, and pupillary muscles) is evaluated by the pupillary light response (PLR).[1] Although physical examination of PLR is the usual method of evaluation, use of a device called a pupillometer offers more diagnostic sensitivity than physical examination alone.[2] Commercial pupillometers are both costly and unavailable in clinical practice, especially in developing countries. Also, they lack flexibility and versatility for research purposes where light stimulation under different paradigms may be required. This paper addresses this issue.

Address for Correspondence: Nefati Kıylıoğlu MD, Adnan Menderes University Faculty of Medicine, Department of Neurology, Division of Clinical Neurophysiology, Aydın, Turkey Phone: +90 532 516 51 88 E-mail: knefati@gmail.com **ORCID-ID:** orcid.org/0000-0001-5783-1719
Received: 09.12.2017 **Accepted:** 23.03.2018

We have developed a viable pupillometer system for real-time video recording of pupil response to light stimulation and video analysis software for characterizing PLR. The overall system was validated and its merits were investigated with the data acquired from healthy individuals subjected to periodic white light stimulations with short and long pulse durations.

Materials and Methods

Video Acquisition and Recording Hardware

Video acquisition and recording functions in the pupillometer system were achieved in a cost-effective manner using a common web camera (INCA_IC-3562 model) attached to a standard laptop PC via a USB cable and a software package (AMCAP Version 8.11). The camera was modified by removing the infrared filter in front of its lens. This expanded the operation of the camera into a near-infrared spectrum and allowed visualization of the pupil in both dark and light conditions. The frame rate of the camera was set at 30 frame/second, but the actual rate was determined to be 25 frame/second for the real video recordings in mpeg4 format. During the examination, the subject sat on a chair in an upright position, placed his/her chin on a metal structure to which the camera was mounted, and was asked to focus on the camera (Figure 1). Eye-to-camera position was carefully leveled to remain horizontal, and the distance between was maintained at 24 cm.

Infrared and White Light Setup

The stimulation arrangement consisted of infrared and white light emitting diodes, placed separately on a specially designed circuit board. Four diodes were placed side-by-side as a bank. White lights were positioned below the infrared diodes. The printed circuit board spanned both eyes and was placed near the cheek, below the eyes. It was oriented at an angle of approximately 130-140° to the horizontal, sloping away from the subject. This orientation prevented white light reflections as they remained below the pupil during the recordings. Otherwise, the reflections within the pupil interfered with the process of pupil size estimation during the off-line video analysis. This approach improved the accuracy of the estimates calculated using semi-automatic software developed in-house as discussed below.

Both the white light and infrared diodes were connected electrically to a microcontroller board (Arduino UNO). It was programmed (Arduino 1.6.0) to carry out the specific stimulation paradigms by periodically turning the white light diodes on and off for a predefined duration while leaving the infrared diodes on for the entire recording time. The peak wavelength of the infrared diode was 940 nm. Turning this diode on alone did not induce any pupillary reaction nor interfere with the eye response induced by the white light.

In a PLR examination, both eyes were stimulated simultaneously with light-dark periods and the responses of both pupils were recorded throughout the session. The resulting video was appropriately named and stored digitally for post-processing.

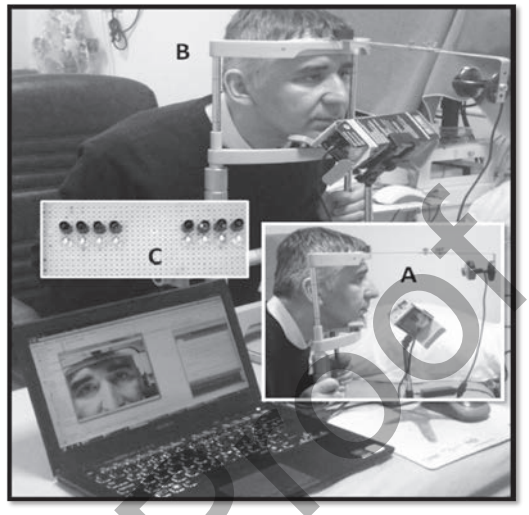

Figure 1. Custom-made pupillometer system used in this study. A) Lateral view, B) Antero-lateral view, C) Placement of infrared (lower) and white light diodes (upper) from the front view

Video Processing Software

The video files were analyzed using software developed in the Matlab environment (Matlab Version R2015A, The MathWorks Inc., Natick, MA). The Matlab code is given in Figure 2. The program runs in semiautomatic mode. The code opens the video file, starts with a predefined video frame, and lets the user manually mark the centers of the pupils in both eyes. The pupils in the first and the following frames were identified automatically. Also, the pupils were segmented out and their sizes were calculated pixel-wise, both automatically, in each video frame and recorded sequentially in a text file along with the frame number. Estimating pupil size was not possible in some frames due to eye blinking or closing. These data points were filled with zero automatically.

Validation Measurements of Repeatability

The light stimulation paradigms used for validation purposes involved periodic short 1 second light/1 second dark or long 2 second light/2 second dark pulses. Each recording started with a baseline acquisition of 5 second followed by at least 12 periods of light/dark stimulus cycles. Under each paradigm, the intensity produced by white light was measured using a power meter (Lutron-Model LX-1108) which was placed at the same level as the left eye. During the examination, videos were acquired with both 1 second and 2 second stimulation paradigms. To test repeatability, the same paradigm was repeated in each session with a 2 minute rest interval in between. The videos were processed off-line using the code in Figure 2. The pupil size estimates for both eyes in the frames under each stimulation paradigm were sequentially stored in text files.

Ethical Issues, Inclusion and Exclusion Criteria

The study was approved by the Medical Ethics Committee of Adnan Menderes University (2015/577). Signed consent forms were obtained from the volunteers. Inclusion criteria were: having no history of any previous disorders which caused

```
xyloObj=VideoReader('file.avi') ;
nFrames = xyloObj.NumberOfFrames
vidHeight = xyloObj.Height;
vidWidth = xyloObj.Width;
mov(1:nFrames) = struct('cdata', zeros(vidHeight, vidWidth, 3, 'uint8'),'colormap', []);
start=1; stop=nFrames;
esik_yansima=240; %threshold for filling possible reflections in pupil
esik_pupilsegment=60; % segmentation out of pupil
alan=200;      % area of connected regions
for k = start : stop
 k; cdata = read(xyloObj, k); A=double(rgb2gray(cdata)) ;
 if k==start
     imagesc(A); colormap(gray); [c,r,P] = impixel ;
     Mask=A;
     for ix=1:640
     for iy=1:480
      Mask(iy,ix)=0;
      if sqrt( (ix-c(1))^2+ (iy-r(1))^2) <25
        Mask(iy,ix)=1;
      end
      if sqrt( (ix-c(2))^2+ (iy-r(2))^2) <25
        Mask(iy,ix)=1;
      end
     end
     end
     imshow(Mask); ioutside=find(Mask==0) ; C=A.*Mask;
     iinside=find(C>esik_yansima) ;  %find bright points inside pupil and fix it
     C(iinside)=0; C(ioutside)=255; imagesc(C); pause(1)
     BW = roicolor(C,0,esik_pupilsegment);
     BW2 = bwselect(BW,c,r); BW2=bwfill(BW2,'holes'); imagesc(A.*(1-BW2));
     L = bwlabel(BW2); stats = regionprops(L,'all') ;
     j=1; ab=[stats(:).Area]; ab(ab>alan); area=[j,ab(ab>alan)] ; pause(1)
 elseif (k>start & k<stop)
     C=A.*Mask; iinside=find(C>esik_yansima) ; C(iinside)=0; C(ioutside)=255;
     BW = roicolor(C,0,esik_pupilsegment); BW2=bwfill(BW,'holes');
     imagesc(A.*(1-BW2))
     L = bwlabel(BW2); stats = regionprops(L,'all') ;
     j=j+1 ; ab=[stats(:).Area] ; ab(ab>alan); sdim=size(ab(ab>alan)) ;
     if sdim(2) ==2
       area=cat(1,area,[j,ab(ab>alan)]) ;
     else
       area=cat(1,area,[j,0,0]) ;
     end
     pause(0.05)
 else
 end ;
end
fid = fopen('area.txt','w');
fprintf(fid,'%6d %6d %6d\n',area');
fclose(fid)
```

Figure 2. Matlab code for video processing to estimate pupil sizes in both eyes. The variables "esik_yansima", "esik_pupilsegment" and 'alan' in the program may require adjustments based on the purpose of the video analysis in order to improve the accuracy of the pupil size estimates

transient visual loss, being free from any medication, and having no sleep complaints. After being informed about the procedures, volunteers underwent a full ophthalmological evaluation either between 10:00 and 12:00 am or between 1:00 and 4:00 pm.[3] Those with a best corrected visual acuity of 20/20 in both eyes were subjected to further examination for PLR. All volunteers completed the evaluation process.

Temporal Analysis of Pupil Size Changes with Light Stimulus

The text files were analyzed in Excel (MS Office) and the temporal data were plotted as a function of frame number. Data series with zero values or those identified with eye movement or with abnormally high or low values were excluded from the analysis. Once satisfied with the behavior of the displayed graphs, we went back and normalized the pupil size measurements frame-by-frame by the baseline recording (averaged over 5 s of time duration). That is, all pupil size estimates including the baselines were scaled according to the following formula:[4]

Normalized pupil area (NPA) = (Average baseline - Pupil size)/Average baseline x 100.

The resulting NPA readings were equivalent to the percentage reduction in pupil size. Normalization also reduced the effect of aging on the temporal dynamics of pupil size, according to a previous report.[5]

Next, the time signals were consecutively extracted period by period (i.e. over the total duration of 12 consecutive light and darkness) and the segments were further averaged temporally to obtain a single trace of pupil response profile for each eye. This approach eliminated the variation in pupil response with the stimulus cycle. The resulting signal profile was described by a set of parameters which were then measured from the data gathered from all research participants and further analyzed statistically.

Statistical Analysis

The data included temporal variations of NPA. The periodic signals obtained from both right and left eyes under the stimulation protocols were investigated for compatibility, consistency, and repeatability by intra-class correlation coefficient test (single-measurement, absolute-agreement, 2-way mixed effects model).[6]

Results

Thirty-seven volunteers, 16 females (age: mean 34; min 20 and max 61 years old) and 21 males (age: mean 36; min 20 and max 60 years old), were included in this study. The test runs with the stimulation paradigms producing light intensities listed in Table 1. The intensity values represent the average over 12 periods of dark and light durations. The light levels achieved with the paradigms were sufficiently high to induce strong pupil responses. Figure 3 shows the representative graphs of NPAs as obtained from an examination session with the procedures described above. In both eyes, NPAs exhibited identical behaviors, indicating the capability of the system to promptly follow changes in pupil size in response to the light stimulus.

Intra-class correlation coefficient calculations from the first and second trials under both paradigms are summarized in Table 2. Most cases had moderate to excellent repeatability scores (87.8% for the 1 second and 86.8% for the 2 second stimulation paradigms). These findings confirmed the quality of the match between the signal pairs obtained with repetitions.[6,7]

Figure 4 shows representative mean traces (average over 12 cycles) of the pupil response in Figure 3. The corresponding plots for each eye also exhibit very close traces.

Discussion

In spite of commercial availability, there are still attempts to build custom-made pupillometers to address specific concerns.[7] Parameters such as initial pupil size and duration/velocity/latency of pupillary contraction and dilatation are of clinical interest as they reflect the functional state of the eye. Classically, the V-shaped response was observed with the light stimulus. When the light was on, the pupil first contracts and then dilates after the light turns off (Figures 3, 4). The temporal appearances of PLR traces for the 1 second and 2 second stimulus

Table 1. Light intensities measured under each light stimulation paradigm

	Luminance (lux)		
Paradigms	**Baseline**	**Light on**	**Light off**
Short (1 s light/1 s dark)	0.26	31.51	7.39
Long (2 s light/2 s dark)		36.43	2.09

Baseline acquisitions in all cases were 5 s long. The rest of the trials with the two stimulation paradigms were 2 min long
s: second

Table 2. Intraclass correlation coefficient values calculated from the normalized pupil area signal pairs (first and second trials) gathered from all subjects (n=37) for both eyes (74 eyes)

Score	Frequency	
	1 s light/1 s dark n (%)	**2 s light/2 s dark n (%)**
Excellent (ICC >0.90)	12 (16%)	2 (2.9%)
Good (ICC 0.75-0.90)	25 (33.8%)	38 (55.9%)
Moderate (ICC 0.50-0.75)	27 (37.8%)	19 (28%)
Poor (ICC <0.50)	9 (12.2%)	9 (13.2%)
Total*	63 (100%)	68 (100%)

*Totals do not add up to 74 because sufficient pupil size data could not be obtained in some cases ICC: Intraclass correlation coefficient
s: second

paradigms were similar to those produced by the commercial pupillometers.[7] However, while commercial devices typically produce data from a single stimulus with a fixed period and duty cycle, our system is capable of handling periodic stimulations with different periods and duty cycles. The system is also flexible in the sense that white diodes can be replaced by those with different colors of interest to facilitate PLR studies concerning color dependence. Moreover, the continuous stimulation does not lead to habituation.

Eye movements (saccades) affect video-based estimates of pupil size, especially when a computer screen is used for stimulation purposes.[8] In our setup, the patient was asked to focus on the camera's shutter during the examination. The software monitored the stability of the eye by tracking the center of mass of the pupil segment in each frame. Positional shifts of more than 10 pixels in length were considered as indicative of eye movement. These efforts ensured increased accuracy in the pupil capturing area. However, in a very small number of cases, data gathering and analysis were limited due to low eyelid position, frequent blinking, insufficient data capturing of pupil area because of interference with shadow due to light-dark cycle, and also interference related to make-up in female subjects. This is why the total numbers in the frequency column of Table 2 do not add up to 74 (37 participants with 2 eyes), meaning that it was not feasible to estimate the pupil size even after filling the missing data points with zero. Nevertheless, in the absence of such issues, the custom-made pupillometer and video analysis software platform developed in this study revealed

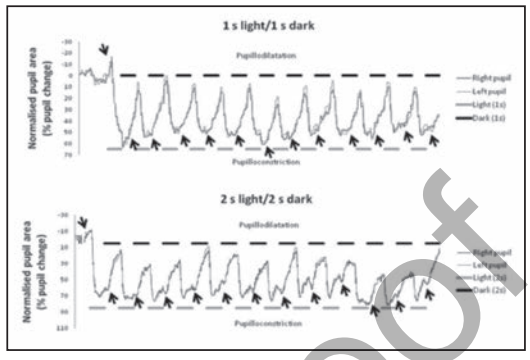

Figure 3. Temporal profiles of normalized pupil areas in both eyes under the stimulation paradigms as encoded by the black and gray bars. The single arrow at upper left points to small pupil dilatation when the lights were off and the lower twelve arrows point to pupil constrictions when the lights were on

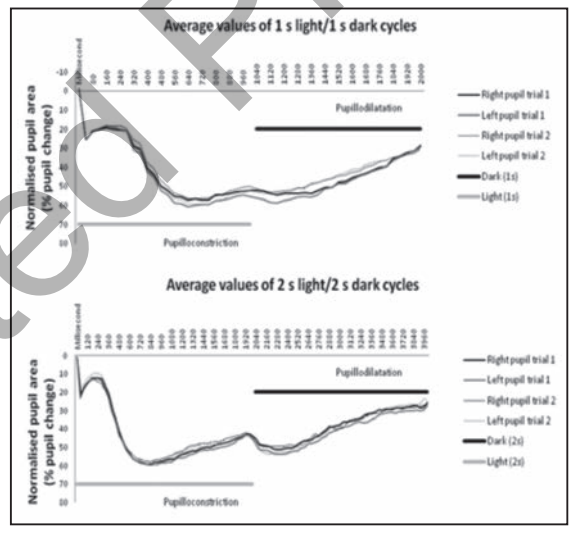

Figure 4. Mean response profiles of pupil size to 1 second light/1 s dark (top trace) and 2 second light/2 second dark (bottom trace) stimulus durations as encoded by the black and gray bars

moderate to excellent repeatability scores (greater than 85% of the people investigated) and its performance was comparable to the test-retest repeatability of the previous pupillometer scores.[2,7] Lei et al.[7] evaluated the test-retest reliability of hemifield, central-field, and full-field chromatic pupillometry. For the post-illumination pupil response, they determined intra-class correlation coefficients of 0.84 (0.69-0.95) and 0.94 (0.83-0.98) at full field stimulation with blue light. Unlike our study, which did not assess interobserver variability, Couret et al.[2] investigated the interobserver variability and reported intra-class correlation coefficients of 0.95 and 0.87 for pupil size at both resting and after light stimulation, respectively. Our intra-class correlation coefficient values were similar, confirming that the pupillometer system can be used reliably to evaluate PLR.[6]

The potential value of PLR evaluations in normal and disease conditions have been investigated in many studies in areas such as the autonomic nervous system, cognitive function, drug metabolism, pain response, psychology, fatigue, and sleep

disorders.[9,10,11,12,13,14,15,16,17,18,19,20] There is a growing interest in diagnosis in these areas, and our custom-made pupillometer may be useful as an easily-applicable, non-invasive diagnostic tool.

Study Limitations

As mentioned earlier, in a few cases there were limitations in data gathering and analysis due to low eyelid position, frequent blinking, insufficient data capturing due to shadowing, and interference related to cosmetics worn by female subjects. Extracting data from the videos was also time-consuming.

Conclusion

Our study demonstrates that our custom-made pupillometer and video analysis software platform can be used to reliably evaluate PLR. However, further development and implementation are needed to potentially turn it into a low-cost alternative.

Ethics

Ethics Committee Approval: Adnan Menderes University, Medical Faculty Ethic Committee 2015-577.

Informed Consent: Signed consent was obtained from the volunteers.

Peer-review: Externally and internally peer-reviewed.

Authorship Contributions

Concept: Nefati Kıylıoğlu, Mehmet Bilgen, Tolga Kocatürk, Design: Mehmet Bilgen, Mahmut Alp Kılıç, Nefati Kıylıoğlu, Data Collection or Processing: Nefati Kıylıoğlu, Mahmut Alp Kılıç, Analysis or Interpretation: Nefati Kıylıoğlu, Mehmet Bilgen, Tolga Kocatürk, Mahmut Alp Kılıç, Seyhan Bahar Özkan, Literature Search: Nefati Kıylıoğlu, Mehmet Bilgen, Mahmut Alp Kılıç, Tolga Kocatürk, Writing: Nefati Kıylıoğlu, Mehmet Bilgen.

Conflict of Interest: No conflict of interest was declared by the authors.

Financial Disclosure: The authors declared that this study received no financial support.

References

1. Kardon R. Regulation of Light through the Pupil. In: Levin L, Nilsson S, Ver Hoeve J, Wu S, Kaufman P, Alm A, eds. Adler's Physiology of the Eye. (11th ed). Elsevier; 2011:502-525.
2. Couret D, Boumaza D, Grisotto C, Triglia T, Pellegrini L, Ocquidant P, Bruder NJ, Velly LJ. Reliability of standard pupillometry practice in neurocritical care: an observational, double-blinded study. Crit Care. 2016;20:99.
3. Zele AJ, Feigl B, Smith SS, Markwell EL. The circadian response of intrinsically photosensitive retinal ganglion cells. PLoS One. 2011;6:e17860.
4. Kardon R, Anderson SC, Damarjian TG, Grace EM, Stone E, Kawasaki A. Chromatic pupil responses: preferential activation of the melanopsin-mediated versus outer photoreceptor-mediated pupil light reflex. Ophthalmology. 2009;116:1564-1573.
5. Adhikari P, Pearson CA, Anderson AM, Zele AJ, Feigl B. Effect of Age and Refractive Error on the Melanopsin Mediated Post-Illumination Pupil Response (PIPR). Sci Rep. 2015;5:17610.
6. Koo TK, Li MY. A Guideline of Selecting and Reporting Intraclass Correlation Coefficients for Reliability Research. J Chiropr Med. 2016;15:155-163.
7. Lei S, Goltz HC, Chandrakumar M, Wong AM. Test-Retest Reliability of Hemifield, Central-Field, and Full-Field Chromatic Pupillometry for Assessing the Function of Melanopsin-Containing Retinal Ganglion Cells. Invest Ophthalmol Vis Sci. 2015;56:1267-1273.
8. Adhikari S, Stark DE. Video-based eye tracking for neuropsychiatric assessment. Ann N Y Acad Sci. 2017;1387:145-152.
9. Fotiou F, Fountoulakis KN, Goulas A, Alexopoulos L, Palikaras A. Automated standardized pupillometry with optical method for purposes of clinical practice and research. Clin Physiol. 2000;20:336-347.
10. Adhikari P, Zele AJ, Feigl B. The post-illumination pupil response (PIPR). Investig Ophthalmol Vis Sci. 2015;56:3838-3849.
11. Taşkıram Çömez A, Kömür B, Eser İ. Assessment of Pupil Diameters of Emmetropes and Myopes under Photopic, Mesopic and Scotopic Conditions, Using the Infrared Pupillometer Integrated Within Schwind Sirius Multifunctional Diagnostic Device. Turkiye Klin J Med Sci. 2012;32:1226-1234.
12. Türk A, Durmuş Aykut A, Kola M, Erdöl H. The Effect of Phacoemulsification Surgery on Pupil Size in Diabetic and Nondiabetic Cases. Turkiye Klin J Med Sci. 2014;34:145-151.
13. McLaren JW, Hauri PJ, Lin SC, Harris CD. Pupillometry in clinically sleepy patients. Sleep Med. 2002;3:347-352.
14. Hublin C, Matikainen E, partinen M. Autonomic nervous system function in narcolepsy. J Sleep Res. 1994;3:131-137.
15. Philby MF, Aydinoz S, Gozal D, Kilic S, Bhattacharjee R, Bandla HP, Kheirandish-Gozal L. Pupillometric findings in children with obstructive sleep apnea. Sleep Med. 2015;16:1187-1191.
16. Nikolaou A, Schiza SE, Giakoumaki SG, Roussos P, Siafakas N, Bitsios P. The 5-min pupillary alertness test is sensitive to modafinil: A placebo controlled study in patients with sleep apnea. Psychopharmacology (Berl). 2008;196:167-175.
17. de Seze J, Arndt C, Stojkovic T, Ayachi M, Gauvrit JY, Bughin M, Saint Michel T, Pruvo JP, Hache JC, Vermersch P. Pupillary disturbances in multiple sclerosis: Correlation with MRI findings. J Neurol Sci. 2001;188:37-41.
18. Fotiou F, Fountoulakis KN, Tsolaki M, Goulas A, Palikaras A. Changes in pupil reaction to light in Alzheimer's disease patients: A preliminary report. Int J Psychophysiol. 2000;37:111-120.
19. Fountoulakis K, Fotiou F, Iacovides A, Tsiptsios J, Goulas A, Tsolaki M, Ierodiakonou C. Changes in pupil reaction to light in melancholic patients. Int J Psychophysiol. 1999;31:121-128.
20. Connelly MA, Brown JT, Kearns GL, Anderson RA, St Peter SD, Neville KA. Pupillometry: a non-invasive technique for pain assessment in paediatric patients. Arch Dis Child. 2014;99:1125-1131.

DOI: 10.4274/tjo.20270
Turk J Ophthalmol 2018;48:190-195

Original Article

The Effects of Anti-Vascular Endothelial Growth Factor Drugs on Retinal Pigment Epithelial Cell Culture

Mustafa Şahiner*, Dilek Bahar**, Ayşe Öner*, Zeynep Burçin Gönen***, Metin Ünlü*, Duygu Gülmez Sevim*, Çağatay Karaca*, Galip Ertuğrul Mirza*
*Erciyes University Faculty of Medicine, Department of Ophthalmology, Kayseri, Turkey
**Erciyes University Betül-Ziya Eren Genome and Stem Cell Center, Kayseri, Turkey
***Erciyes University Faculty of Dentistry, Department of Oral and Maxillofacial Surgery, Faculty of Dentistry, Kayseri, Turkey

Abstract

Objectives: To assess the effects of anti-vascular endothelial growth factor (VEGF) drugs on retinal pigment epithelium cell culture.

Materials and Methods: Aflibercept (0.5 mg/mL), bevacizumab (0.3125 mg/mL), and ranibizumab (0.125 mg/mL) were applied to retinal pigment epithelium cell cultures isolated from the enucleated eyes of New Zealand white rabbits. Viability, apoptosis, proliferation, and senescence of the cells were evaluated in control and drug-treated cultures at the end of 72 hours.

Results: Cells treated with aflibercept showed increased viability and decreased apoptosis compared to the control culture and both the bevacizumab- and ranibizumab-treated groups ($p<0.05$). Statistically increased apoptosis and decreased viability were found in the bevacizumab and ranibizumab-treated groups compared with the control group ($p<0.05$). There were no statistically significant differences in cell proliferation and senescence between the groups ($p>0.05$).

Conclusion: Anti-VEGF drugs did not affect senescence or proliferation of retinal pigment epithelium cells. Aflibercept was found to decrease apoptosis and increase cell viability, while ranibizumab and bevacizumab increased apoptosis and reduced cell viability in retinal pigment epithelium culture.

Keywords: Anti-VEGF, cell culture, senescence, retinal pigment epithelial cell

Introduction

It is well known that vascular endothelial growth factor A (VEGF-A) is a main mediator of angiogenesis and increased vascular permeability in retinal vascular disorders.[1,2,3,4] The inhibition of vascular endothelial growth factor (VEGF) has been a key point in experimental and clinical studies under research. The effectiveness of intravitreal administration of various anti-VEGF agents is well established in the treatment of macular edema of different origins.[5] The mechanism of action of these drugs when delivered intravitreally is complex and involves the blocking of various types of VEGFs, decreased permeability of newly formed blood vessel walls, and reduced swelling of the retinal layers. In recent years, several reports have demonstrated the impact of anti-VEGF drugs upon different cell cultures in vitro.[6,7,8,9,10,11] Our goal was to investigate the effects of anti-VEGF drugs on viability, apoptosis, proliferation, and senescence in retinal pigment epithelium (RPE) cell culture, which can serve as an in vitro model.

In this study, we compared the proliferative and cytotoxic effects of aşibercept (0.5 mg/mL), bevacizumab (0.3125 mg/mL), and ranibizumab (0.125 mg/mL) on RPE cell cultures by evaluating viability, apoptosis, proliferation, and senescence in control and drug-treated cells after 72 hours.

Address for Correspondence: Metin Ünlü MD, Erciyes University Faculty of Medicine, Department of Ophthalmology, Kayseri, Turkey
Phone: +90 536 830 59 72 E-mail: drunlumetin@hotmail.com **ORCID-ID:** orcid.org/0000-0003-2505-9853
Received: 21.11.2017 **Accepted:** 02.03.2018

Materials and Methods

Animals

Eyes were obtained from 4 New Zealand white rabbits that weighed between 1.5 and 2.2 kg. Animal care and surgical procedures were attempted in scrupulous agreement with the approval of the Ethical Committee of Erciyes University (TTU-2015-5996). The rabbits were killed by injecting a lethal dose of ketamine/xylazine. The globes were enucleated and placed in Ca^{2+} and Mg^{2+}-free phosphate buffered saline augmented with penicillin/streptomycin (GIBCO, 15140-0122).

Isolation and Culture of Rabbit Retinal Pigment Epithelium

Rabbit RPE cells were isolated and maintained as described by Chang et al.[12] After incubating the globes with 2% dispase for 15 minutes, an incision was made 3 mm from the limbus and continued circumferentially. After removal of the cornea and lens, 4 radial incisions were made in the posterior segment, and this part was incubated in Dulbecco's modified Eagle's medium/ Ham's F12 (DMEM/ F12) medium augmented with 10% fetal bovine serum for 2 hours. Finally, the RPE cells were separated from the neural retina and choroid as a sheet with micropipettes and observed under a stereo microscope (Olympus BX51, Japan). Passage 3 cells were used for the study and drugs were applied to the cultures 24 hours after fresh cell plating.

Ranibizumab (Lucentis, Novartis, Switzerland), a fragment of a human monoclonal antibody against VEGF-A selectively binds all isoforms of VEGF-A (VEGF110, VEGF121, and VEGF165), was applied at a concentration of 0.125 mg/mL. Bevacizumab (Avastin, Genetech/Roche, USA), a monoclonal antibody against VEGF which is used off-label to treat various eye diseases, was added to the cultures at a concentration of 0.3125 mg/mL. Aflibercept (Eylea, Bayer Health Care, Germany), a fusion protein that binds to circulating VEGF (subtypes VEGF-A and VEGF-B) and placental growth factor (PGF), was used at a concentration of 0.5 mg/mL.

Immunocytochemistry Staining

For immunofluorescence staining, the RPE cells were fixed with 0.4% paraformaldehyde in PBS and permeabilized with 0.4% Triton X-100. Bovine serum albumin (10 mg/mL) was used as a stabilizing agent for proteins such as antibodies and enzymes. The cells were incubated overnight with primary antibody (zonula occludens protein 1 [Zo-1] invitrogen, 330100 and cytokeratin 18 chemicon, MAB3234). Labeled cells were detected with secondary antibodies for 1 hour, after each incubation, cells were washed with PBS 3-5 times, 5 minute each wash and assessed under a fluorescent microscope (Olympus BX51, Japan).

MTT Proliferation Analysis

The 3-(4,5-dimethylthiazol-2-yl)-2,5-diphenyltetrazolium bromide (MTT) analysis is an established assay for evaluating metabolic activity of cells, and can be useful for the measurement of cell viability. MTT analysis was accomplished as previously reported for determining the metabolic activity of RPE cells.[13] The medium was removed, the cells were washed with PBS, 1000 mL/well MTT solution was added, and the cells were incubated at 37 °C for 1 hour. The formazan crystals were dissolved after the administration of DMSO (1000 mL/well). Absorption was evaluated by a scanning spectrophotometer (Promega Glomax MultiDetection System Plate reader, USA) at 560 nm. The procedures were carried out 3 times. Treatment-naive RPE of the same passage served as the control.

Senescence-associated β-galactosidase Activity

The percentage of RPE cells for positive senescence-associated (SA) β-galactosidase activity was detected as previously reported by Dimri et al.[14] Concisely, treated RPE cells were washed twice with PBS and fixed with 2% formaldehyde and 0.2% glutaraldehyde in PBS (pH 6.0) at room temperature for 4 min. The cells were then washed twice with PBS and incubated for 8 hours at 37°C with freshly prepared SA β-galactosidase staining solution in darkness. Finally, SA β-galactosidase staining solution was eliminated, cells were washed with PBS, and the development of blueish color was visualized by light microscope.

Detection of Apoptosis

The level of apoptosis was determined on the same cultures in which the cellular vital indices were analyzed. Apoptotic cells were identified by Muse™ Annexin V&Dead Cell Kit MCH100105 according to the manufacturer's protocol. The cells were first washed in PBS and then detached for 10 minutes in trypsin and suspended again in PBS. Finally, the cells were centrifuged (1400 rpm, 5 minute) and resuspended in propidiumiodide (1 g/mL). The level of apoptosis was determined according to the number of apoptotic cells in pre-G1 phase using flow cytometry (Millipore Muse® Cell Analyzer, Germany).

Statistical Analysis

SPSS version 22.0 for Windows (Chicago, IL, USA) was used for statistical analysis. Descriptive data were presented as mean and standard deviation and percentages. Results were statistically analyzed by one-way ANOVA. P-values <0.05 were considered significant. All procedures were carried out 3 times.

Results

Evaluation of Retinal Pigment Epithelium Cell Morphology

In comparison of phase-contrast appearance of RPE culture cells 72 hours after supplementation with aflibercept (0.5 mg/mL), bevacizumab (0.3125 mg/mL), and ranibizumab (0.125 mg/mL), and control culture, phase contrast images showed no morphological changes in the RPE culture cells with any drug and RPE cells maintained their hexagonal morphology (Figure 1).

Expression of Cytokeratin 18 and Zonula Occludens Protein 1

Immunocytochemistry images demonstrated expression of intermediate protein cytokeratin 18 (Figure 2A) and tight junction protein ZO-l (Figure 2B) in the RPE sheets.

Effect of Anti-Vascular Endothelial Growth Factor Agents on Cell Viability

We attempted to assess if the 3 anti-VEGF drugs caused cytotoxic effects at the end of 72 hours. RPE cells were cultured until they reached 90% confluency and cytotoxicity was evaluated by MTT assay. There was significantly increased viability of the cells in the aflibercept-treated culture versus control culture (p=0.002) (Figure 3A). Statistically decreased viability was found in the bevacizumab and ranibizumab-treated groups versus control culture (p=0.003 and p=0.0001, respectively) (Figure 3A).

Proliferation and Apoptosis of Retinal Pigment Epithelium Cells

Incubation for 72 hours with aşibercept (0.5 mg/mL), bevacizumab (0.3125 mg/mL), and ranibizumab (0.125 mg/mL) did not significantly affect cell proliferation when compared to control cell cultures (Figure 3B).

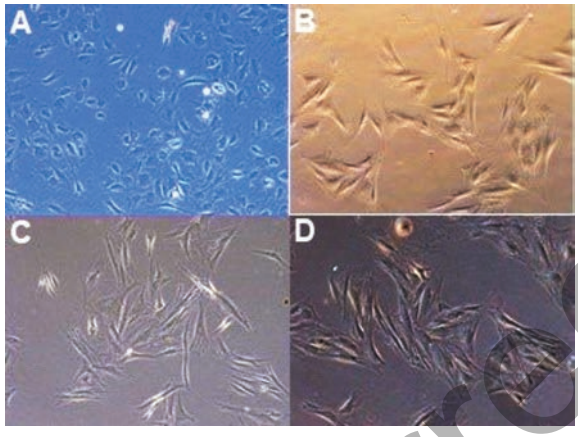

Figure 1. Comparison of phase-contrast microscopic appearance of 3 anti-vascular endothelial growth factor drugs and control culture showed no morphological changes of the retinal pigment epithelium (RPE) cell culture with any drug, and RPE cells maintain the hexagonal morphology at the end of 72 hours in the (A) control, (B) aflibercept (0.5 mg/mL), (C) bevacizumab (0.3125 mg/mL), and (D) ranibizumab (0.125 mg/mL) groups

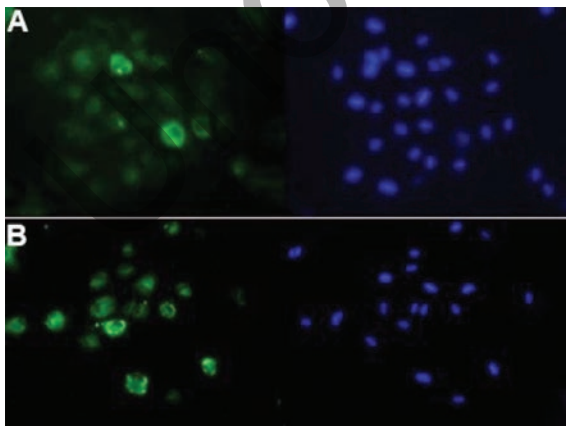

Figure 2. Immunocytochemistry staining of retinal pigment epithelium cell culture demonstrates expression of cytokeratin 18 (A) and tight junction protein zonula occludens protein 1 (B)

Apoptosis rates were significantly higher in the cultures treated with bevacizumab (0.3125 mg/mL) and ranibizumab (0.125 mg/mL) compared to the control group (p=0.001 and p=0.0001, respectively). There was a statistically significant decrease in the apoptosis of cells treated with aflibercept versus the control group (p=0.001) (Figure 3C).

Senescence-associated β-galactosidase Activity

There was no statistically significant difference between the 3 anti-VEGF drugs at the end of 72 hours when evaluating their effects on cell senescence (p>0.05) (Figure 3D).

Discussion

This is the first study in the literature to assess the senescence effects of anti-VEGF drugs and to identify that these agents do not seem to have a significant effect on the senescence of RPE cells in vitro. In addition, we have showed that RPE morphology and proliferation are also not affected by the anti-VEGF drugs most commonly used in retinal diseases. However, aflibercept increased viability and decreased apoptosis, while bevacizumab and ranibizumab had the opposite effect.

Intravitreal injection has become a widely used delivery route of various therapeutic agents for the treatment of vasoproliferative ocular diseases.[15] Current anti-VEGF therapies delivered intravitreally include ranibizumab and aflibercept, as well as off-label bevacizumab. A main functional difference between aflibercept and other anti-VEGF agents is blockage of VEGF-B, PGF1, and PGF-2 in addition to VEGF-A isoforms. To best of our knowledge there are limited in vitro studies in

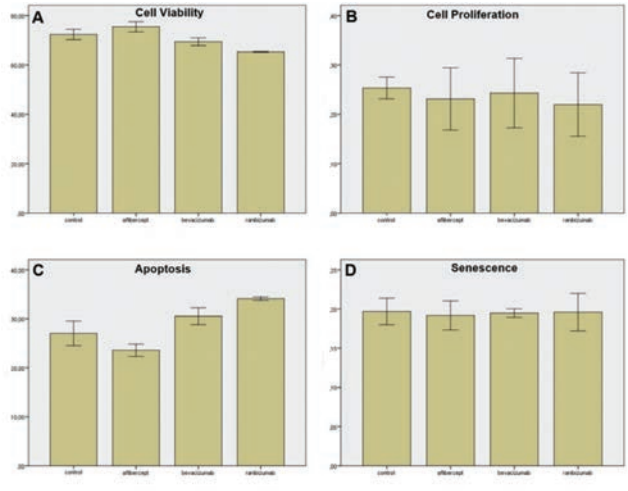

Figure 3. Bar graphs representing cell viability (A), cell proliferation (B), apoptosis (C), and senescence (D) in retinal pigment epithelium cell cultures 72 h after supplementation with aflibercept (0.5 mg/mL), bevacizumab (0.3125 mg/mL), and ranibizumab (0.125 mg/mL). A) Bevacizumab and ranibizumab decreased cell viability while aflibercept increased cell viability compared to the control group; B) None of the anti-vascular endothelial growth factor (VEGF) drugs showed a significant negative effect on cell proliferation; C) Bevacizumab and ranibizumab increased apoptosis while aflibercept significantly decreased apoptosis compared to the control group; D) None of the anti-VEGF drugs showed a significant effect on senescence

the literature evaluating the safety and efficacy of ranibizumab, aflibercept, and bevacizumab. In the present study, aflibercept was found to decrease apoptosis and increase cell viability. In contrast, ranibizumab and bevacizumab were observed to increase apoptosis and reduce cell viability in RPE cultures. Retinal pigment epithelium-derived VEGF is a vital mediator for support of the choriocapillaris. Several clinical studies have shown a correlation between subfoveal choroidal thickness and RPE atrophy progression, which suggested that decreased blood supply might promote RPE atrophy during anti-VEGF treatment.[16,17] We also noticed that most of the experimental studies on the adverse effects of the anti-VEGF drugs were carried out on RPE cell linings with intact choriocapillaris. Our study is performed on an isolated RPE cell line and may be able to show the direct toxic effects of anti-VEGF drugs on RPE. In a study performed on newborn rabbits, Cam et al.[18] showed that at 3 weeks after injection, all anti-VEGF drugs caused low levels of serum anti-VEGF concentrations and induced apoptosis as determined with apoptotic index, which was described as the percentage of apoptotic TdT-mediated dUTP-digoxigenin nick end labeling (TUNEL) positive cells of tissues. Malik et al.[19] also studied the safety profiles of various concentrations of anti-VEGF drugs on human RPE cells. They reported that while ranibizumab and aflibercept did not cause mitochondrial toxicity or cell death, bevacizumab and aflibercept revealed mild mitochondrial toxicity, though they also did not cause significant cell death at clinical doses. However, in our study all of the drugs caused a significant difference in cell viability. Malik et al.[19] treated the culture media with anti-VEGF drugs at concentrations they considered to be the clinical dose, assuming the amount of intravitreal injected drug spreads equally throughout the 4 mL human vitreous and modifying the doses accordingly. No such modification was performed in our study, which is a limitation of our study and could explain our conflicting results.

In our study, anti-VEGF drugs had no effect on the senescence or proliferation of RPE cells at after 72 hours. Cellular senescence is a program activated by normal cells in reaction to various stress factors such as oxidative stress, DNA damage, oncogene activity, and inadequate culturing conditions.[20,21] Conventionally, when cells enter senescence they exhibit substantial morphological changes. The cells spread out and flatten, which is usually followed by increasing SA β-galactosidase activity.[14] To best of our knowledge there are no studies evaluating the effects of anti-VEGF drugs on senescence in the current literature. Our data showed that none of the anti-VEGF drugs affected senescence in RPE cells at the end of the 72 hours. Recently, Zhuge et al.[22] reported that fullerenol, an effective free radical scavenger and antioxidant, could salvage RPE cells from oxidative stress-induced senescence due to its antioxidant effect. They suggested that the protective effect of fullerenol is crucial for the development of new treatment strategies in oxidative stress-associated retinal disorders such as age-related macular degeneration (AMD). In addition, Kernt et al.[23] investigated the antiapoptotic and cytoprotective effects of idebenone, a benzoquinone derivative that is structurally related to ubiquinone (coenzyme Q10), on optic nerve head astrocytes (ONHA) under oxidative stress. They concluded that idebenone reduced senescence, oxidative stress, and apoptotic cell death in cultured ONHA in vitro. One of the limitations of our study is that we studied the effects of drugs in healthy retinas, not under the drugs' indicated disease states such as AMD, which would have already had oxidative stress and changes in RPE senescence. Therefore, we do not know the senescence effects of the drugs in already oxidative stress-induced conditions.

Recently, Spitzer et al.[8] compared the antiproliferative and cytotoxic effects of bevacizumab, pegaptanib, and ranibizumab on different ocular cells. When applied to choroidal epithelial cells, they observed reductions in cell proliferation of 44.1% with ranibizumab versus 38.2% and 35.1% with bevacizumab and pegaptanib, respectively, although the difference between them was not statistically significant. They reported that bevacizumab, pegaptanib, and ranibizumab significantly suppressed choroidal endothelial cell proliferation and concluded that when used at the currently established doses, none of the drugs was superior over the others in respect to endothelial cell growth inhibition. Our study showed no difference in the proliferation rate of the RPE line in the treated groups compared to controls.

Another study compared the effects of ranibizumab, pegaptanib, and bevacizumab at intravitreal dose range on human umbilical vein endothelial cells (HUVEC).[10] The results indicated that ranibizumab and bevacizumab significantly increased apoptosis of HUVEC, similar to our results in RPE cells. Clinically applied doses of these drugs, but not pegaptanib, caused significantly reduced cellular proliferation without causing cytotoxic effects at all concentrations used. In addition, the active form of VEGF receptor-2 expression was decreased relative to controls after incubation with bevacizumab (to 66% of control values), ranibizumab (78%), and pegaptanib (86%).

Schnichels et al.[11] investigated the cytotoxicity and antiproliferative activity of aflibercept, bevacizumab, and ranibizumab on different ocular cells (ARPE19, RGC-5, and 661W) and concluded that aflibercept does not cause changes in cell morphology, induce apoptosis, or permanently decrease cell viability, cell density, or proliferation in any cell line or concentration investigated. In addition, aflibercept slightly upregulated or downregulated certain VEGF-related factors, but the changes were not significant when compared to bevacizumab and ranibizumab. The ARPE19 cell line was derived from human RPE in their study, whereas ours was derived from rabbits. VEGF-Trap$_{R1R2}$ (aflibercept) is composed of entirely human sequences and was constructed to bind human VEGF isoforms.[24] Holash et al.[24] stated that despite its wholly human nature, VEGF-Trap$_{R1R2}$ binds all species of VEGF tested, from human to chicken VEGF, yet in their study the experiments were shown on mouse, rat, and humans. The conflicting results obtained in our study and that of Schnichels et al.[11] may be attributable to different responses shown by the cell lines of different origin used in the studies.

It is known that most eyes with AMD require long-term anti-VEGF treatment, and it is the constant neutralization of VEGF, which is crucial for ocular homeostasis, that may lead to adverse effects.[25]

Study Limitations

One of the limitations of our study is that anti-VEGF drugs are used repeatedly, most commonly administered as 3 monthly loading doses followed by repeated injections monthly or pro re nata (as needed) thereafter. In contrast, our study represents results after a single injection, and longitudinal studies showing the effects of more and repeated injections as in real life should be planned.

Conclusion

In conclusion, our study reveals that anti-VEGF drugs had no effects on senescence and proliferation of RPE cells. Aflibercept was found to decrease apoptosis and increase cell viability. In contrast, ranibizumab and bevacizumab were observed to increase apoptosis and reduce RPE cell viability. In the literature, there are no studies evaluating the effects of anti-VEGF drugs on senescence. We believe that our study will guide future research in this respect and experimental and preclinical studies will be needed to confirm our in vitro findings.

Ethics

Ethics Committee Approval: Erciyes University Local Ethics Committee for Animal Experiments date: 14/01/2015, number: 15/12.

Peer-review: Externally peer-reviewed.

Authorship Contributions

Surgical and Medical Practices: Zeynep Burçin Gönen, Mustafa Şahiner, Ayşe Öner, Concept: Galip Ertuğrul Mirza, Ayşe Öner, Mustafa Şahiner, Zeynep Burçin Gönen, Dilek Bahar, Design: Ayşe Öner, Mustafa Şahiner, Zeynep Burçin Gönen, Dilek Bahar, Data Collection or Processing: Zeynep Burçin Gönen, Dilek Bahar, Analysis or Interpretation: Zeynep Burçin Gönen, Dilek Bahar, Metin Ünlü, Duygu Gülmez Sevim, Çağatay Karaca, Literature Search: Metin Ünlü, Duygu Gülmez Sevim, Çağatay Karaca, Writing: Metin Ünlü, Duygu Gülmez Sevim, Çağatay Karaca.

Conflict of Interest: No conflict of interest was declared by the authors.

Financial Disclosure: The authors declared that this study received no financial support.

References

1. Aiello LP, Pierce EA, Foley ED, Takagi H, Chen H, Riddle L, Ferrara N, King GL, Smith LE. Suppression of retinal neovascularization in vivo by inhibition of vascular endothelial growth factor (VEGF) using soluble VEGF-receptor chimeric proteins. Proc Natl Acad Sci U S A. 1995;92:10457-10461.
2. Presta LG, Chen H, O'Connor SJ, Chisholm V, Meng YG, Krummen L, Winkler M, Ferrara N. Humanization of an anti-vascular endothelial growth factor monoclonal antibody for the therapy of solid tumors and other disorders. Cancer Res. 1997;57:4593-4599.
3. Qaum T, Xu Q, Joussen AM, Clemens MW, Qin W, Miyamoto K, Hassessian H, Wiegand SJ, Rudge J, Yancopoulos GD, Adamis AP. VEGF-initiated blood-retinal barrier breakdown in early diabetes. Invest Ophthalmol Vis Sci. 2001;42:2408-2413.
4. Gragoudas ES, Adamis AP, Cunningham ET Jr, Feinsod M, Guyer DR; VEGF Inhibition Study in Ocular Neovascularization Clinical Trial Group. Pegaptanib for neovascular age-related macular degeneration. N Engl J Med. 2004;351:2805-2816.
5. Wells JA, Glassman AR, Ayala AR, Jampol LM, Bressler NM, Bressler SB, Brucker AJ, Ferris FL, Hampton GR, Jhaveri C, Melia M, Beck RW; Diabetic Retinopathy Clinical Research Network. Aflibercept, Bevacizumab, or Ranibizumab for Diabetic Macular Edema: Two-Year Results from a Comparative Effectiveness Randomized Clinical Trial. Ophthalmology. 2016;123:1351-1359.
6. Wang Y, Fei D, Vanderlaan M, Song A. Biological activity of bevacizumab, a humanized anti-VEGF antibody in vitro. Angiogenesis. 2004;7:335-345.
7. Spitzer MS, Wallenfels-Thilo B, Sierra A, Yoeruek E, Peters S, Henke-Fahle S, Bartz-Schmidt KU, Szurman P; Tuebingen Bevacizumab Study Group. Antiproliferative and cytotoxic properties of bevacizumab on different ocular cells. Br J Ophthalmol. 2006;90:1316-1321.
8. Spitzer MS, Yoeruek E, Sierra A, Wallenfels-Thilo B, Schraermeyer U, Spitzer B, Bartz-Schmidt KU, Szurman P. Comparative antiproliferative and cytotoxic profile of bevacizumab (Avastin), pegaptanib (Macugen) and ranibizumab (Lucentis) on different ocular cells. Graefes Arch Clin Exp Ophthalmol. 2007;245:1837-1842.
9. Kaempf S, Johnen S, Salz AK, Weinberger A, Walter P, Thumann G. Effects of bevacizumab (Avastin) on retinal cells in organotypic culture. Invest Ophthalmol Vis Sci. 2008;49:3164-3171.
10. Carneiro A, Falcao M, Pirraco A, Milheiro-Oliveira P, Falcao-Reis F, Soares R. Comparative effects of bevacizumab, ranibizumab and pegaptanib at intravitreal dose range on endothelial cells. Exp Eye Res. 2009;88:522-527.
11. Schnichels S, Hagemann U, Januschowski K, Hofmann J, Bartz-Schmidt KU, Szurman P, Spitzer MS, Aisenbrey S. Comparative toxicity and proliferation testing of aflibercept, bevacizumab and ranibizumab on different ocular cells. Br J Ophthalmol. 2013;97:917-923.
12. Chang CW, Roque RS, Defoe DM, Caldwell RB. An improved method for isolation and culture of pigment epithelial cells from rat retina. Curr Eye Res. 1991;10:1081-1086.
13. Kernt M, Neubauer AS, Liegl RG, Hirneiss C, Alge CS, Wolf A, Ulbig MW, Kampik A. Sorafenib prevents human retinal pigment epithelium cells from light-induced overexpression of VEGF, PDGF and PlGF. Br J Ophthalmol. 2010;94:1533-1539.
14. Dimri GP, Lee X, Basile G, Acosta M, Scott G, Roskelley C, Medrano EE, Linskens M, Rubelj I, Pereira-Smith O, et al. A biomarker that identifies senescent human cells in culture and in aging skin in vivo. Proc Natl Acad Sci U S A. 1995;92:9363-9367.
15. Avery RL, Bakri SJ, Blumenkranz MS, Brucker AJ, Cunningham ET Jr, D'Amico DJ, Dugel PU, Flynn HW Jr, Freund KB, Haller JA, Jumper JM, Liebmann JM, McCannel CA, Mieler WF, Ta CN, Williams GA. Intravitreal injection technique and monitoring: updated guidelines of an expert panel. Retina. 2014;34(Suppl 12):1-18.
16. Cho HJ, Kim HS, Yoo SG, Han JI, Lew YJ, Cho SW, Lee TG, Kim JW. Retinal Pigment Epithelial Tear After Intravitreal Ranibizumab Treatment for Retinal Angiomatous Proliferation. Am J Ophthalmol. 2015;160:1000-1005.
17. Hata M, Yamashiro K, Oishi A, Ooto S, Tamura H, Miyata M, Ueda-Arakawa N, Kuroda Y, Takahashi A, Tsujikawa A, Yoshimura N. Retinal Pigment Epithelial Atrophy after Anti-Vascular Endothelial Growth Factor Injections for Retinal Angiomatous Proliferation. Retina. 2017;37:2069-2077.
18. Cam D, Berk AT, Micili SC, Kume T, Ergur BU, Yilmaz O. Histological and Immunohistochemical Retinal Changes Following the Intravitreal Injection of Aflibercept, Bevacizumab and Ranibizumab in Newborn Rabbits. Curr Eye Res. 2017;42:315-322.

19. Malik D, Tarek M, Caceres del Carpio J, Ramirez C, Boyer D, Kenney MC, Kuppermann BD. Safety profiles of anti-VEGF drugs: bevacizumab, ranibizumab, aflibercept and ziv-aflibercept on human retinal pigment epithelium cells in culture. Br J Ophthalmol. 2014;98(Suppl 1):11-16.
20. Chen Q, Fischer A, Reagan JD, Yan LJ, Ames BN. Oxidative DNA damage and senescence of human diploid fibroblast cells. Proc Natl Acad Sci U S A. 1995;92:4337-4341.
21. Serrano M, Lin AW, McCurrach ME, Beach D, Lowe SW. Oncogenic ras provokes premature cell senescence associated with accumulation of p53 and p16INK4a. Cell. 1997;88:593-602.
22. Zhuge CC, Xu JY, Zhang J, Li W, Li P, Li Z, Chen L, Liu X, Shang P, Xu H, Lu Y, Wang F, Lu L, Xu GT. Fullerenol protects retinal pigment epithelial cells from oxidative stress-induced premature senescence via activating SIRT1. Invest Ophthalmol Vis Sci. 2014;55:4628-4638.
23. Kernt M, Arend N, Buerger A, Mann T, Haritoglou C, Ulbig MW, Kampik A, Hirneiss C. Idebenone prevents human optic nerve head astrocytes from oxidative stress, apoptosis, and senescence by stabilizing BAX/Bcl-2 ratio. J Glaucoma. 2013;22:404-412.
24. Holash J, Davis S, Papadopoulos N, Croll SD, Ho L, Russell M, Boland P, Leidich R, Hylton D, Burova E, Ioffe E, Huang T, Radziejewski C, Bailey K, Fandl JP, Daly T, Wiegand SJ, Yancopoulos GD, Rudge JS. VEGF-Trap: a VEGF blocker with potent antitumor effects. Proc Natl Acad Sci U S A. 2002;99:11393-11398.
25. Kuroda Y, Yamashiro K, Tsujikawa A, Ooto S, Tamura H, Oishi A, Nakanishi H, Miyake M, Yoshikawa M, Yoshimura N. Retinal Pigment Epithelial Atrophy in Neovascular Age-Related Macular Degeneration After Ranibizumab Treatment. Am J Ophthalmol. 2016;161:94-103.

DOI: 10.4274/tjo.53179
Turk J Ophthalmol 2018;48:196-201

Review

Optical Coherence Tomography Angiography in Glaucoma

Gábor Holló
Semmelweis University, Department of Ophthalmology, Unit of Head, Glaucoma and Perimetry, Budapest, Hungary

Abstract

Optical coherence tomography angiography (OCTA) comprises different OCT-based technologies developed for non-invasive assessment and measurement of optic nerve head and retinal perfusion. Currently the most clinically established approach is based on the split spectrum amplitude decorrelation algorithm, which detects moving red blood cells and eliminates all other information. The two main clinical fields in which OCTA offers clinically useful information are investigation of the macular retina (e.g. in macular degeneration and diabetic macular disease) and glaucoma. For glaucoma, the optic nerve head and the peripapillary retinal perfusion in the retinal nerve fiber layer, and the superficial perifoveal macular vasculature are the areas of interest. This review provides a comprehensive summary of the most important current and potential future applications of OCTA in glaucoma, but does not address the nonglaucomatous optic nerve head or peripapillary and macular diseases.

Keywords: Glaucoma, OCTA, optical coherence tomography angiography, perfusion, peripapillary retinal nerve fiber layer, macula

What is Optical Coherence Tomography Angiography?

Optical coherence tomography angiography (OCTA) comprises various OCT-based technologies.[1] These methods all offer noninvasive assessment of perfusion in various retinal layers separately, or allow assessment of iris and corneal neovascularization and filtering bleb vascularity. Various instrument families from different manufacturers (e.g. Optovue, Zeiss, Heidelberg, Topcon, Nidek and Canon) are currently used in clinical practice. All of these systems offer perfusion images but currently not all instrument and software versions provide objective measurements. It is important to note that due to the technical differences, conversion of the parameters and measured values between the different instrument systems is not possible.

This review and the presented images are based on the most commonly used OCTA system, the Angiovue OCT (Optovue Inc., Fremont, CA, USA), but the main findings are also valid for most other OCTA instruments. In the Angiovue OCT, the measurement principle is based on split spectrum amplitude decorrelation algorithm (SSADA).[1] This algorithm detects red blood cell movement independently from the direction of movement. At the same time, all static (structural) information is removed by the software. Thus, in contrast to fluorescein angiography, data in OCTA are derived from the red blood cells rather than plasma. It is important to note that "nonperfusion" in OCTA does not necessarily mean missing or obstructed vessels, or lack of capillary plasma perfusion; it simply means that at the time of image acquisition, no moving red blood cells were present in the "nonperfused" areas. For both research purposes and glaucoma practice, the most informative parameters are peripapillary vessel density (angioflow vessel density) in the peripapillary retinal nerve fiber layer (RNFL) (Figures 1 and 2) and superficial perifoveal vessel density in the macula (Figure 3).[1] Vessel density is the perfused area expressed as a percentage of the total examined area or its predefined sectors within a retinal layer of interest.[1,2] OCTA of the disc area is technically available in most systems, but the presence of the large vessels and the variability and complexity of the three-dimensional optic nerve head structure make the measured results difficult to interpret. In order to correctly interpret the results, both the OCTA image and the corresponding structural image (en face

Address for Correspondence: Gabor Hollo MD, Semmelweis University, Department of Ophthalmology, Unit of Head, Glaucoma and Perimetry, Budapest, Hungary
Phone: +90 212 801 44 36 E-mail: hollo.gabor@med.semmelweis-univ.hu
Received: 20.06.2018 **Accepted:** 28.06.2018

OCT image) need to be used (Figures 1 and 2).[3,4] In the most advanced systems, capillary vessel density and all-vessel density are measured separately for each retinal layer.[5,6]

Are Optical Coherence Tomography Angiography Measurements Reliable?

Retinal perfusion is autoregulated, but vascular dysfunction is common in open-angle glaucoma.[7] In addition, systemic blood pressure and other systemic parameters may vary between visits, as is commonly seen in the elderly glaucoma population. Therefore, short-term repeatability and long-term reproducibility of vessel density measurements in the peripapillary RNFL and the superficial perifoveal macular layer were investigated by several groups.[3,8,9] In general, both parameter types show high repeatability and long-term reproducibility in both normal and glaucomatous eyes when the image quality is high. In our reproducibility study, the long-term reproducibility of peripapillary vessel density measurements was less than 4%,[3] and in another study the between-visit reproducibility of superficial perifoveal macular vessel density was less than 9%.[9] We and others have also shown that long-term reproducibility of peripapillary vessel density measurements is independent of RNFL thickness, thus the reproducibility is similar in healthy, early and advanced glaucomatous eyes.[3,8] Another important question is whether peripapillary vessel density values reflect the perfusion of the peripapillary RNFL thickness. We and others have consistently found a strong relationship between vessel density and glaucomatous damage through the spectrum of glaucoma disease severity.[3,10,11]

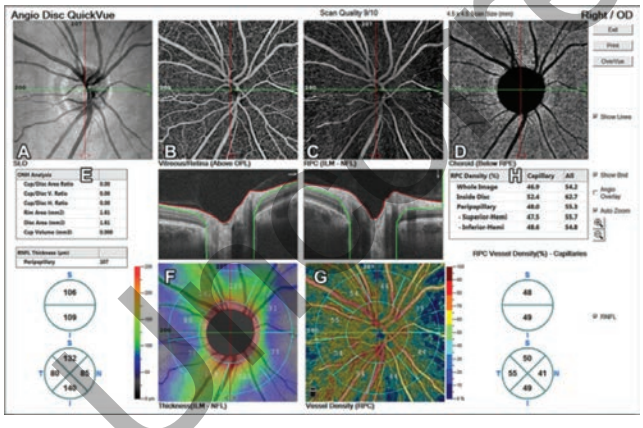

This image and permission for use were obtained from Gábor Holló's archive. All rights belong to Gábor Holló.

Figure 1. Peripapillary optical coherence tomography angiography (OCTA) report of a healthy eye with the Optovue OCTA system. A) Scanning laser ophthalmoscopy image of the measurement area; B) Vitreous-retinal perfusion map. C) Perfusion map in the radial peripapillary capillaries layer which corresponds to the retinal nerve fiber layer. D) Perfusion map in the choroid level. E) Optic nerve head and retinal nerve fiber layer thickness measurement results. F) Color-coded retinal nerve fiber layer thickness image. G) Color-coded vessel density map and its sectors in the radial peripapillary capillaries layer. H) Capillary and all-vessels density values for various sectors of the peripapillary area in the radial peripapillary capillaries layer
RNFL: Retinal nerve fiber layer, OD: Right eye, ILM: Internal limiting membrane, NFL: Nerve fiber layer

Can Vessel Density Measurements Be Used to Diagnose Glaucoma?

For some instrument and software types, differentiation of open-angle glaucoma and normal eyes using peripapillary vessel density or superficial perifoveal macular vessel density measurements is similar to of even better than that with RNFL thickness.[12] However, the accuracy of the different instrument systems seems to vary considerably.[12,13,14,15,16,17] Currently no head-to-head comparison study is available. Using the Angiovue OCT system, discrimination between perimetric open-angle glaucoma eyes and normal eyes was stronger with peripapillary vessel density than RNFL thickness,[12] but the opposite was found for distinguishing angle-closure glaucoma eyes from normal eyes.[15] Together with other results shown later in this review, this result suggests that for open-angle glaucoma, in which vascular dysregulation frequently plays a role in the development of the disease, vessel density measurements may offer advantages in early diagnosis; in contrast, in angle closure

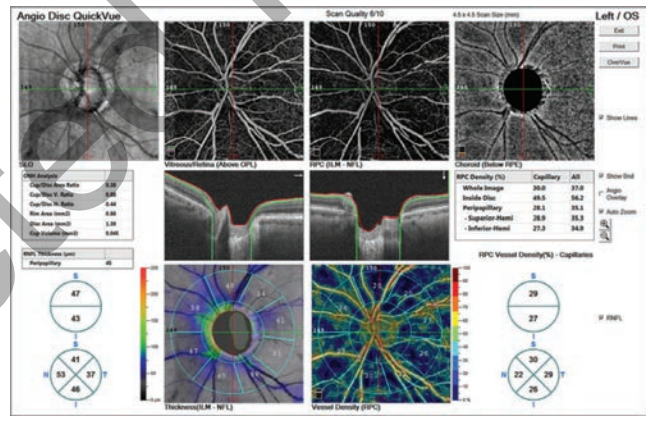

This image and permission for use were obtained from Gábor Holló's archive. All rights belong to Gábor Holló.

Figure 2. Peripapillary optical coherence tomography angiography report of an eye with advanced glaucomatous damage
RNFL: Retinal nerve fiber layer, OS: Left eye, ILM: Internal limiting membrane

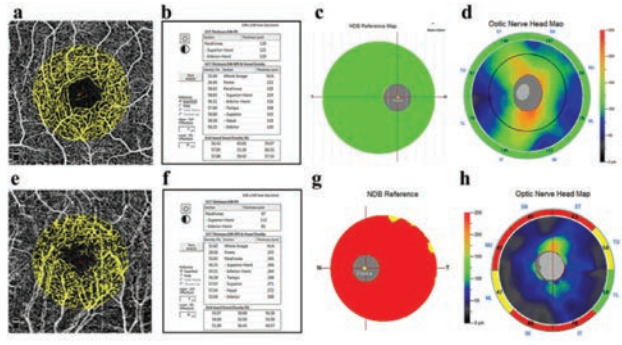

This image and permission for use were obtained from Gábor Holló's archive. All rights belong to Gábor Holló.

Figure 3. Superficial perifoveal macular vessel density and the corresponding macular inner retina thickness and retinal nerve fiber layer thickness in a healthy eye (A to D) and in an advanced glaucoma eye (E to H). A and E: Color coded perfusion maps, B and F: Vessel density measurement values, C and G: Macular inner retina thickness maps, D and H: Retinal nerve fiber layer thickness maps

glaucoma, in which intraocular pressure elevation has a major or exclusive pathophysiological role, the structural parameters perform better.

It was shown that localized RNFL bundle defects are spatially associated with localized peripapillary vessel density reductions (Figure 4), even in early and preperimetric open-angle glaucoma.[4] Strong spatial correspondence between peripapillary vessel density reduction and deep lamina cribrosa defects was also confirmed.[18]

Structure-function Relationship with Optical Coherence Tomography Angiography

In OCTA, the "structure-function relationship" is in fact a "function-function relationship" in which localized and generalized OCTA parameters are related to the spatially corresponding visual field sensitivity or damage values. However, the most interesting part of these investigations is when structural parameters (RNFL thickness, sector RNFL thickness, inner macular retina thickness and its hemifields) are also included in the analysis. In general, for both the Humphrey and Octopus perimetry systems a strong negative relationship was found between peripapillary, whole image, and macular vessel density parameters and the corresponding visual field deterioration.[19,20,21] It is even more interesting that in primary open-angle glaucoma, the relationship is particularly strong for superotemporal and inferotemporal peripaillary vessel density and the spatially corresponding visual field sectors, and this relationship can be significantly stronger than that seen for the spatially corresponding sector RNFL thickness value.[19,20] These results support the pathophysiological hypothesis which suggests a causative role of vascular dysregulation in the development and progression of primary open-angle glaucoma, particularly in the inferotemporal and superotemporal peripapillary areas, where glaucomatous RNFL loss appears early and progresses rapidly.[7]

It is also interesting that a strong relationship was found between mean paracentral visual field defect values in Octopus perimetry and temporal peripapillary vessel density values.[22] The temporal peripapillary area (the papillomacular RNFL bundle) has been considered a particularly stable sector of the RNFL which does not thin until the latest stages of glaucoma. However, the perfusion-function relationship suggests that some mild vascular dysfunction or damage may start in the papillomacular area much earlier than previously thought. Recently a similar relationship was published for superficial perifoveal macular vessel density and mean sensitivity of the central 10-degree visual field in Humphrey perimetry,[23] and correspondence was found between the presence of central visual field defects and increased size of the foveal avascular zone in glaucoma.[24]

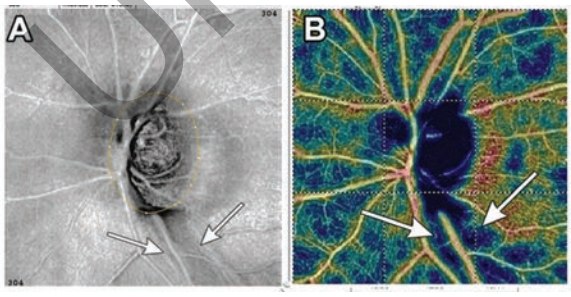

This image and permission for use were obtained from Gábor Holló's archive. All rights belong to Gábor Holló.

Figure 4. A localized retinal nerve fiber bundle defect and the spatially corresponding localized peripapillary vessel density reduction (arrows) in glaucoma

Myopia and Peripapillary Vessel Density

Since RNFL thickness measurements are influenced by myopia and atypical optic nerve head morphology, it was important to investigate the clinical applicability of vessel density measurements in myopic eyes.[25,26,27] Few studies to date have addressed this problem. In glaucoma with high myopia, the regional relationship of visual field and peripapillary vessel density is significantly greater than that with the corresponding RNFL thickness.[25] In myopia without glaucoma, peripapillary vessel density is lower than in normal eyes, and in myopic glaucoma it is even more reduced.[26] Similarly to RNLF thickness, perifoveal perfusion is altered in myopia with disc torsion.[27] Thus, in myopic glaucoma we cannot expect considerably better diagnostic accuracy from OCTA than from structural OCT parameters.

Image Quality and Artifacts in Optical Coherence Tomography Angiography

Similar to structural OCT measurements, OCTA is seriously influenced by image artifacts, most commonly vitreous floaters. Collagen opacities, which are common in glaucoma,[28] may cause shadow effect by blocking the return of the illumination light from the retina.[29] The shadow effect results in an OCT image and vessel density values which falsely imitate reduced or missing perfusion (Figure 5). Other artifacts known in structural OCT imaging may also have a significant impact on OCTA image quality and the measured values.[29,30]

Can Optical Coherence Tomography Angiography Be Used to Distinguish Glaucoma from Other Optic Nerve Diseases?

The peripapillary OCTA alterations are unfortunately not disease-specific. Reduction of perfusion is determined by disease severity rather than disease type.[30] Figure 6 illustrates how different optic nerve head diseases appear very similar in OCTA images. Thus, detailed evaluation of the optic nerve head and peripapillary retina remains mandatory for disease classification even in the age of modern OCTA technology.

Influence of Intraocular Pressure on Measured Vessel Density Values

The potential relationship between intraocular pressure or intraocular pressure reduction and peripapillary perfusion has been an important question in glaucoma management for decades. The structural parameters (RNFL thickness and inner macular retina thickness) do not react in an active way to pressure-lowering treatment. In a proof-of-concept investigation conducted on systemically healthy, young, and newly diagnosed open-angle glaucoma and ocular hypertensive patients whose untreated intraocular pressure was high but decreased by at

least 50% to 18 mmHg or less under treatment, we found a clinically very significant improvement in the initially reduced peripapillary vessel density (Figure 7).[31] Later other investigators using other OCTA systems and intraocular pressure-lowering interventions confirmed our results.[32,33] The results achieved with intraocular pressure reduction suggest that in relatively early glaucoma, the change of vessel density may potentially be used for early assessment of the interventions' long-term beneficial effect on visual field preservation.

Can We Use Vessel Density for the Measurement of Glaucomatous Progression?

The current standard of detection and measurement of glaucomatous progression is serial visual field testing and software-based visual field progression analysis. However, structural OCT parameters (RNFL thickness, inner macular retina thickness) have also been investigated for their applicability for the measurement of glaucomatous progression. Recently, structural progression measurements became a part of modern glaucoma care and progression analysis. In some of our latest studies we prospectively investigated early (2-year) glaucomatous progression with peripapillary vessel density and RNFL thickness measurements.[34,35] Progression was better detected with RNFL thickness progression analysis. Statistically significant peripapillary capillary vessel density progression was found in 17% of the study eyes, and half of the progressing cases also showed significant and spatially corresponding RNFL thickness progression.[35] It is important to note that in contrast to structural OCT parameters, which are not under physiological regulation, vessel density reflects intraocular pressure changes, status of systemic perfusion, glaucomatous vascular dysregulation, retinal oxygenation, and hypercapnia. Thus, vessel density is less stable than RNFL thickness. Therefore, we cannot expect to see an easy-to-understand vessel density progression pattern when the gradual glaucoma-related perfusion changes are small, or smaller than the fluctuations induced by factors which are not related to glaucomatous progression.

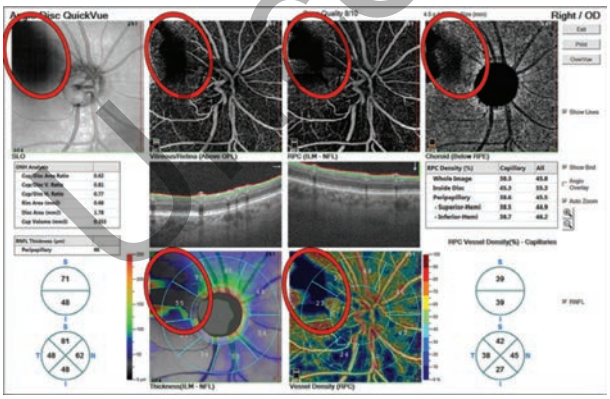

Figure 5. Influence of a vitreous floater (encircled with a red ellipse) on the peripapillary optical coherence tomography angiography measurement
RNFL: Retinal nerve fiber layer, OD: Right eye, ILM: Internal limiting membrane, NFL: Nerve fiber layer

In another recent investigation, we evaluated the potential influence of breath holding on vessel density measurements using a standardized and extreme form of breath holding, the Valsalva maneuver.[36] Breath holding and the Valsalva maneuver do influence retinal perfusion. Due to the increased intrathoracic pressure, the venous outflow from the eye decreases and as a consequence, retinal perfusion is temporally reduced. Since vessel density measurements are time-consuming (image acquisition for peripapillary measurements may take up to 16 seconds), the reduction of capillary perfusion in the RNFL needs to be

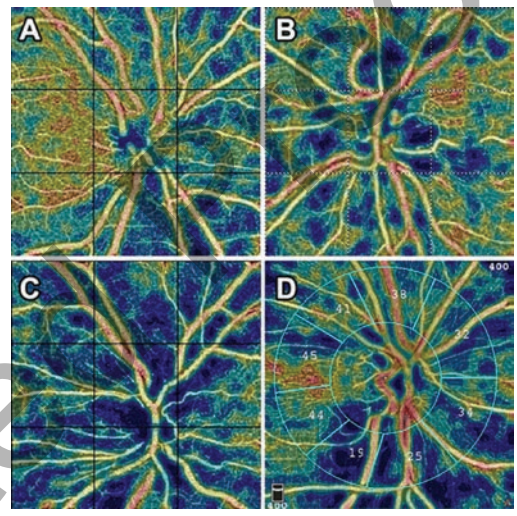

Figure 6. Color-coded peripapillary optical coherence tomography angiography images of four eyes with four different optic nerve head diseases. A) Compression due to optic nerve head drusen, B) Retinal vein occlusion earlier in life, C) Chronic non-arteritic anterior ischemic optic neuropathy, D) Advanced glaucoma

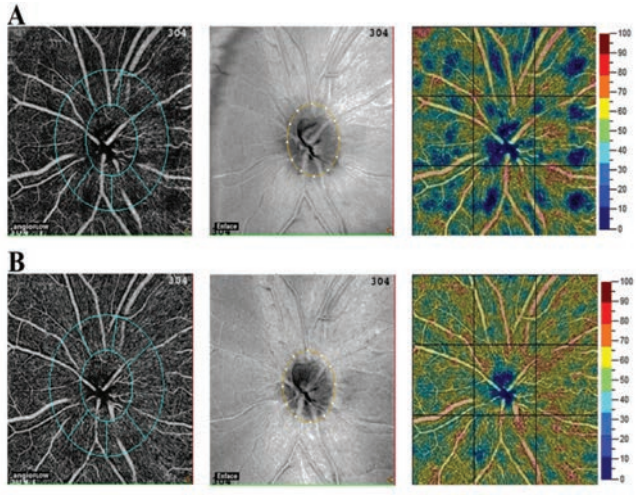

Figure 7. Influence of large intraocular pressure reduction on peripapillary vessel density in ocular hypertension. A) Untreated eye with high intraocular pressure. B) The same eye one month later under combined intraocular pressure-lowering medication and with more than 50% intraocular pressure reduction. The peripapillary vessel density map shows a clear increase in capillary perfusion

considered. Our results, however, clearly showed that the Valsalva maneuver does not influence the measured peripapillary vessel density values with the Optovue OCTA system. This result does not mean that breath holding has no influence on ocular blood flow, but it clearly shows that with the SSADA software, slowing the movement of red blood cells does not influence the measured vessel density as long as the red blood cells keep moving in the capillaries of the peripapillary RNFL.

Future of Optical Coherence Tomography Angiography in the Management of Glaucoma

OCTA appeared in clinical glaucoma research and practice four years ago, and software development is rapid. Results achieved with one software or hardware version may not be valid for the newer versions, which are usually superior to the previous ones. Thus, currently no final decision can be made on the various OCTA parameters' usefulness for the measurement of glaucomatous progression or conversion of ocular hypertension to glaucoma, their diagnostic value in preperimetric glaucoma, or their utility as indicators of visual field preservation after intraocular pressure-lowering interventions. These limitations, however, are temporary. In the coming years, OCTA will remain one of the most exciting clinical research areas, which deserves attention from both glaucoma specialists and general ophthalmologists treating glaucoma patients.

Ethics

Peer-review: Internally peer-reviewed.

Financial Disclosure: The author declared that this study received no financial support.

Note: All figures within the article are taken from the archive of Gábor Holló. All rights of usage are belong to Gábor Holló.

References

1. Tan ACS, Tan GS, Denniston AK, Keane PA, Ang M, Milea D, Chakravarthy U, Cheung CMG. An overview of the clinical applications of optical coherence tomography angiography. Eye (Lond). 2018;32:262-286.
2. Jia Y, Morrison JC, Tokayer J, Tan O, Lombardi L, Baumann B, Lu CD, Choi W, Fujimoto JG, Huang D. Quantitative OCT angiography of optic nerve head blood flow. Biomed Opt Express. 2012,3:3127-3137.
3. Holló G. Intrasession and between visit variability of sector peripapillary angioflow vessel density values measured with the Angiovue optical coherence tomograph in different retinal layers in ocular hypertension and glaucoma. PLoS ONE. 2016;11:e0161631.
4. Holló G. Vessel density calculated from OCT angiography in 3 peripapillary sectors in normal, ocular hypertensive and glaucoma eyes. Eur J Ophthalmol. 2016;26:42-45.
5. Holló G. Valsalva maneuver and peripapillary OCT angiography vessel density. J Glaucoma. 2018;27:133-136.
6. Holló G. Influence of removing the large retinal vessels-related effect on peripapillary vessel density progression analysis in glaucoma. J Glaucoma. 2018;27:137-139.
7. Grieshaber MC, Mozaffarieh M, Flammer J. What is the link between vascular dysregulation and glaucoma? Surv Ophthalmol. 2007;52(Suppl 2):144-154.
8. Venugopal JP, Rao HL, Weinreb RN, Pradhan ZS, Dasari S, Riyazuddin M, Puttiah NK, Rao DAS, Devi S, Mansouri K, Webers CA. Repeatability of vessel density measurements of optical coherence tomography angiography in normal and glaucoma eyes. Br J Ophthalmol. 2018;102:352-357.
9. Manalastas PIC, Zangwill LM, Saunders LJ, Mansouri K, Belghith A, Suh MH, Yarmohammadi A, Penteado RC, Akagi T, Shoji T, Weinreb RN. Reproducibility of optical coherence tomography angiography macular and optic nerve head vascular density in glaucoma and healthy eyes. J Glaucoma. 2017;26:851-859.
10. Geyman LS, Garg RA, Suwan Y, Trivedi V, Krawitz BD, Mo S, Pinhas A, Tantraworasin A, Chui TYP, Ritch R, Rosen RB. Peripapillary perfused capillary density in primary open-angle glaucoma across disease stage: an optical coherence tomography angiography study. Br J Ophthalmol. 2017;101:1261-1268.
11. Lommatzsch C, Rothaus K, Koch JM, Heinz C, Grisanti S. OCTA vessel density changes in the macular zone in glaucomatous eyes. Graefes Arch Clin Exp Ophthalmol. 2018;256:1499-1508.
12. Yarmohammadi A, Zangwill LM, Diniz-Filho A, Suh MH, Manalastas PI, Fatehee N, Yousefi S, Beghiht A, Saunders LJ, Medeiros FA, Huang D, Weinreb RN. Optical coherence tomography angiography vessel density in healthy, glaucoma suspect, and glaucoma eyes. Invest Ophthalmol Vis Sci. 2016;57:451-459.
13. Rao HL, Kadambi SV, Weinreb RN, Puttaiah NK, Pradhan ZS, Rao DAS, Kumar RS, Webers CAB, Shetty R. Diagnostic ability of peripapillary vessel density measurements of optical coherence tomography angiography in primary open-angle and angle-closure glaucoma. Br J Ophthalmol. 2017;101:1066-1070.
14. Rao HL, Dasari S, Riyazuddin M, Puttaiah NK, Pradhan ZS, Weinreb RN, Mansouri K, Webers CAB. Diagnostic ability and structure-function relationship of peripapillary optical microangiography measurements in glaucoma. J Glaucoma. 2018;27:219-226.
15. Rao HL, Pradhan ZS, Weinreb RN, Riyazuddin M, Dasari S, Venugopal JP, Puttaiah NK, Rao DAS, Devi S, Mansouri K, Webers CAB. Vessel density and structural measurements of optical coherence tomography in primary angle closure and primary angle closure glaucoma. Am J Ophthalmol. 2017;177:106-115.
16. Wan KH, Lam AKN, Leung CK. Optical coherence tomography angiography compared with optical coherence tomography macular measurements for detection of glaucoma. JAMA Ophthalmol. 2018;136:866-874.
17. Richter GM, Madi I, Chu Z, Burkemper B, Chang R, Zaman A, Sylvester B, Reznik A, Kashani A, Wang RK, Varma R. Structural and functional associations of macular microcirculation in the ganglion cell-inner plexiform layer in glaucoma using optical coherence tomography angiography. J Glaucoma. 2018;27:281-290.
18. Suh MH, Zangwill LM, Manalastas PI, Belghith A, Yarmohammadi A, Medeiros FA, Diniz-Filho A, Saunders LJ, Yousefi S, Weinreb RN. Optical coherence tomography angiography vessel density in glaucomatous eyes with focal lamina cribrosa defects. Ophthalmology. 2016;123:2309-2317.
19. Holló G. Relationship between optical coherence tomography sector peripapillary angioflow-density and Octopus visual field cluster mean defect values. PLoS One. 2017;12:e0171541.
20. Rao HL, Pradhan ZS, Weinreb RN, Dasari S, Riyazuddin M, Raveendran S, Puttaiah NK, Venugopal JP, Rao DAS, Devi S, Mansouri K, Webers CAB. Relationship of optic nerve structure and function to peripapillary vessel density measurements of optical coherence tomography angiography in glaucoma. J Glaucoma. 2017;26:548-554.
21. Yarmohammadi A, Zangwill LM, Diniz-Filho A, Suh MH, Yousefi S, Saunders LJ, Belghith A, Manalastas PI, Medeiros FA, Weinreb RN. Relationship between optical coherence tomography angiography vessel density and severity of visual field loss in glaucoma. Ophthalmology. 2016;123:2498-2508.
22. Holló G. Relationship between OCT angiography temporal peripapillary vessel-density and Octopus perimeter paracentral cluster mean defect. J Glaucoma 2017;26:397-402.
23. Penteado RC, Zangwill LM, Daga FB, Saunders LJ, Manalastas PIC, Shoji T, Akagi T, Christopher M, Yarmohammadi A, Moghimi S, Weinreb RN. Optical coherence tomography angiography macular vascular density measurements and the central 10-2 visual field in glaucoma. J Glaucoma. 2018;27:481-489.
24. Kwon J, Choi J, Shin JW, Lee J, Kook MS. Alterations of the foveal avascular zone measured by optical coherence tomography angiography in glaucoma

patients with central visual field defects. Invest Ophthalmol Vis Sci. 2017;58:1637-1645.
25. Shin JW, Kwon J, Lee J, Kook MS. Relationship between vessel density and visual field sensitivity in glaucomatous eyes with high myopia. Br J Ophthalmol. 2018.
26. Suwan Y, Fard MA, Geyman LS, Tantraworasin A, Chui TY, Rosen RB, Ritch R. Association of myopia with peripapillary perfused capillary density in patients with glaucoma: an optical coherence tomography angiography study. JAMA Ophthalmol. 2018;136:507-513.
27. Sung MS, Lee TH, Heo H, Park SW. Association between optic nerve head deformation and retinal microvasculature in high myopia. Am J Ophthalmol. 2018;188:81-90.
28. Schwab C, Glatz W, Schmidt B, Lindner E, Oettl K, Riedl R, Wedrich A, Ivastinovic D, Velikay-Parel M, Mossboeck G. Prevalence of posterior vitreous detachment in glaucoma patients and controls. Acta Ophthalmol. 2017;95:276-280.
29. Ghasemi Falavarjani K, Al-Sheikh M, Akil H, Sadda SR. Image artefacts in swept-source optical coherence tomography angiography. Br J Ophthalmol. 2017;101:564-568.
30. Holló G. Optical coherence tomography angiography and glaucoma. In: Chow DR, de Olivieria RPC, eds. OCT angiography. New York; Thieme Medical Publishers Inc; 2017:112-126.
31. Holló G. Influence of large intraocular pressure reduction on peripapillary OCT vessel density in ocular hypertensive and glaucoma eyes. J Glaucoma. 2017;26:7-10.
32. Shin JW, Sung KR, Uhm KB, Jo J, Moon Y, Song MK, Song JY. Peripapillary microvascular improvement and lamina cribrosa depth reduction after trabeculectomy in primary open-angle glaucoma. Invest Ophthalmol Vis Sci. 2017;58:5993-5999.
33. Alnawaiseh M, Müller V, Lahme L, Merté RL, Eter N. Changes in flow density measured using optical coherence tomography angiography after iStent insertion in combination with phacoemulsification in patients with open-angle Glaucoma. J Ophthalmol. 2018;2018:2890357.
34. Holló G. Comparison of peripapillary OCT angiography vessel density and retinal nerve fiber layer thickness measurements for their ability to detect progression in glaucoma. J Glaucoma. 2018;27:302-305.
35. Holló G. Influence of removing the large retinal vessels-related effect on peripapillary vessel density progression analysis in glaucoma. J Glaucoma. 2018;27:137-139.
36. Holló G. Valsalva maneuver and peripapillary OCT angiography vessel density. J Glaucoma. 2018;27:133-136.

DOI: 10.4274/tjo.49799
Turk J Ophthalmol 2018;48:202-205

Case Report

Optic Neuropathy and Macular Ischemia Associated with Neurosarcoidosis: A Case Report

Burak Tanyıldız*, Gizem Doğan*, Nilüfer Zorlutuna Kaymak*, Mehmet Engin Tezcan**, Ahmet Kasım Kılıç***, Sevda Şener Cömert****, Aysu Karatay Arsan*

*University of Health Sciences, Kartal Dr. Lütfi Kırdar Training and Research Hospital, Ophthalmology Clinic, İstanbul, Turkey
**University of Health Sciences, Kartal Dr. Lütfi Kırdar Training and Research Hospital, Rheumatology Clinic, İstanbul, Turkey
***University of Health Sciences, Kartal Dr. Lütfi Kırdar Training and Research Hospital, Neuorology Clinic, İstanbul, Turkey
****University of Health Sciences, Kartal Dr. Lütfi Kırdar Training and Research Hospital, Pulmonary Diseases Clinic, İstanbul, Turkey

Abstract

In this study, we present a case of bilateral optic neuropathy and macular ischemia in the right eye associated with neurosarcoidosis. A 26-year-old woman presented to our clinic with complaints of bilateral blurred vision. Bilateral granulomatous anterior uveitis, vitritis, optic neuropathy, and macular ischemia were detected in the right eye in slit-lamp examination. She also reported complaints of fever, weakness, sweating, arthralgia, and headache for 2 months. She was referred to the pulmonary diseases unit of our hospital due to hilar lymphadenopathy seen in her chest x-ray, and biopsies were taken for diagnostic purposes. Histological analysis of the mediastinal lymph node biopsies revealed chronic, non-caseating, granulomatous inflammation. Furthermore, the patient was referred to a neurologist due to concomitant complaint of intense headaches. She was diagnosed with neurosarcoidosis supported by findings on cranial magnetic resonance imaging and lumbar puncture. She received a 3-day course of high-dose (1 g/day) intravenous steroid treatment (methylprednisolone) followed by a tapering dose of oral prednisone. The patient began receiving oral methotrexate 15 mg/week as a steroid-sparing agent. Significant improvement in neurological and ophthalmological symptoms occurred in the first week of treatment. In this case report, we emphasized that neurosarcoidosis should be included in the differential diagnosis of patients with both bilateral optic neuropathy and macular ischemia. Furthermore, early diagnosis and timely treatment of neurosarcoidosis are important for favorable visual outcomes.

Keywords: Macular ischemia, methotrexate, neurosarcoidosis, optic neuropathy

Introduction

Sarcoidosis can affect multiple organs and is histologically characterized by non-caseified granulomas.[1] Ocular involvement is observed in 25-50% of patients with systemic sarcoidosis.[2] The most common findings are uveitis and conjunctival nodules.[3,4]

Neurosarcoidosis is found in 5-15% of those with systemic disease.[5,6] In patients with neurosarcoidosis, ophthalmic symptoms are mostly associated with cranial nerve involvement and uveitis. The facial, trigeminal, oculomotor, and optic nerves are the most commonly involved cranial nerves.[7]

Presented herein is a patient with bilateral uveitis, unilateral macular ischemia, bilateral optic disc involvement, and a biopsy-confirmed diagnosis of pulmonary sarcoidosis. This case report emphasizes that optic disc involvement may be a sign of neurosarcoidosis in patients with sarcoidosis and that macular ischemia may develop due to reduced flow in the retinal artery resulting from inflammation.

Case Report

A 26-year-old female patient presented to our clinic with blurred vision in both eyes for 2 weeks. She reported no

Address for Correspondence: Burak Tanyıldız MD, University of Health Sciences, Kartal Dr. Lütfi Kırdar Training and Research Hospital, Ophthalmology Clinic, İstanbul, Turkey Phone: +90 554 277 57 17 E-mail: buraktanyildiz@yahoo.com **ORCID-ID:** orcid.org/0000-0001-8245-8389
Received: 19.12.2017 **Accepted:** 18.02.2018

history of any major illness, but had complaints of fever, sweating, exhaustion, joint pain, and headache starting 2 months earlier. Upon presentation to another center for these complaints, chest x-ray revealed hilar fullness and a thoracic computed tomography (CT) scan was performed. Thoracic CT revealed bilateral hilar lymphadenopathy, and the patient was referred to our hospital for further diagnosis and treatment, where she underwent endobronchial ultrasound-assisted lymph node biopsy in our pulmonary diseases unit. Histopathological examination revealed granulomatous structures, lymphocytes, and sporadic bronchial epithelial cells.

The patient was not under treatment when she presented to our clinic. Physically, she exhibited somnolence and clouding of consciousness. Her visual acuity was 20/25 in the right eye and 20/20 vision in the left eye. Granulomatous keratic precipitates and +1 Tyndall effect were detected in both eyes in anterior segment examination. In both eyes, +1 vitritis was observed in the anterior vitreous.

On fundus examination, the optic discs of both eyes were edematous and hyperemic. In the right eye, a soft exudate was observed inferior to the optic disc and the lower half of the macula was ischemic (Figures 1A, 1B). The patient was started on topical treatment with 1% prednisolone acetate 4 times daily and 0.5% tropicamide 3 times daily.

Neurology consultation was requested due to the patient's complaints of intense headaches and the presence of bilateral optic disc involvement. However, no pathology was detected on neuromuscular examination. Cranial imaging and a lumbar puncture were performed. Diffusion magnetic resonance imaging (MRI) revealed extending nodular enhancements within and adjacent to the optic chiasm, at the basal cisternal level, and in the leptomeningeal layers in the posterior fossa. Thoracic and cervical MRI revealed leptomeningeal enhancement adjacent to the entire spinal cord. Cranial MR venography was normal.

Laboratory tests revealed low hemoglobin (10.7 g/dL; normal: 12-17), high sedimentation rate (57 mm/h; normal: 6-12), elevated CRP (9.4 mg/dL; normal: 0-3.5), and high urinary calcium (324 mg/24 hours; normal: 0-250). Anticardiolipin antibodies and lupus anticoagulants were negative. Cerebrospinal fluid (CSF) analysis showed high protein (145 mg/dL; normal: 15-45) and normal glucose (47 mg/dL; normal: 40-70), cell count in the cytological specimen was high (8500 cells/mL; normal: 0-10), and CSF pressure was normal (12 cm H_2O; normal: 8-18). CSF tuberculosis culture and acid-fast bacilli staining was negative. Based on the laboratory values, lymph node biopsy, and imaging findings, the patient was diagnosed with neurosarcoidosis-associated optic neuropathy and treatment was initiated with intravenous 1 g methylprednisolone for 3 days followed by oral methylprednisolone at 1 mg/kg/day. The macular ischemia initially observed in the right eye regressed within 1 week. The patient's general condition improved significantly with treatment and fundus fluorescein angiography (FFA) was performed. In both eyes, hyperfluorescence beginning in the early phase and increasing in the late phase was observed in the optic discs (Figures 2A-D) and a hyperfluorescent spot that increased in intensity in the late phase was observed on the vessel passing superiorly over the left fovea (Figure 2D). Hyperfluorescent leakage that increased toward the late phase was observed in the lower peripheral retinal vessels of both eyes (Figures 3A, 3B).

Although systemic steroid therapy was reduced, it was decided to initiate systemic immunosuppressive therapy; oral methotrexate 15 mg/week and folic acid 5 mg/day were added to her treatment. Her vision was 20/20 in both eyes after 3 months of treatment. Anterior segment examination was normal. Fundus examination showed regression of the optic disc edema (Figures 4A, 4B). Follow-up diffusion MRI revealed that the extending nodular enhancements within and adjacent to the optic chiasm at the basal cisternal level and in the leptomeningeal layers in the posterior fossa had disappeared. In addition, thoracic and cervical MRI showed that the leptomeningeal enhancements along the spinal cord had completely resolved and the hilar lymphadenopathy had disappeared.

The patient had no systemic or ophthalmological recurrence while under oral 15 mg/week methotrexate and 5 mg/day folic

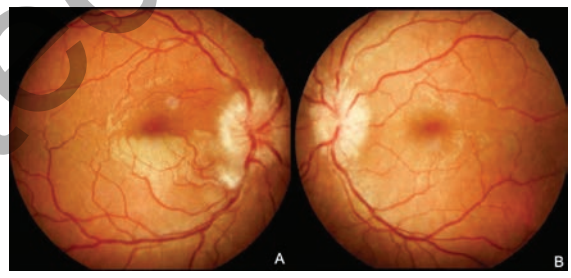

Figure 1. Color fundus photograph of a 26-year-old female patient at initial presentation: (A) Optic disc edema, soft exudate in the inferotemporal part of the optic disc, and ischemia in the inferior half of the macula is seen in the right eye; (B) optic disc edema is seen in the left eye

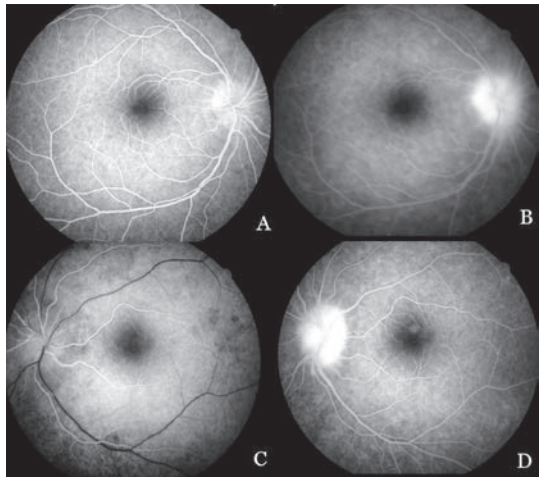

Figure 2. Fundus fluorescein angiography image obtained 2 weeks after initial presentation: (A-D) Optic disc hyperfluorescence beginning in the early phase and increasing in the late phase is seen in both eyes; (D) a hyperfluorescent spot increasing in intensity in the late phase is seen in the superior aspect of the left fovea

acid therapy or during the 15-month follow-up period. No side effects related to systemic immunosuppressive therapy were observed.

Discussion

Although the lungs are most commonly affected, sarcoidosis can manifest with extrapulmonary involvement including dermal, ocular, neurological, cardiac, renal, and gastrointestinal involvement.[8] Neurological involvement is uncommon in sarcoidosis. Neurosarcoidosis is seen in 5-15% of patients with systemic sarcoidosis.[5,6]

Turner et al.[9] reported that the central nervous system is also involved in 37% of patients with intraocular sarcoidosis. In a study by Menezo et al.[7], it was found that 7.4% of patients with neurosarcoidosis had optic nerve involvement. In a series of 19 patients with systemic sarcoidosis, optic neuropathy was accompanied by granulomatous anterior uveitis in 10 patients, retinal vasculitis and cotton-wool spots in 2 patients each, and isolated vitritis, panuveitis, isolated choroidal involvement, macular exudates, and episcleritis in 1 patient each.[10] In our case, the patient had systemic sarcoidosis with ocular involvement manifesting as bilateral anterior uveitis, vitritis, and macular ischemia in the right eye. When the patient underwent neurological evaluation for bilateral optic nerve involvement and headaches, we found that she also had neurosarcoidosis.

Yu and Yannuzzi[11] associated bilateral decreased vision in a patient who had pulmonary neurosarcoidosis and neurosarcoidosis with findings of avascular zone enlargement on FFA and cystic changes in the macula on OCT. The patient was found to have bilateral perifoveal ischemia, which was presented as a rare finding of sarcoidosis involvement. Sarcoidosis usually causes non-ischemic retinal vasculitis.[12] The macular ischemia in the right eye of our patient and the soft exudate in the lower temporal part of the optic disc may be attributable to reduced flow in the retinal artery due to inflammation. The macular ischemia and exudate regressed within the first week of treatment. Due to the poor general condition of the patient, OCT and FFA were not done during this period.

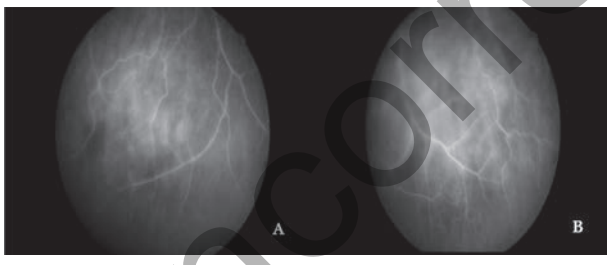

Figure 3. Peripheral fundus fluorescein angiography image shows leakage increasing in the late phase in the retinal vessels in the (A) right and (B) left eyes

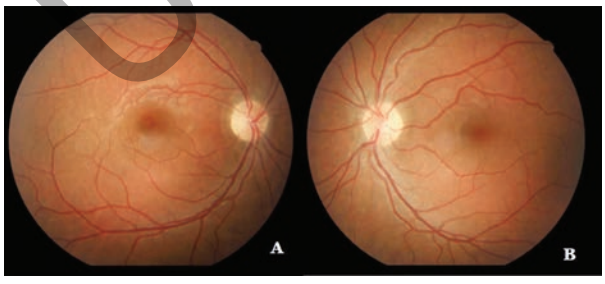

Figure 4. Fundus photograph taken 3 months after treatment: (A) Complete resolution of the optic disc edema and ischemia in the inferior macula is seen in the right eye; (B) Regression of the optic disc edema is seen in the left eye

Unlike pulmonary sarcoidosis, spontaneous resolution of neurosarcoidosis is uncommon. Neurosarcoidosis-related morbidity and mortality are minimized with treatment.[13] Although corticosteroids appear to be the first choice for the treatment of neurosarcoidosis, response rates to treatment with corticosteroids alone are lower in patients with neurosarcoidosis compared to patients with pulmonary sarcoidosis.[14,15] In the long-term treatment of neurosarcoidosis, reactivation has been reported when the corticosteroid dose is reduced to 20-25 mg.[15] The addition of immunosuppressive agents such as methotrexate,[14] azathioprine,[16] mycophenolate mofetil,[16] and chlorambucil[17] to corticosteroid therapy has been reported in case reports. There are also studies in which the anti-TNF inhibitor infliximab has been used as a biological agent.[18] In one report, a 61% remission rate was achieved in neurosarcoidosis by discontinuing corticosteroids and treating with methotrexate.[14] In the present case, full remission with no recurrence during the 15-month follow-up period was achieved with methotrexate treatment.

In conclusion, neurosarcoidosis should be included in the differential diagnosis of patients with bilateral optic neuropathy and uveitis. Although macular ischemia is a rare finding of sarcoidosis, we should bear in mind that it may arise as a result of reduced flow in the retinal artery due to inflammation. Early diagnosis and treatment improve the prognosis of the disease and of ocular involvement if present. Sarcoidosis requires a multidisciplinary approach, and ophthalmologists play a key role in diagnosis and treatment planning.

Ethics

Informed Consent: It was taken.

Peer-review: Externally peer-reviewed.

Authorship Contributions

Surgical and Medical Practices: Burak Tanyıldız, Nilüfer Zorlutuna Kaymak, Mehmet Engin Tezcan, Ahmet Kasım Kılıç, Sevda Şener Cömert, Aysu Karatay Arsan, Concept: Burak Tanyıldız, Gizem Doğan, Nilüfer Zorlutuna Kaymak, Mehmet Engin Tezcan, Aysu Karatay Arsan, Design: Burak Tanyıldız, Gizem Doğan, Nilüfer Zorlutuna Kaymak, Mehmet Engin Tezcan, Aysu Karatay Arsan, Data Collection or Processing: Burak Tanyıldız, Gizem Doğan, Analysis or Interpretation: Burak Tanyıldız, Literature Search: Burak Tanyıldız, Writing: Burak Tanyıldız.

Conflict of Interest: No conflict of interest was declared by the authors.

Financial Disclosure: The authors declared that this study received no financial support.

References

1. Costabel U, Hunninghake GW. ATS/ERS/WASOG statement on sarcoidosis. Sarcoidosis Statement Committee. American Thoracic Society. European Respiratory Society. World Association for Sarcoidosis and Other Granulomatous Disorders. Eur Respir J. 1999;14:735-737.
2. Bradley D, Baughman RP, Raymond L, Kaufman AH. Ocular manifestations of sarcoidosis. Semin Respir Crit Care Med. 2002;23:543-548.
3. Karma A. Ophthalmic changes in sarcoidosis. Acta Ophthalmol Suppl. 1979:1-94.
4. Obenauf CD, Shaw HE, Sydnor CF, Klintworth GK. Sarcoidosis and its ophthalmic manifestations. Am J Ophthalmol. 1978;86:648-655.
5. Stern BJ, Krumholz A, Johns C, Scott P, Nissim J. Sarcoidosis and its neurological manifestations. Arch Neurol. 1985;42:909-917.
6. Delaney P. Neurologic manifestations in sarcoidosis: review of the literature, with a report of 23 cases. Ann Intern Med. 1977;87:336-345.
7. Menezo V, Lobo A, Yeo TK, du Bois RM, Lightman S. Ocular features in neurosarcoidosis. Ocul Immunol Inflamm. 2009;17:170-178.
8. Rao DA, Dellaripa PF. Extrapulmonary manifestations of sarcoidosis. Rheum Dis Clin North Am. 2013;39:277-297.
9. Turner RG, James DG, Friedmann AI, Vijendram M, Davies JP. Neuro-ophthalmic sarcoidosis. Br J Ophthalmol. 1975;59:657-663.
10. Kidd DP, Burton BJ, Graham EM, Plant GT. Optic neuropathy associated with systemic sarcoidosis. Neurol Neuroimmunol Neuroinflamm. 2016;3:e270.
11. Yu S, Yannuzzi LA. Bilateral perifoveal macular ischemia in sarcoidosis. Retin Cases Brief Rep. 2014;8:212-214.
12. Talat L, Lightman S, Tomkins-Netzer O. Ischemic retinal vasculitis and its management. J Ophthalmol. 2014;2014:197675.
13. Judson MA, Boan AD, Lackland DT. The clinical course of sarcoidosis: presentation, diagnosis, and treatment in a large white and black cohort in the United States. Sarcoidosis Vasc Diffuse Lung Dis. 2012;29:119-127.
14. Lower EE, Broderick JP, Brott TG, Baughman RP. Diagnosis and management of neurological sarcoidosis. Arch Intern Med. 1997;157:1864-1868.
15. Zajicek JP, Scolding NJ, Foster O, Rovaris M, Evanson J, Moseley IF, Scadding JW, Thompson EJ, Chamoun V, Miller DH, McDonald WI, Mitchell D. Central nervous system sarcoidosis--diagnosis and management. QJM. 1999;92:103-117.
16. Baughman RP, Lower EE. Treatment of Sarcoidosis. Clin Rev Allergy Immunol. 2015;49:79-92.
17. Gelwan MJ, Kellen RI, Burde RM, Kupersmith MJ. Sarcoidosis of the anterior visual pathway: successes and failures. J Neurol Neurosurg Psychiatry. 1988;51:1473-1480.
18. Gelfand JM, Bradshaw MJ, Stern BJ, Clifford DB, Wang Y, Cho TA, Koth LL, Hauser SL, Dierkhising J, Vu N, Sriram S, Moses H, Bagnato F, Kaufmann JA, Ammah DJ, Yohannes TH, Hamblin MJ, Venna N, Green AJ, Pawate S. Infliximab for the treatment of CNS sarcoidosis: A multi-institutional series. Neurology. 2017;89:2092-2100.

DOI: 10.4274/tjo.98522
Turk J Ophthalmol 2018;48:206-208

Case Report

Possible Association of Papillophlebitis with Guillain-Barré Syndrome: Case Report

Müge Çoban Karataş*, Merih Soylu**

*Başkent University Faculty of Medicine, Department of Ophthalmology, Ankara, Turkey
**Private Practice, Adana, Turkey

Abstract

In this case report, we presented a patient with visual deterioration as a result of papillophlebitis in the right eye who was later diagnosed with Guillain-Barré syndrome (GBS). Upon systemic and laboratory work-up to determine the etiology of papillophlebitis, the diagnosis of GBS was made and treatment was initiated immediately. The ocular and systemic symptoms resolved quickly after starting intravenous immunoglobulin therapy. We present this case to emphasize the importance of etiological diagnosis in papillophlebitis and the unusual presentation of GBS.

Keywords: Papillophlebitis, Guillain-Barré syndrome, visual deterioration

Introduction

Papillophlebitis is an uncommon ocular condition of undetermined etiology. Unlike classic central retinal vein occlusion, patients suffering from this disease are usually healthy and younger than 50 years of age.[1,2] Most patients complain of blurred vision and photopsia. Typical findings include dilatation and tortuosity of the major retinal veins with retinal hemorrhage and optic disc edema.[2] Traditional treatment for papillophlebitis includes systemic and periocular steroid therapy, intravitreal triamcinolone, intravitreal anti-VEGF inhibitors, platelet inhibitors, and anticoagulation.[3,4,5] Guillain-Barré syndrome (GBS) is an immune-mediated acute polyneuropathy principally affecting motor nerves and causing paralysis.[6] It is the most common cause of acute muscle weakness associated with peripheral neuropathy in adults and can be lethal if not treated early.[7] GBS is reported to be associated with Zika virus infection.[8] There are a few case presentations in the literature reporting total ophthalmoplegia, optic nerve involvement, ptosis, Vogt-Koyanagi-Harada, and uveitis as ocular findings of GBS.[9,10,11,12]

Here we report a case with visual deterioration in the right eye with numbness, pain, and tingling sensation in both lower legs.

Case Report

A 53-year-old woman presented with complaints of visual deterioration in the right eye. Her anamnesis revealed no ocular or systemic diseases except a mild influenza-like illness a week earlier. Her best corrected visual acuity (BCVA) was 0.5 in the right and 1.0 in the left eye. Anterior segment examination and intraocular pressure was within normal range in both eyes. Fundoscopic examination of the right eye revealed splinter hemorrhages, optic nerve head hemorrhage, and cotton wool spots in the superior arcuate region, and the patient was diagnosed with papillophlebitis (Figure 1). Fundus fluorescein angiography revealed no ischemic areas; however, there was hypofluorescence in the areas corresponding to hemorrhages, and hyperfluorescence in the optic nerve head (Figure 2). Optical coherence tomography revealed macular edema and intraretinal edema and hyperreflective spots in the nasal fovea

Address for Correspondence: Müge Çoban Karataş MD, Başkent University Faculty of Medicine, Department of Ophthalmology, Ankara, Turkey
Phone: +90 322 327 27 27 E-mail: bkaratas99@hotmail.com **ORCID-ID:** orcid.org/0000-0002-7903-5075
Received: 24.11.2017 **Accepted:** 13.02.2018

corresponding to the areas affected by the occlusion (Figure 3). Laboratory and radiological tests were requested to determine the etiology of the papillophlebitis. One week after onset of these complaints, the patient began to experience numbness, pain, and tingling sensation in both lower legs. Motor weakness became progressively severe in both extremities and she was admitted to the neurology clinic for advanced examination and treatment. No abnormalities were detected in magnetic resonance imaging of the brain and spinal cord. Complete blood count, electrolytes and blood chemistry and urinalysis were normal. Coagulation tests, including serum levels of homocysteine, protein C and S, partial thromboplastin time, and prothrombin time were normal. Erythrocyte sedimentation rate and anticardiolipin G and M were within normal range. Lumbar puncture revealed no pathology. She was diagnosed with GBS and treated with intravenous immunoglobulin (IVIg) therapy. Her symptoms improved in the following 3 months. During follow-up, her BCVA in the right eye returned to 1.0 without any treatment for ocular findings (Figure 4).

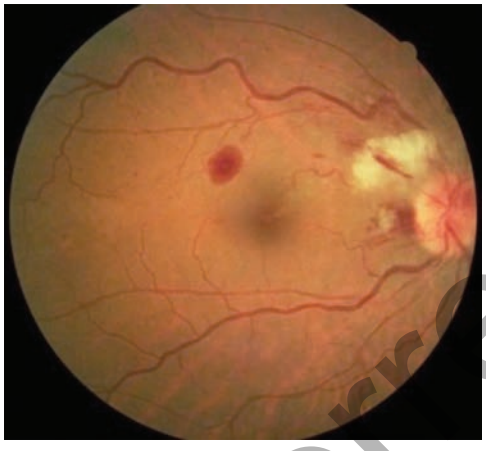

Figure 1. Fundoscopic examination revealed splinter hemorrhages, optic nerve head hemorrhage, and cotton wool spots due to ischemia in the superior arcuate region and a diagnosis of papillophlebitis was made

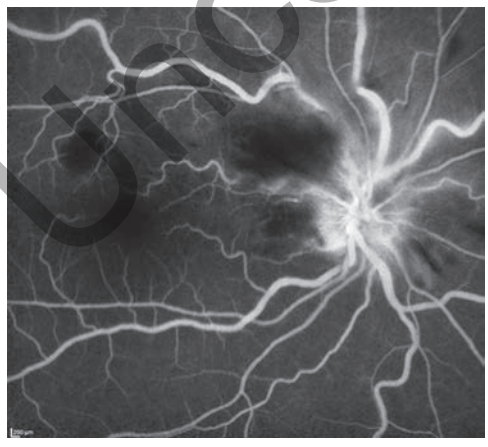

Figure 2. Fundus fluorescein angiography revealed no ischemic areas; however, there was hypofluorescence in the areas corresponding to hemorrhages and hyperfluorescence in the optic nerve head

Discussion

GBS is usually preceded by infection or other immune stimulation that induces an aberrant autoimmune response targeting the peripheral nerves and their spinal roots.[13,14] Two-thirds of adult patients report preceding symptoms of a respiratory or gastrointestinal tract infection within 4 weeks of onset.[15] Underlying systemic diseases such as systemic lupus erythematosus (SLE), sarcoidosis, Hodgkin disease, and other neoplasms have been known to cause a small number of GBS cases.[16]

The pathogenesis of GBS as a manifestation of active SLE is not clear, but both cell-mediated and humoral processes may play a significant role.[17] Ocular findings in SLE include hemorrhage, retinal cotton wool spots, microangiopathy, and vaso-occlusion as a result of immune complex deposition. The role of immune complex deposition is highlighted in vascular pathogenesis in the eye.[15]

Our patient was relatively young and did not suffer from any systemic diseases. Her anamnesis revealed only an influenza-like illness with mild symptoms the week before. To the best of our knowledge, there are no previous reports in the literature of papillophlebitis as the initial presentation of GBS. Although the two clinical presentations may be coincidental, it may be postulated that papillophlebitis in our patient was related to the immune-mediated etiology of GBS, as is seen in SLE.

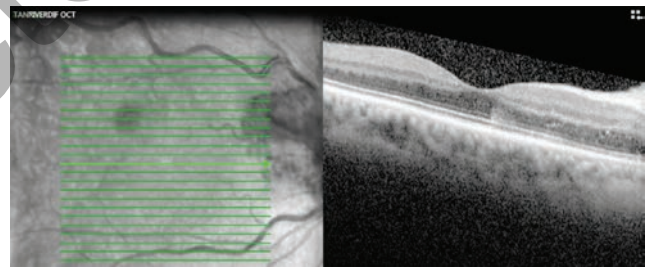

Figure 3. Optical coherence tomography revealed macular edema and intraretinal edema and hyperreflective spots in the nasal fovea corresponding to the areas affected by the occlusion

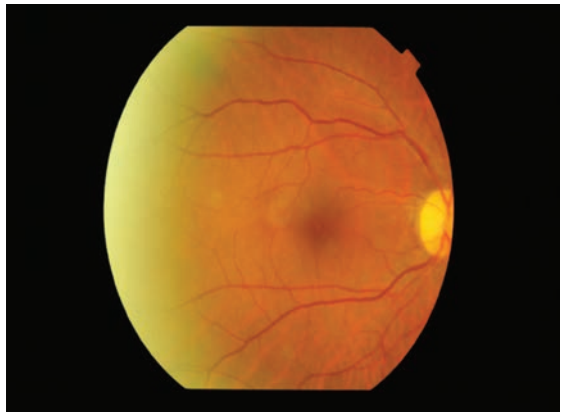

Figure 4. During follow-up, the patient's best corrected visual acuity in the right eye returned to 1.0 without any treatment for ocular findings. Hemorrhages and cotton wool spots improved without any specific ocular treatment

In conclusion, we present this case in order to emphasize the importance of etiologic diagnosis in papillophlebitis. Papillophlebitis may be an initial finding of GBS, which may lead to serious neurologic complications if not treated early. Treatment modalities may differ with the etiologic diagnosis. Early initiation of IVIg or plasma exchange is of proven benefit and crucial in GBS.[19] In our patient, no specific treatment for ocular findings was applied, as the papillophlebitis resolved with systemic treatment of GBS without leaving any sequelae. This may also be the result of the benign course of the papillophlebitis and the reversal of the findings of papillophlebitis may be the natural outcome.

Ethics

Informed Consent: It was taken.

Peer-review: Externally peer-reviewed.

Authorship Contributions

Surgical and Medical Practices: Müge Çoban Karataş, Merih Soylu, Concept: Müge Çoban Karataş, Merih Soylu, Design: Müge Çoban Karataş, Merih Soylu, Data Collection or Processing: Müge Çoban Karataş, Merih Soylu, Analysis or Interpretation: Müge Çoban Karataş, Merih Soylu, Literature Search: Müge Çoban Karataş, Merih Soylu, Writing: Müge Çoban Karataş, Merih Soylu.

Conflict of Interest: No conflict of interest was declared by the authors.

Financial Disclosure: The authors declared that this study received no financial support.

References

1. Ellenberger C, Messner KH. Papillophlebitis: benign retinopathy resembling papilledema or papillitis. Ann Neurol. 1978;3:438-440.
2. Sanborn GE, Magargal LE. Papillophlebitis:an update. In: smith JL,eds. Neurophthalomology Entering the 90's. Masson; New York; 1988:47-54.
3. Chang YC, Wu WC. Intravitreal triamcinolone acetonide fort he management of papillophlebitis and associated macular edema. Int Ophthalmol. 2008;28:291-296.
4. Fong ACO, Schatz H, McDonald HR, Burton TC, Maberley AL, Joffe L, Zegarra H, Nadel AJ, Johnson RN. Central retinal vein occlusion in young adults (papillophlebitis). Retina. 1992;12:3-11.
5. Güngör İ, Konuk GE, Süllü Y, Arıtürk N. Papillophlebitis: Treatment of vision loss due to subretinal fluid with intravitreal ranibizumab. Neuroophthalmology. 2014;38:336-339.
6. Miller NR, Newman NJ, Biousse V, Kerrison JB. Walsh & Hoyt's Clinical Neuro-Ophthalmology. 6th edition. Vol 1. Philadelphia PA; Lippicott Williams & Wilkins; 2004.
7. Wang Y, Lang W, Zhang Y, Ma X, Zhou C, Zhang HL. Long-term prognosis of Guillain-Barré syndrome not determined by treatmentoptions? Oncotarget. 2017;8:79991-80001.
8. Méndez N, Oviedo-Pastrana M, Mattar S, Caicedo-Castro I, Arrieta G. Zika virus disease, microcephaly and Guillain-Barré syndrome in Colombia: epidemiological situation during 21 months of the Zika virus outbreak, 2015-2017. Arch Public Health. 2017;75:65.
9. Panosyan FB. Bilateral Ptosis due to Sympathetic Dysfunction as a Feature of Guillain-Barre Syndrome. J Clin Neuromuscul Dis. 2017;19:38-42.
10. Rajska K, Rożniecki J, Loba P, Zielińska M, Broniarczyk-Loba A. Total ocular akinesis: Miller Fisher or Guillain-Barré syndrome? Neurol Neurochir Pol. 2011;45:297-300.
11. Najman-Vainer J, Levinson RD, Graves MC, Nguyen BT, Engstrom RE Jr, Holland GN. An association between Vogt-Koyanagi-Harada disease and Guillain-Barré syndrome. Am J Ophthalmol. 2001;131:615-619.
12. Maca SM, Scharitzer M, Barisani-Asenbauer T. Uveitis and neurologic diseases: an often overlooked relationship. Wien Klin Wochenschr. 2006;118:273-279.
13. Hughes RA, Cornblath DR. Guillain-Barré syndrome. Lancet. 2005;366:1653-1666.
14. Van den Berg B, Walgaard C, Drenthen J, Fokke C, Jacobs BC, van Doorn PA. Guillain-Barré syndrome: pathogenesis, diagnosis, treatment and prognosis. Nat Rev Neurol. 2014;10:469-482.
15. Jacobs BC, Rothbarth PH,van der Meché FG, Herbrink P, Schmitz PI, de Klerk MA, van Doorn PA. The spectrum of antedecedent infections in Guillain-Barré syndrome:a case-control study. Neurology. 2010;74:581-87.
16. Ropper AH. The Guillain Barre syndrome. N Engl J Med. 1992;326:1130-1136.
17. Robson MG, Walport MJ, Davies KA. Systemic lupus erythematosus and acute demyelinating polyneuropathy. Br J Rheumatol. 1994;33:1074-1077.
18. Nag TC, Wadhwa S. Vascular changes of the retina and choroid in systemic lupus erythematosus: pathology and pathogenesis. Curr Neurovasc Res. 2006;3:159-168.
19. Willison HJ, Jacobs BC, van Doorn PA, Guillain-Barré syndrome. Lancet 2016;388:717-727.

DOI: 10.4274/tjo.09076
Turk J Ophthalmol 2018;48:209-211

Case Report

Intravitreal Aflibercept as an Adjunct to Systemic Therapy in a Case of Choroidal Neovascular Membrane Associated with Sympathetic Ophthalmia

Ali Osman Saatçi, Ziya Ayhan, Şefik Can İpek, Meltem Söylev Bajin
Dokuz Eylül University Faculty of Medicine, Department of Ophthalmology, İzmir, Turkey

Abstract

Choroidal neovascular membrane (CNV) is a very rare complication in patients with sympathetic ophthalmia. We hereby report a 38-year-old man who developed a type 2 CNV in his only seeing (left) eye while under systemic steroid treatment. Systemic therapy was revised and a total of 5 intravitreal aflibercept injections (2 mg each) were administered over a period of 8 months. Good anatomic and functional outcome was noted at the last visit. Anti-vascular endothelial growth factor injection may be an important adjunct to systemic therapy in eyes with with sympathetic ophthalmia-associated CNV.

Keywords: Aflibercept, choroidal neovascular membrane, prednisolone, sympathetic ophthalmia

Introduction

Sympathetic ophthalmia (SO) is a rare bilateral granulomatous inflammation that follows an accidental or surgical insult to the uvea.[1] Choroidal neovascular membrane (CNV) may complicate the disease course and negatively affect visual outcome in patients with SO.[2,3,4,5,6,7,8,9]

In a retrospective cohort study including 4041 eyes of 2307 patients with posterior uveitis and panuveitis, 81 eyes (2%) had CNV at presentation.[10] In this study, the number of patients with SO and CNV was not given as it was too small. Recently, in another retrospective study involving 6850 uveitis patients, 73 eyes of 60 patients (0.87%) were found to have inflammatory CNV.[11] Of these 73 eyes, 52% (38 eyes of 29 patients) had CNV at the first presentation and the remaining 48% (35 eyes of 31 patients) developed CNV during the course of follow-up. Only 1 patient with CNV had a diagnosis of SO.

Here we report a one-eyed patient with SO who developed CNV during follow-up and was treated with intravitreal aflibercept injections in addition to ongoing systemic therapy.

Case Report

The blind and painful right eye of a 38-year-old man was eviscerated in September 2016. The patient stated that his right eye had been blind since early childhood due to a unilateral congenital anomaly complicated by secondary glaucoma. He received the diagnosis of SO in January 2017 after he experienced visual loss in his only seeing (left) eye. At the time of diagnosis, the patient was admitted to the hospital and meticulously investigated for possible infectious and noninfectious causes to rule out other uveitic entities, but without any positive findings. At that time, his best-corrected visual acuity was 6/10. Slit-lamp examination yielded some vitreous cells in the left eye. Fundoscopy showed a few scattered pigmented chorioretinal scars and discrete yellowish round choroidal lesions throughout the left fundus (Figure 1A). Fluorescein angiogram delineated the active lesions as early hypofluorescent (Figure 1B) with late staining. Left macular contour was normal on optical coherence tomography (OCT) examination (Figure 1C). He was started on oral prednisolone (64 mg) for 2 weeks with gradual tapering of 8 mg per week. Despite initial visual improvement, he

Address for Correspondence: Ali Osman Saatçi MD, Dokuz Eylül University Faculty of Medicine, Department of Ophthalmology, İzmir, Turkey
Phone: +90 532 743 70 71 E-mail: osman.saatci@yahoo.com **ORCID-ID:** orcid.org/0000-0001-6848-7239
Received: 13.12.2017 **Accepted:** 24.01.2018

experienced another episode of visual decline while taking 32 mg of prednisolone. His best-corrected visual acuity decreased to 2/10 and he had grade 4 vitreous haze according to the Miami grading.[12] Fundus examination showed marked yellowish-white discoloration of the macula with some evidence of intraretinal hemorrhage (Figure 2A and B). He was hospitalized and treated with pulse methylprednisolone 1 g (250 mg 4 times daily) for 3 days. Following pulse therapy, 64 mg oral prednisolone and 150 mg (50 mg 3 times daily) azathioprine were co-administered. Two weeks after the completion of pulse therapy, his visual acuity was still 2/10 despite a significant reduction in vitreous haze. Fluorescein angiogram and OCT demonstrated type 2 choroidal neovascularization (Figure 3A-C). Five intravitreal 2 mg aflibercept injections were given within a period of 8 months. His final visual acuity was 6/10 with a stable-looking macula (Figure 4A and B) and he was continued on a treatment regimen of 150 mg azathioprine and 8 mg prednisolone daily.

Discussion

CNV can be associated with various inflammatory choroidal diseases, as cytokines together with vascular endothelial growth factor (VEGF) are implicated in the pathogenetic mechanisms, leading to impaired permeability and altered angiogenesis.[13,14] The presence of Dalen-Fuchs nodules may be the cause of the disruption of the Bruch's membrane in eyes with SO.[7]

CNV in eyes with SO has been observed to resolve spontaneously[2,3] and to respond to immunosuppressive agents (cyclosporine and azathioprine),[4,7] photodynamic therapy,[6] thermal laser,[5] and intravitreal bevacizumab injection.[8] Even submacular surgery to remove CNV has been attempted.[9]

Steroids and immunosuppressives are generally used in uveitis to reduce the inflammatory stimulus which seems to play a role in CNV formation and also partly due to their antiangiogenic effect.[15] Anti-VEGF agents have also been used in addition to systemic therapy in eyes with inflammatory CNV in case reports and series. In a randomized study investigating the efficacy and safety of ranibizumab for the treatment of CNV due to uncommon causes in a group of 178 patients, 18 (15.1%) had postinflammatory type CNV and a single loading dose followed by a pro re nata regimen seemed to succeed statistically both in anatomic and visual outcome.[16] Julian et al.[8] reported using intravitreal bevacizumab therapy in a group of 15 patients with uveitis-related CNV and only 1 of the 15 patients had SO. This patient was also receiving systemic steroid and interferon alpha. The number of bevacizumab injections was not mentioned. In our case, the patient developed CNV in his only eye while he was on systemic steroids and 5 consecutive 2 mg aflibercept

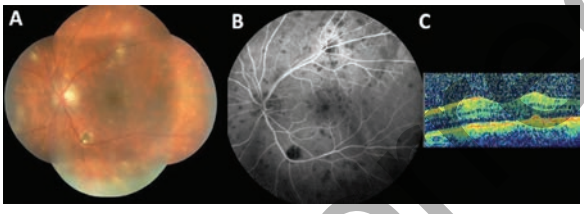

Figure 1. A) Composite color fundus photograph of the left eye showing scattered roundish yellow-white infiltrates throughout the fundus; B) venous phase of the angiogram depicting the widespread hypofluorescent dots under the retina in 360 degrees; C) optical coherence tomography section showing the nearly normal foveolar contour and some hyperreflective dots corresponding to posterior vitreous inflammatory cell clusters at the time of the diagnosis of sympathetic ophthalmia

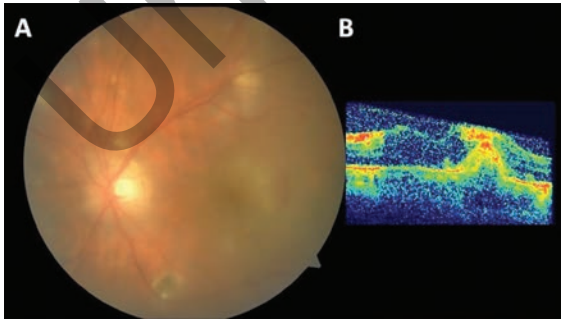

Figure 2. A) Color fundus photograph of the left eye demonstrating the hazy view of the posterior fundus and yellow-white foveolar infiltration with indistinct borders and the presence of some retinal hemorrhage; B) optical coherence tomography section of the left eye delineating the possible choroidal neovascular membrane

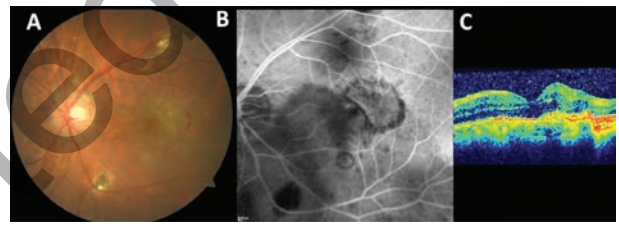

Figure 3. A) Color fundus photograph of the left eye showing the juxtafoveolar choroidal neovascular membrane and scattered chorioretinal scars; B) fluorescein angiography image depicting the hyperfluorescent well-demarcated classic type of choroidal neovascular membrane; C) optical coherence tomography section showing type 2 membrane with some intraretinal fluid

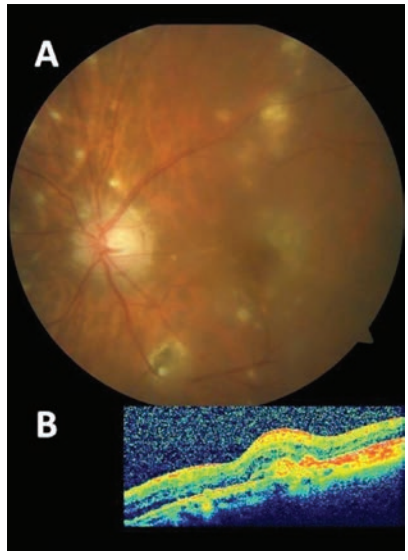

Figure 4. A) Color fundus photograph showing the diminished choroidal neovascular membrane area and persistent 360-degree chorioretinal scars at the last follow-up visit; B) optical coherence tomography section showing the fibrotic-looking choroidal neovascular membrane

injections administered over 8 months helped us to improve his vision. Together with azathioprine maintenance therapy, he achieved relatively good anatomic and visual outcomes.

Clinicians should be careful to differentiate the signs of choroidal subretinal neovascular membrane from the signs of already present uveal inflammation, as even eyes under immunosuppressive treatment may develop CNV. Anti-VEGF agents (aflibercept in the present case) seems to be a very valuable adjunct to obtain a good anatomic and functional outcome in inflammatory type subretinal choroidal neovascular membranes and systemic immunosuppression should also be used to suppress the inflammatory stimulus.

Ethics

Informed Consent: Received.

Peer-review: Externally peer-reviewed.

Authorship Contributions

Surgical and Medical Practices: Ali Osman Saatçi, Meltem Söylev Bajin, Ziya Ayhan, Şefik Can İpek, Concept: Ali Osman Saatçi, Design: Ali Osman Saatçi, Data Collection or Processing: Ali Osman Saatçi, Analysis or Interpretation: Ali Osman Saatçi, Literature Search: Ali Osman Saatçi, Ziya Ayhan, Şefik Can İpek, Writing: Ali Osman Saatçi.

Conflict of Interest: No conflict of interest was declared by the authors.

Financial Disclosure: The authors declared that this study received no financial support.

References

1. Chu XK, Chan CC. Sympathetic ophthalmia: to the twenty-first century and beyond. J Ophthalmic Inflamm Infect. 2013;3:49.
2. Chew EY, Crawford J. Sympathetic ophthalmia and choroidal neovascularization. Case report. Arch Ophthalmol. 1988;106:1507-1508.
3. Carney MD, Tessler HH, Peyman GA, Goldberg MF, Williams DP. Sympathetic ophthalmia and subretinal neovascularization. Ann Ophthalmol. 1990;22:184-186.
4. Kilmartin DJ, Forrester JV, Dick AD. Cyclosporine-induced resolution of choroidal neovascularization associated with sympathetic ophthalmia. Arch Ophthalmol. 1998;116:249-250.
5. Borkowski LM, Weinberg DV, Delany CM, Milsow L. Laser photocoagulation for choroidal neovascularization associated with sympathetic ophthalmia. Am J Ophthalmol. 2001;132:585-587.
6. Kinge B, Syrdalen P, Bjornsson OM. Photodynamic therapy for choroidal neovascularization secondary to sympathetic ophthalmia. Retina. 2005;25:375-377.
7. Vianna RN, Ozdal P, Souza Filho JP, Deschenes J. Choroidal neovascularization associated with sympathetic ophthalmia: case report. Arq Bras Oftalmol. 2005;68:397-400.
8. Julian K, Terrada C, Fardeau C, Cassoux N, Francais C, LeHoang P, Bodaghi B. Intravitreal bevacizumab as first local treatment for uveitis-related choroidal neovascularization: long-term results. Acta Ophthalmol. 2011;89:179-184.
9. Bom S, Young S, Gregor Z, Lightman S. Surgery for choroidal neovascularization in sympathetic opthalmia. Retina. 2002;22:109-111.
10. Baxter SL, Pistilli M, Pujari SS, Liesegang TL, Suhler EB, Thorne JE, Foster CS, Jabs DA, Levy-Clarke GA, Nussenblatt RB, Rosenbaum JT, Kempen JH. Risk of choroidal neovascularization among the uveitides. Am J Ophthalmol. 2013;156:468-477.
11. Bansal R, Bansal P, Gupta A, Gupta V, Dogra MR, Singh R, Katoch D. Diagnostic Challenges in Inflammatory Choroidal Neovascular Membranes. Ocul Immunol Inflamm. 2017;25:554-562.
12. Davis JL, Madow B, Cornett J, Stratton R, Hess D, Porciatti V, Feuer WJ. Scale for photographic grading of vitreous haze in uveitis. Am J Ophthalmol. 2010;150:637-641.
13. Battaglia Parodi M, Iacono P, Verbraak FD, Bandello F. Antivascular endothelial growth factors for inflammatory chorioretinal disorders. Dev Ophthalmol. 2010;46:84-95.
14. D'Ambrosio E, Tortorella P, Iannetti L. Management of uveitis-related choroidal neovascularization: from the pathogenesis to the therapy. J Ophthalmol. 2014;2014:450428.
15. Bhende M. AAS. Management of Inflammatory CNV. In: Biswas J. MP, ed. Uveitis: An Update. New Delhi; Springer; 2016:109-117.
16. Lai TYY, Staurenghi G, Lanzetta P, Holz FG, Melissa Liew SH, Desset-Brethes S, Staines H, Hykin PG; MINERVA study group. Efficacy and safety of ranibizumab for the treatment of choroidal neovascularization due to uncommon cause: Twelve-Month Results of the MINERVA Study. Retina. 2018;38:1464-1477.

DOI: 10.4274/tjo.03185
Turk J Ophthalmol 2018;48:212-214

Case Report

Familial Exudative Retinopathy: A Case and Family Analysis

Hazan Gül Kahraman, Feray Koç, Nazife Sefi Yurdakul
İzmir Atatürk Training and Research Hospital, Ophthalmology Clinic, İzmir, Turkey

Abstract

Familial exudative vitreoretinopathy (FEVR) is a rare inherited disorder of retinal angiogenesis. A 49-year-old male patient was referred to our clinic for retinal vascular occlusion. His history, clinical findings, and fundus fluorescein angiography findings were evaluated. Family members were called and eye examinations were performed. Our patient was not born preterm and he reported decreased visual acuity after a traffic accident during childhood. He had laser treatment when he was 12 years old and again 1 month before our examination. He also had laser-assisted in situ keratomileusis surgery for both eyes in 2002. On examination, his visual acuity was 0.4 in the right eye and 0.3 in the left eye. He had cortical cataract in both eyes. Macula OCT revealed macular contour irregularity due to epiretinal membrane in his right eye and minimal perifoveal thinning in his left eye. On fundus photography, straightening of the retinal vessels, macular dragging, retinal folds on temporal retina, preretinal fibrosis, and laser spots were seen. FFA revealed avascular retinal areas with incomplete laser spots in the temporal, inferior, and superior parts of retina. He also had neovascularization with leakage in the temporal retina of his right eye. The patient's brother, who was also born at full term, also had excessive branching of the vascular structures in the temporal peripheral retina, non-perfused cord vessels and avascular areas. In light of all these findings, we diagnosed our patient with Stage 2A FEVR and his brother with Stage 1 FEVR. In summary, FEVR is a clinically diagnosed disease. Because FEVR is inherited and potentially sight-threatening, family examination is helpful and important so that affected family members can be diagnosed and followed up.

Keywords: Retina, familial exudative vitreoretinopathy, genetics

Introduction

Familial exudative vitreoretinopathy (FEVR) is a rare hereditary disease affecting retinal vascular development, and was first described in 1969 by Criswick and Schepens.[1] The vascular pathologies were characterized by Canny and Oliver[2] in 1976 using fundus fluorescein angiography (FFA). The primary clinical manifestation of the disease is an avascular peripheral retina. Subsequent ischemia may lead to other findings of FEVR, including serious problems such as neovascularization (NVE), fibrosis, posterior pole traction, retinal folds, and even retinal detachment.[3] Diagnosis can be made based on the presence of these findings on fundus examination, but evaluation of family members can also support the diagnosis in advanced cases with complicated findings. Ranchod et al.[4] and Pendergast and Trese.[5] reported positive family history in 37% and 57.7% of patients with FEVR, respectively. In a study conducted in Turkey, 7 out of 10 patients were found to have a positive family history.[6] In this report, we present the findings of a patient diagnosed with FEVR and another affected member of his family.

Case Report

A 49-year-old male patient was referred to our clinic with a prediagnosis of retinal vascular occlusion. In his medical history, he reported developing low vision after a traffic accident in childhood, having laser treatment in both eyes at 12 years of age and again 1 month earlier, and undergoing bilateral laser-assisted in situ keratomileusis in 2002. His medical and family histories were otherwise unremarkable. Following fundus examination and FFA, he was questioned again about his birth and he stated that he had been born full term by normal delivery.

Address for Correspondence: Hazan Gül Kahraman MD, İzmir Atatürk Training and Research Hospital, Clinic of Ophthalmology, İzmir, Turkey
Phone: +90 538 540 11 23 E-mail: hazangulakduman@hotmail.com **ORCID-ID:** orcid.org/0000-0003-0865-1580
Received: 20.09.2017 **Accepted:** 20.02.2018

On ophthalmologic examination, his visual acuity was 0.4 in the right eye and 0.3 in the right eye, with mild cortical lens opacities. Fundus photography showed straightening of the temporal retinal vascular arcades and temporal dragging of the macula in both eyes (Figure 1).

Previously applied laser spots with corresponding preretinal fibrosis were observed in the temporal periphery. Although the nonperfused areas in the temporal retina had been partially laser treated, FFA revealed leakage due to persistent retinal NVE in the right eye (Figure 2).

Optical coherence tomography revealed disrupted macular contour associated with epiretinal membrane in the right macula and minimal perifoveal thinning in the left macula (Figure 3).

Suspecting FEVR, the patient's family members were invited for ophthalmologic examination. The patient's father had normal ocular findings, while his brother showed straightening of the temporal vascular arcades in both eyes and excessive vascular branching and nonperfusing cord vessels in the peripheral vasculature, as well as temporal avascular areas (Figure 4).

His brother was also not born prematurely. FFA was not performed for his brother because he did not return for the procedure. FFA in the patient's father was within normal limits. Based on the brother's findings and the revised Pendergast and Trese[7] classification, the patient was diagnosed with stage 2A FEVR and his brother was diagnosed with stage 1A FEVR (Table 1). The patient's other family members did not appear for examination. Additional laser therapy to the nonperfused areas was recommended due to persistent NVE. When obtaining his family history, it was learned that his parents were second-degree cousins.

Discussion

FEVR is diagnosed clinically. In the early stages, it is important to differentiate FEVR from retinopathy of prematurity. However, in older patients presenting with findings such as proliferative vitreoretinopathy (PVR), retinal detachment, and vitreous hemorrhage, especially those with asymmetric involvement, pathologies such as Coats disease, Eales disease, retinosis, sickle cell anemia, and toxocariasis must be excluded. Patients may also present with various combinations of macular dragging, radial retinal folds, NVE, preretinal vitreous organization, vitreoretinal proliferation, subretinal exudation, and retinal detachment. PVR is more common in advanced disease, and requires multiple surgical interventions.[8]

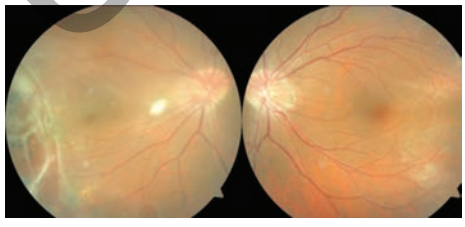

Figure 1. Fundus photographs of a patient with familial exudative vitreoretinopathy showing straightening of the temporal retinal vascular arcades, temporal dragging of the macula that was more prominent in the right eye, and laser spots with preretinal fibrosis in the right fundus temporal to the macula

Milder forms of FEVR may manifest with peripheral avascularity accompanied by vitreoretinal adhesions, veno-venous anastomoses, increased vascular branching, and V-shaped

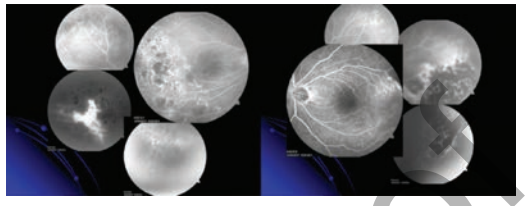

Figure 2. Fundus fluorescein angiography showing partially laser-treated avascular areas in the temporal retina of both eyes and leakage due to persistent retinal neovascularization in the right eye

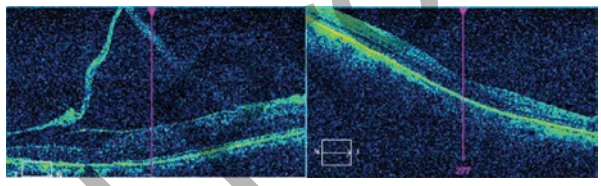

Figure 3. Macular optical coherence tomography showing disrupted macular contour associated with epiretinal membrane in the right macula and minimal perifoveal thinning in the left macula

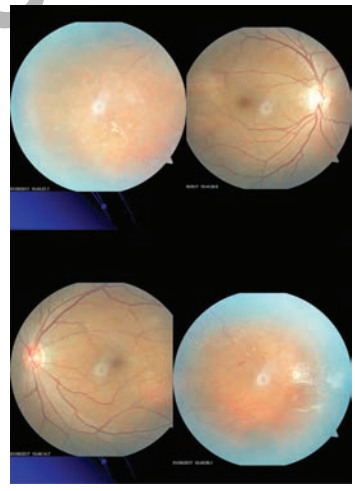

Figure 4. Color fundus photograph showing avascular areas, excessive vascular branching, and nonperfusing cord vessels in the temporal retinas of both eyes

Table 1. Updated clinical classification of familial exudative vitreoretinopathy

Stage	Exudate*		Clinical features
	(-)	(+)	
1	A	B	Avascular retinal periphery
2	A	B	Extraretinal neovascularization
3	A	B	Extramacular retinal detachment
4	A	B	Retinal detachment involving the macula
5	A (open funnel)	B (closed funnel)	Total retinal detachment

*: For stages 1-4

retinochoroidal degeneration.[9] Some FEVR patients who are asymptomatic with approximately normal fundus examination are reported to have smaller optical disc diameter, greater optic disc-macular distance/optic disc diameter ratio, and higher vessel density from the optic disc compared to a control group.[10] We also observed these findings in the patient's brother. These findings may support a diagnosis of FEVR in suspected cases.

To date, mutations in 5 genes have been associated with the AEVR phenotype (*NDP, FZD4, LRP5, TSPAN12, ZNF408*).[11,12] Autosomal recessive, autosomal dominant, and X-related inheritance patterns have been reported. Therefore, while patients may have a positive family history, a negative family history may not be significant because family members can exhibit different clinical severity. One of the main challenges to diagnosis is that the patient's parents are often healthy. The examination of other family members, especially siblings, is important to prevent further suffering associated with the disease.[13] Because FEVR carries the risk of blindness, screening family members not only facilitates diagnosis, but is also key for follow-up and future genetic counseling for these patients. In addition, evaluating family members can expand our knowledge of the clinical course of the various phenotypes of this rare condition. Our patient had undergone laser therapy at another center and was undiagnosed when he was referred to our clinic. His family members were evaluated for this purpose for the first time and FEVR was detected in his brother. Because we could not perform genetic analysis in this case, the affected gene and inheritance pattern could not be determined, but the patient's family was made aware of the possible complications and genetic transmission of this disease.

FEVR can present in older patients. Family screening assists diagnosis and also enables affected individuals to be identified before becoming symptomatic. These individuals can be informed about and followed for the possible complications of the disease. Furthermore, inheritance pattern may be determined based on the affected family members and genetic counseling can be provided for future generations.

Ethics

Informed Consent: The patient's consent was not received because this case report is retrospective and any information that will reveal the patient's identity is not shared.

Peer-review: Externally and internally peer-reviewed.

Authorship Contributions

Surgical and Medical Practices: Feray Koç, Hazan Gül Kahraman, Concept: Feray Koç, Design: Feray Koç, Data Collection or Processing: Feray Koç, Hazan Gül Kahraman, Analysis or Interpretation: Feray Koç, Hazan Gül Kahraman, Nazife Sefi Yurdakul, Literature Search: Feray Koç, Hazan Gül Kahraman, Writing: Feray Koç, Hazan Gül Kahraman.

Conflict of Interest: No conflict of interest was declared by the authors.

Financial Disclosure: The authors declared that this study received no financial support.

References

1. Criswick VG, Schepens CL. Familial exudative vitreoretinopathy. Am J Ophthalmol. 1969;68:578-594.
2. Canny CL, Oliver GL. Fluorescein angiographic findings in familial exudative vitreoretinopathy. Arch Ophthalmol. 1976;94:1114-1120.
3. Gilmour DF. Familial exudative vitreoretinopathy and related retinopathies. Eye (Lond). 2015;29:1-14.
4. Ranchod TM, Ho LY, Drenser KA, Capone A Jr, Trese MT. Clinical presentation of familial exudative vitreoretinopathy. Ophthalmology. 2011;118:2070-2075.
5. Pendergast SD, Trese MT. Familial exudative vitreoretinopathy. Results of surgical management. Ophthalmology. 1998;105:1015-1023.
6. Cebeci Z, Yıldız Ekinci D, Bayraktar Ş, Kır N. Familial exudative vitreoretinopathy: Follow-up and treatment results. Turk J Ophthalmol. 2014;44:370-373.
7. Kashani AH, Brown KT, Chang E, Drenser KA, Capone A, Trese MT. Diversity of retinal vascular anomalies in patients with familial exudative vitreoretinopathy. Ophthalmology. 2014;121:2220-2227.
8. Aktan G, Subasi M, Or M, Akbatur H. Results of treatment of familial exudative vitreoretinopathy. Annals of Ophthalmology. 2000;32:212-218.
9. Sızmaz S, Yonekawa Y, Trese MT. Familial exudative vitreoretinopathy. Turk J Ophthalmol. 2015;45:164-168.
10. Yuan M, Yang Y, Yu S, Hu A, Lu L, Ma J, Ding X1, Li J. Posterior pole retinal abnormalities in mild asymptomatic FEVR. Invest Ophthalmol Vis Sci. 201416;56:458-463.
11. Kaderli B. Familyal eksüdatif vitreoretinopati. Ret-Vit. 2012;20:120-124.
12. Chen ZY, Battinelli EM, Fielder A, Bundy's, Sims K, Breakefield XO, Craig IW. A mutation in the Norrie disease gene (NDP) associated with X-linked familial exudative vitreoretinopathy. Nat Genet. 1993;5:180-183.
13. Collin RW, Nikopoulos K, Dona M, Gilissen C, Hoischen A, Boonstra FN, Poulter JA, Kondo H, Berger W, Toomes C, Tahira T, Mohn LR, Blokland EA, Hetterschijt L, Ali M, Groothuismink JM, Duijkers L, Inglehearn CF, Sollfrank L, Strom TM, Uchio E, van Nouhuys CE, Kremer H, Veltman JA, van Wijk E, Cremers FP. ZNF408 is mutated in familial exudative vitreoretinopathy and is crucial for the development of zebrafish retinal vasculature. Proc Natl Acad Sci USA. 2013;110:9856-9861.

2018 INTERNATIONAL CONGRESSES

EURETINA 2018
Sep 20 - 23, 2018, Vienna, Austria
www.euretina.org

ESCRS 2018
Sep 22 - 26, 2018, Vienna, Austria
www.escrs.org

AAO 2018
Oct 27 - 30, 2018, Chicago, USA
www.aao.org

2018 NATIONAL CONGRESSES

TOA 52nd National Congress
Nov 14 - 18, 2018, Antalya, Turkey

TURKISH
JOURNAL OF
OPHTHALMOLOGY
TJO

www oftalmoloji org

Avrupa Konutları Kale, Maltepe Mah. Yedikule Çırpıcı Yolu Sk.9.Blok No:2 Kat.1 Ofis:1 Zeytinburnu-İstanbul-Turkey
Phone: +90 212 801 44 36 -37 Fax: +90 212 801 44 39 E-mail: dergi@oftalmoloji.org

Copyright Transfer Form

Corresponding author:.....

Registered number:.....

Title of Article:.....

We, the undersigned authors, accept that the Turkish Journal of Ophthalmology bears no responsibility for the manuscript concerned prior to its acceptance to the Journal. We guarantee that the submitted paper is original, has not previously been published in any other journal, and that, in the event that it is accepted for publication, in whole or in part, the Turkish Journal of Ophthalmology has obtained all permission necessary for publication, and the original copyright form has been submitted to the responsible directorship of publication of the Turkish Journal of Ophthalmology. By signing this form, we transfer copyright of the manuscript to the Turkish Journal of Ophthalmology.

The Turkish Journal of Ophthalmology follows the criteria defined by the International Committee of Medical Journal Editors for authorship of scientific articles; we hereby acknowledge the requirement that each and every person listed in this work should have made a considerable contribution during the creation of this work (such as study design; gathering, analyzing and interpreting the data; or in the writing and scientific review of the article). By signing the Copyright Transfer Form, we hereby declare that all persons identified within the list of authors below have fulfilled the above-mentioned criteria. The authors reserve the following rights.

Note: When used as stated above, a complete reference should be given indicating that the manuscript has been published in the Turkish Journal of Ophthalmology.

1. All proprietary rights, apart form copyright, such as patent rights, etc.
2. The right to use the manuscript in whole or in part in any future work such as books and lectures, free of charge.
3. The right to copy the manuscript for personal use, provided it is not offered for sale.

All authors sign as follows

Name - Surname.....Signature..... Date .....

Name - Surname.....Signature..... Date .....

Name - Surname.....Signature..... Date .....

Name - Surname.....Signature..... Date .....

Name - Surname.....Signature..... Date .....

Name - Surname.....Signature..... Date .....

Name - Surname.....Signature..... Date .....

Name - Surname.....Signature..... Date .....

Address for Correspondence:

Phone: Fax: E-mail:

This form should be filled out completely, including original signatures, scanned and submitted electronically together with your manuscript.
If you are unable to upload the file, e-mail it as an attachment to dergi@oftalmoloji.org within three days of manuscript submission.

Distance Visual Acuity Measurements Equivalency Table

						Spatial Frequency
ETDRS Standard Line Number	**Qualitative Measurements**	**Decimal**	**Snellen**	**LogMAR**	**Angle of Resolution**	**Cycle per Degree**
-3		2.00	20/10	-0.30	0.5	60.00
-2		1.60	20/12.5	-0.20	0.625	48.00
-1		1.25	20/16	-0.10	0.8	37.50
0		1.00	20/20	0.00	1	30.00
		0.90		0.05		27.00
1		0.80	20/25	0.10	1.25	24.00
		0.70		0.15		21.00
2		0.63	20/32	0.20	1.6	18.75
		0.60		0.22		18.00
3		0.50	20/40	0.30	2	15.00
4		0.40	20/50	0.40	2.5	12.00
		0.30		0.52		9.00
5		0.32	20/63	0.50	3.15	9.52
6		0.25	20/80	0.60	4	7.50
7		0.20	20/100	0.70	5	6.00
8		0.16	20/125	0.80	6.25	4.80
9		0.13	20/160	0.90	8	3.75
10	CF from 6 m	0.10	20/200	1.00	10	3.00
11	CF from 5 m	0.08	20/250	1.10	12.5	2.40
12	CF from 4 m	0.06	20/320	1.20	16	1.88
13	CF from 3 m	0.05	20/400	1.30	20	1.50
14		0.04	20/500	1.40	25	1.20
15	CF from 2 m	0.03	20/640	1.51	32	0.94
16		0.025	20/800	1.60	40	0.75
17		0.020	20/1000	1.70	50	0.60
18	CF from 1 m	0.016	20/1250	1.80	62.5	0.48
21	CF from 50 cm	0.008	20/2500	2.10	125	0.24
31	HM from 50 cm	0.0008	20/25000	3.10	1250	0.02

Abbreviations:
CF: Counting fingers, HM: Perception of hand motions, m= meter, cm= centimeter

Equations of conversions for Microsoft Excel:
- Log10 (Decimal Acuity)= LogMAR Equivalent
Power (10; -Logmar Equivalent)= Decimal Acuity (for English version of Microsoft Excel)
Kuvvet (10; -Logmar Equivalent)= Decimal Acutiy (for Turkish version of Microsoft Excel)

Reference
Eğrilmez S, Akkın C, Erakgün T, Yağcı A. Standardization in evaluation of visual acuity and a comprehensive table of equivalent. Turk J Ophthalmol. 2002;32:132-136.

Near Visual Acuity Measurements Related Equivalency Table*														
Snellen	**20/400**	**20/320**	**20/250**	**20/200**	**20/160**	**20/125**	**20/100**	**20/80**	**20/63**	**20/50**	**20/40**	**20/32**	**20/25**	**20/20**
Decimal	0.05	0.063	0.08	0.10	0.125	0.16	0.20	0.25	0.32	0.40	0.50	0.63	0.80	1.00
Jaeger	J19	J18	J17	J16	J15	J14	J13	J11	J9	J7	J5	J3	J2	J1
Times New Roman Point	60	48	36	30	24	18	14	12	10	8	6	5	4	3
LogMAR	1.3	1.2	1.1	1.0	0.9	0.8	0.7	0.6	0.5	0.4	0.3	0.2	0.1	0.0

*Adapted from Rabbets RB: Visual acuity and contrast sensitivity. In: Rabbets RB, editor. Clinical visual optics. Edinburgh: Butterworth-Heinemann, 1998:19-61.